



AIAA 2000-1771

Contributions of the Langley Transonic Dynamics Tunnel to Rotorcraft Technology and Development

William T. Yeager, Jr.
Vehicle Technology Directorate
U.S. Army Research Laboratory
NASA Langley Research Center
Hampton, VA 23681

and

Raymond G. Kvaternik
NASA Langley Research Center
Hampton, VA 23681

AIAA Dynamics Specialists Conference
April 5-6, 2000
Atlanta, GA

CONTRIBUTIONS OF THE LANGLEY TRANSONIC DYNAMICS TUNNEL TO ROTORCRAFT TECHNOLOGY AND DEVELOPMENT

William T. Yeager, Jr.*
Vehicle Technology Directorate
U.S. Army Research Laboratory
NASA-Langley Research Center
Hampton, VA 23681

Raymond G. Kvaternik†
Aeroelasticity Branch
NASA-Langley Research Center
Hampton, VA 23681

Abstract

A historical account of the contributions of the Langley Transonic Dynamics Tunnel (TDT) to rotorcraft technology and development since the tunnel's inception in 1960 is presented. The paper begins with a summary of the major characteristics of the TDT and a description of the unique capability offered by the TDT for testing aeroelastic models by virtue of its heavy gas test medium. This is followed by some remarks on the role played by scale models in the design and development of rotorcraft vehicles and a review of the basic scaling relationships important for designing and building dynamic aeroelastic models of rotorcraft vehicles for testing in the TDT. Chronological accounts of helicopter and tiltrotor research conducted in the TDT are then described in separate sections. The discussions include a description of the various models employed, the specific objectives of the tests, and illustrative results.

Introduction

The Langley Transonic Dynamics Tunnel (TDT) (fig. 1) and the Aeroelasticity Branch (AB) with which it is associated have a long and substantive history of aeroelastic research which has made creditable contributions to rotorcraft technology and development. That research, extending from shortly after the tunnel's inception in 1960 to the present, has included a wide range of experimental investigations using a variety of scale models and testbeds, and the development and application of essential analyses. The results of that

research have contributed substantially to the technology base needed by the industry for designing and building advanced rotorcraft systems. In particular, the work has contributed to supporting rotorcraft research and development programs, to the fundamental understanding of phenomena involved, and to resolving anomalies. For convenience of discussion, the rotorcraft investigations may be divided into two categories: helicopters and tiltrotors.

Helicopter model testing has been conducted in the TDT since 1963, and has generally taken the form of research testing rather than testing in direct support of any specific helicopter development program. Several testbeds have been used for helicopter testing in the TDT (fig. 2). The first (fig. 2a) was built by Lockheed Aircraft Company and was used for testing of hingeless rotor configurations in support of the XH-51 research helicopter development program. A testbed developed by Bell Helicopter Company was used for two-bladed teetering rotor studies (fig. 2b). The Lockheed testbed was later refurbished in-house at Langley and became known as the Generalized Rotor Aeroelastic Model, or GRAM (fig. 2c). This testbed was used for helicopter rotor testing at the TDT until the late 1970s. The current testbed, known as the Aeroelastic Rotor Experimental System, or ARES (fig. 2d), has been used for all helicopter rotor testing in the TDT since 1977. The ARES testbed has been used for investigations involving rotor performance, loads, stability, and acoustics for a number of rotor models. For example, the ARES has been used for the study of conformable rotors to define their potential for altering blade spanwise and azimuthal airload distributions to improve rotor performance and reduce loads. An active control concept known as Higher Harmonic Control (HHC) was tested on the ARES to confirm predictions as to the level of reduction in fixed-system vibration and blade-vortex interaction noise. The ARES testbed has also been used to obtain aeromechanical stability and loads data for hingeless and bearingless rotor models and to validate existing analytical models. The ARES testbed has

* Senior Research Engineer.

† Senior Research Engineer, Associate Fellow AIAA.

Copyright © 2000 by the American Institute of Aeronautics and Astronautics, Inc. No copyright is asserted in the United States under Title 17, U.S. Code. The U.S. Government has a royalty-free license under the copyright claimed herein for Government Purposes. All other rights are reserved by the copyright owner.

also been used for studies to evaluate rotors incorporating advanced technologies that will be needed to meet military requirements for increased mission effectiveness and improved safety and survivability in future helicopters.

Tiltrotor aeroelastic research in the TDT (fig. 3) has been about equally divided between supporting research and development programs. This work has its roots in propeller whirl flutter studies conducted in the TDT in the early 1960s, and some later fundamental studies into the whirl flutter behavior of propellers having flapping blades. Tiltrotor aeroelastic studies began in 1968 in an exploratory parametric investigation of stability, dynamics, and loads using a model of a proposed Bell Helicopter Company tiltrotor design designated the Model 266. In the early 1970s, aerodynamic and flutter clearance tests were conducted in support of the development program that led to the NASA/Army XV-15 tiltrotor research aircraft. During this same period, a parametric investigation of propeller whirl flutter was conducted using an off-design research configuration of a proposed Grumman tiltrotor design. There was a hiatus in tiltrotor research activity at AB from 1974 until 1984, after which tests were conducted on a Bell tiltrotor model in support of the V-22 development program. A second hiatus in tiltrotor research occurred from 1985 to 1994, after which there was a resurgence of tiltrotor activity within AB/TDT, primarily in anticipation of NASA's Short Haul Civil Tiltrotor program. This led to a new tiltrotor research program using a refurbished version of the V-22 model that was tested earlier in the TDT in support of the V-22 program. The refurbished model has been incorporated into a tiltrotor research testbed called the Wing and Rotor Aeroelastic Testing System (WRATS). In collaboration with Bell Helicopter Textron, studies under the current research program are focusing on a range of aeroelastic technical areas that have been identified as having the potential for enhancing the commercial viability of tiltrotor aircraft. In particular, emphasis is being placed on the development of active and passive techniques for vibration control, stability augmentation, and increased aerodynamic performance of tiltrotor aircraft.

Several overviews of TDT aeroelastic research activities have been published over the years (see, for example, refs. 1-9). However, these reviews have either been generic discussions of work conducted in the TDT without any particular emphasis on rotorcraft, or specific to rotorcraft but incomplete with respect to the scope of the work reviewed. The purpose of this paper is to present a complete and unified historical account of AB/TDT aeroelastic research accomplishments that have contributed to rotorcraft technology and devel-

opment since the inception of the TDT in 1960. Relevant ancillary studies contributing to this technology base are also included. The paper begins with a summary of the major characteristics of the TDT and a description of the unique capability offered by the TDT for testing aeroelastic models by virtue of its heavy gas test medium. This is followed by some remarks on the use of scale models in the design and development of rotorcraft vehicles, and a review of the basic scaling relationships important for designing and building dynamic aeroelastic rotorcraft models for testing in the TDT. Helicopter and tiltrotor tests that have been conducted in the TDT are then described in separate sections. In each of these sections, a chronological account of the pertinent work and contributions is given. These discussions include a statement on the objectives of the tests, a photograph and a description of the various models and testbeds used, and illustrative results that characterize the phenomenon (or phenomena) under investigation. Where and when appropriate, an explanation of the pertinent fundamental mechanisms and interactions involved in the phenomena is included in the discussion. Each section concludes with a résumé of current and planned research activities.

Tunnel Characteristics

The Langley Transonic Dynamics Tunnel (TDT) is a single-return, closed-loop, continuous-flow, variable-pressure, slotted-throat wind tunnel having a test section 16-feet square (with cropped corners). An aerial view of the wind tunnel and its adjoining engineering and equipment building is shown in figure 1. A schematic depicting the general arrangement of the tunnel is shown in figure 4. The tunnel uses either air or a heavy gas as the test medium and can operate at total (stagnation) pressures from near vacuum to atmospheric. It has a Mach number range from near zero to about 1.2, with attendant maximum Reynolds numbers of about three million per foot in air to about ten million per foot in heavy gas. Both Mach number and pressure are independently controllable.

The TDT is specially configured for aeroelastic testing. Large windows are provided for close, unobstructed viewing of the model from the control room. A set of four by-pass valves is present in the wind-tunnel circuit to allow quick reduction in the dynamic pressure in the test section in case of model instability. The tunnel fan blades are protected from debris of damaged models by a wire-mesh safety screen. A variety of model mount systems is available. For helicopter testing, stand-mounted testbeds have been used. For tiltrotor testing, stand-mounted, sidewall-mounted, sting-mounted, and rod-mounted models have been

used. The TDT also offers an airstream oscillator system for gust studies. The system consists of an arrangement of biplane vanes located on either side of the tunnel entrance section (fig. 5). Vane frequency and amplitude are adjustable and the two pairs of vanes may be operated either in phase or out of phase to provide vertical or rolling gust fields.

The tunnel was originally constructed as a 19-foot diameter subsonic pressure tunnel in 1938 (ref. 10). In the late 1950s, the facility was converted to a transonic dynamics tunnel to fill the need for a wind tunnel dedicated to the testing of large aeroelastic models of aerospace flight vehicles from low subsonic through transonic speeds. This new aeroelastic testing capability was made possible by using the high-molecular-weight gas R-12 as the test medium (ref. 11). A number of subsequent comparative tests (see, for example, refs. 12-15) confirmed pre-conversion studies as to the soundness of testing aeroelastic models in R-12 instead of air. Environmental concerns raised in the late-1980s regarding the continued widespread use of R-12 led to a NASA decision to replace the R-12 used in the TDT with the environmentally acceptable and essentially equivalent refrigerant R-134a. Conversion of the TDT heavy gas test medium from R-12 to R-134a was completed in 1997 and is described in references 16-17. Subsequent wind tunnel characterization and calibration tests were completed in 1998, after which normal tunnel operations resumed. Because R-12 and R-134a have comparable properties, the primary flow characteristics of the TDT for R-134a operations are not much different from those for R-12, as was expected. For this reason, the advantages of testing in heavy gas will continue with R-134a. However, because the speed of sound in R-134a is slightly higher than in R-12 rotorcraft models tested in R-134a must be operated at higher rotor rotational speeds to maintain Mach scaling.

Since its inception, the TDT has been a unique national facility for testing aeroelastic models of a variety of aircraft, spacecraft, and launch vehicles (see, for example, refs. 1-2). The heavy gas feature of the tunnel (in combination with its large size) offers several advantages over air with respect to designing, building, and testing aeroelastic models. For example, improved model-to-full scale similitude, eased fabrication requirements, lower model vibration frequencies, reduced test section flow velocities, larger test Reynolds numbers, and reduced tunnel power requirements. The size of the test section easily accommodates model rotors up to 10 feet in diameter. More detailed descriptions of the TDT and its capabilities may be found in references 16-17.

Some Remarks on the Use of Scale Models

Aeroelastically-scaled wind-tunnel models have played an important role in the design, development, and verification process in diverse fields of engineering, including aerospace engineering (see, for example, refs. 18-23). Their use is particularly prolific in the field of aeronautics wherein dynamic aeroelastic (i.e., flutter) models are extensively employed both to substantiate that an aircraft design is free of aeroelastic instabilities within its flight envelope, and to validate analyses. Analytical capabilities for addressing aeroelastic design issues of aircraft have improved significantly over the years. However, because aircraft have continued to increase in structural and aerodynamic complexity, the need to rely on wind-tunnel tests of sub-scale models to verify predicted behavior and performance before entering the flight test stage of a development program remains. Such models are also widely used in research investigations dealing with such issues as active control of aeroelastic stability and response, buffet load alleviation, and for the validation of analytical and computational methods used in design.

The importance of sub-scale models for helicopter research has been recognized as early as 1950 (refs. 24-25). However, sub-scale models have also played a valuable, although perhaps less prominent, role in the design and development of helicopters, tiltrotors, and V/STOL aircraft (for example, see refs. 22-23, 26-27). The importance and role of sub-scale models in rotorcraft research and development have been recognized by both government and industry on many occasions. For example, references 28-29 emphasized the importance of a properly conducted wind-tunnel test program that includes both model-scale and full-scale testing to reduce the technical risk of a rotorcraft development program, and to lessen the chance for surprises in the flight test stage.

Model Scaling Considerations

Dynamic aeroelastic models may be classified into two general groups: (1) research models, and (2) prediction models. Research models do not represent any particular aircraft and are at most only broadly representative of full-scale designs. They are used primarily to gain insight into aeroelastic problems (e.g., identify the types of flutter which may be associated with a new or unusual configuration), to provide experimental data for comparison with analysis, and to provide general design information on flutter trends that occur with variations in system parameters. Prediction models are based on actual full-scale designs and are intended to

predict the full-scale behavior of specific aircraft. These models are related to the full-scale designs that they represent by certain scaling relationships. It should be noted that prediction models can also be used effectively as research models.

A model will exhibit similitude or similarity to a full-scale structure provided certain dimensionless ratios have the same values for both. These dimensionless ratios may be determined by dimensional analysis of all the quantities involved in the problem or (if the structure is simple enough) from the differential equations which define the system. The objective of the theory of similitude (refs. 18, 19, 30-32) is to establish those relationships that must be maintained to permit reliable predictions to be made from measured model behavior. Usually, not all dimensionless ratios can be maintained at full-scale values with reasonable choices of materials and scale factors in available test facilities. In such cases, complete similarity cannot be maintained and compromises must be made, based on experience and knowledge of the problem, by which the less important dimensionless ratios are allowed to deviate from full-scale values. Fortunately, a model is usually designed to study only a particular phenomenon (or class of phenomena), in which case only those dimensionless ratios important for the phenomena of interest need be maintained at their full-scale values.

The requirements for achieving dynamic and aeroelastic similitude of model and full-scale aircraft and helicopters are replete in the literature (see, for example, refs. 31-36) and will be reviewed here only briefly as they apply to rotorcraft. As mentioned above, the similarity requirements can be obtained either by applying dimensional analysis to the problem or by examining the appropriate governing equations written in nondimensional form. Application of such procedures results in the identification of the basic independent nondimensional parameters that must have a one-to-one correspondence between model and full scale to ensure adequate representation. For the study of dynamic aeroelasticity and unsteady aerodynamics phenomena, five basic similarity parameters are indicated: Mach number, advance ratio (reduced frequency), Lock number (mass ratio), Reynolds number, and Froude number. The other dependent ratios relating model quantities to full-scale quantities can be derived from these basic similarity parameters. The models must also be geometrically similar to their full-scale equivalents in external shape as well as in their distribution of mass and stiffness. In addition, any important body degrees-of-freedom must be included in the models.

The simultaneous satisfaction of the five similarity parameters noted above is not possible because of conflicting requirements which result for the design of a model. In conventional wind tunnels using atmospheric pressure air as the test medium, only three of the five parameters can be maintained at their full-scale values. For the simulation of flight conditions where compressibility effects are important, it is well established that the full-scale values of Mach number, advance ratio, and Lock number must be maintained in the model. This is true whether the model is to be tested in air or heavy gas. However, if the model is designed for testing in heavy gas, Froude number may be maintained simultaneously with Mach number, advance ratio, and Lock number by selecting an appropriate length scale factor (about .20 to .29 depending on the simulated full-scale altitude). For simulation of flight conditions where compressibility effects are not important models are usually designed to maintain full-scale values of advance ratio, Froude number, and Lock number when tested in air. However, for suitable length scale factors, these models can simultaneously obtain near full-scale values of Mach number when tested in heavy gas. It is generally not possible to simulate full-scale Reynolds number in either the air or heavy gas test mediums of the TDT. However, the use of heavy gas permits a nearly three-fold increase in Reynolds number over comparable conditions in air.

Some of the more important aeroelastic scale factors applicable to rotorcraft models in the TDT are summarized in table 1. Scale factors are tabulated for testing in air, R-12, and R-134a for the cases in which either Mach or Froude number is maintained at its full-scale value in addition to Lock number and advance ratio.

Helicopter Research Contributions

Tests Utilizing the Lockheed Aircraft Testbed

1963 - 1964

The initial model helicopter tests in the TDT were conducted in 1963 and 1964 as part of a cooperative effort between the U. S. Army, Lockheed Aircraft, and NASA to conduct hingeless rotor research investigations (refs. 37-40). The tests were conducted using a 1/3-size hingeless rotor model that was 10 feet in diameter (fig. 2a). The model blades were ballasted to allow testing in R-12 at a density of 0.008 slugs/ft³. A number of configurations were tested resulting in research information that included structural loads and aerodynamic data for all the configurations tested. The 1963 and 1964 tests included rotor configurations with

three, four, and six blades as well as variations in the blade flapwise and chordwise stiffnesses and stiffness distributions. Each configuration was tested through a forward speed and load factor range simulating conventional helicopter and compound helicopter operation (refs. 37-38).

The 1963 test involved only a three-bladed hingeless rotor configuration with matched root stiffness. Testing was conducted at simulated forward speeds from 60 to 240 mph over a range of rotor load factors at advancing tip Mach numbers up to 0.91. Data were obtained for helicopter, unloaded rotor, and compound helicopter modes of operation and indicated a beneficial influence of blade twist on chordwise cyclic loads in forward flight. This rotor was designed to enable wide variations in dynamic characteristics and therefore was not representative of an optimized design. The test in 1964 was conducted using a blade and rotor hub design that was optimized for low drag. The blade flapwise and chordwise stiffnesses were also approximately matched along the blade span. This test involved three-, four-, and six- bladed rotors with the four-bladed configuration considered as the baseline. As in the 1963 test, all configurations were tested over a range of forward speeds and rotor load factors to obtain structural loads and performance data. Results indicated that the optimized rotor design with low chordwise stiffness blades showed considerable promise from the standpoint of structural loads, vibration, and performance. The results of these two hingeless rotor tests were encouraging with regard to the use of hingeless rotor configurations and were of use in the development of the Lockheed XH-51 helicopter.

Tests Utilizing Bell Helicopter Company Testbed

In the late 1960s and into the 1970s, the emphasis in helicopter testing at the TDT was on two-bladed teetering rotor configurations. The tests conducted in this timeframe used 1/4- and 1/5- size teetering rotor models mounted on the testbed developed by Bell Helicopter Company (fig. 2b).

1969

In 1969, a teetering rotor test (ref. 13) was conducted to obtain data to assess three areas of interest: 1) the aerodynamic characteristics of rotors operating at combinations of high advance ratio and high advancing tip Mach number; 2) the feasibility of obtaining rotor structural and aerodynamic loads from a dynamically similar scaled model; and 3) the validity of data obtained in an R-12 atmosphere. This test used a 1/4-size, geometrically and dynamically scaled rotor system representative of those used on Bell Helicopter

Company UH-1C and AH-1G aircraft. An additional 1/4-size model rotor was used that had different twist and airfoil characteristics than the scaled rotor system. Assessment of the wind-tunnel results was made by comparing to existing full-scale wind-tunnel data and full-scale flight data. Comparisons of theoretical calculations with the wind-tunnel data were also made. Results documented in reference 13 show that model and full-scale experimental rotor performance as a function of advance ratio showed no significant trend differences. Comparisons of model and full-scale rotor performance showed good agreement with variations in advancing tip Mach number. Calculated rotor performance trends with advance ratio and with advancing tip Mach number were not found to be in as good agreement with full-scale data as was the wind-tunnel results. Correlation of model and full-scale blade oscillatory loads did not yield the accuracy desired. It was concluded that non-scaled rotor hub impedance and discrepancies in the full-scale blade stiffness values used to produce the model blades probably caused this lack of agreement. Finally, it was concluded that trend correlations showed that full-scale loads could be determined in an R-12 atmosphere using a properly scaled rotor model.

1973

References 15 and 41 document results of a teetering rotor test conducted in 1973 using the same testbed as the 1969 test. This test continued the evaluation of R-12 as a suitable test medium for model helicopter rotors (ref. 15), and investigated the effects of hub in-plane support parameters ("hub impedance") on the chordwise oscillatory loads of a two-bladed teetering rotor (ref. 41). To evaluate the suitability of R-12 as a test medium, the studies involved testing a 1/5-size aeroelastically scaled helicopter rotor in R-12 at the same advance ratios, tip Mach numbers, shaft angles of attack, and collective pitch values as a full-size helicopter rotor tested in air. Reynolds number variations were achieved through controlled R-12 density changes and the use of a wide chord model rotor that was not aeroelastically scaled. Integrated rotor performance from the aeroelastically scaled model rotor provided data trends and magnitudes that agreed well with full-scale rotor data (figs. 6-7) even at the lower values of model Reynolds numbers. An exact match of full-scale rotor Reynolds number was accomplished by utilizing the wide chord model rotor, but with accompanying mismatches in rotor solidity and aeroelastic scaling. Performance results obtained for the full-scale and model-scale rotors are summarized in figure 8. Region B of figure 8 illustrates the expected performance trend with decreasing Reynolds number for the wide chord blade, i.e., more torque required at a given rotor lifting task. An unexpected result of these tests is illustrated

by Region A of figure 8 which shows that better model performance correlation with full-scale values was achieved with a dynamically scaled rotor of the correct solidity than with a rotor that matched Reynolds number but, was not dynamically scaled. It was concluded that Reynolds number effects may be minor in rotor aerodynamic performance testing in comparison to the combined effects of rotor solidity and blade elastic properties.

The determination of the effect of hub inplane support parameters on two-bladed teetering rotor chordwise oscillatory loads consisted of : 1) a shake test to define the impedance of several testbed configurations as a function of frequency, and 2) testing of the configurations in the TDT. Wind-tunnel test results showed that the one-per-rev inplane bending moments could be changed by a factor of two, depending on the testbed configuration, at the same aerodynamic operating condition. The higher harmonic blade loads and pitch link loads were not affected by changes in inplane hub impedance. Additionally, the test results generally substantiated the predicted trends, although differences in the magnitude of the blade bending moments were observed when compared to predicted results. Some of these differences were attributed to the influence of the testbed strain-gage balance or tunnel floor on hub impedance. A definitive reason for the difference between the measured and calculated blade bending moments was not arrived at since neither of these effects were accounted for in the analysis.

Tests Utilizing the GRAM Testbed

In 1974 and 1975 teetering rotor tests were conducted utilizing the GRAM testbed (fig. 2c). These teetering rotor tests (ref. 6) involved a 1/4-size aerodynamically scaled model of a Bell Helicopter Company AH-1G "Cobra" rotor (fig. 9), and two 1/5-size aerodynamically scaled wide-chord rotor configurations, with (fig. 10) and without a mid-span flap hinge (fig. 11).

1974

The purpose of the AH-1G rotor test (ref. 6) was to determine whether two-bladed teetering rotors can experience stall flutter, which is a factor that limits the forward flight speed of articulated rotor configurations. Stall flutter is a phenomenon that is characterized by high oscillatory blade loads at the first torsional frequency of the blade occurring on the retreating side of the rotor disk. Blade loads and rotor performance data were obtained for the AH-1G model rotor up to advance ratios of 0.40. In order to compare the model test conditions with the full-scale aircraft flight envelope, model thrust values for selected test points were converted to full-scale load factors. These results were

plotted on the aircraft flight envelope as shown in figure 12. Based on the comparison with the full-scale load factors in figure 12 it was determined that model data were obtained that corresponded to full-scale thrust values both within and without the aircraft sustained operating envelope. Model thrust data were also obtained outside the sustained operating value of the aircraft, but within the maneuver, or transient, envelope. It should be noted that the model tests did not simulate maneuvers, but rather the model thrust simulated the full-scale thrust required in maneuvering flight. For three of the test points presented in figure 12, the model blade torsional moment waveforms at 45% blade radius are shown for two rotor revolutions. Note that at an advance ratio of 0.2, the torsional waveform at a low thrust condition does not indicate any oscillations on the retreating side of the disk (180 deg. to 360 deg. azimuth) that could be attributable to stall flutter. However, for the higher thrust condition at an advance ratio of 0.2 there are significant torsional oscillations of the model blade on the retreating side of the disk and these oscillations are at the first torsional frequency of the model blade. At an advance ratio of 0.4, the torsional waveform shown corresponds to a maneuver thrust condition for the aircraft, and large torsional oscillations are evident on the retreating side of the rotor disk. The results presented in figure 12 indicate that two-bladed teetering rotors could experience the stall flutter phenomenon experienced by articulated rotor systems. With regard to control system loads, the implications of stall flutter for a teetering rotor may not be as severe as for an articulated rotor since, even for non-stalled conditions, the control system of a teetering rotor must be designed to withstand the typically higher control loads.

1975

The test of the wide-chord teetering rotor (ref. 42) had two purposes. The primary purpose of the test was to evaluate the use of a wide chord blade to increase the aerodynamic performance capabilities of a two-bladed teetering rotor, and to obtain loads data on the wide chord configuration. The secondary purpose of the test was to determine the effectiveness of a mid-span flapping hinge in reducing the flapwise blade loads of the wide-chord blade configuration. Figure 13 shows a comparison of the oscillatory flapwise blade loads as a function of blade radius for the rotor configurations with and without the hinge. As the results in figure 13 show, the mid-span hinge was effective in reducing the oscillatory flapwise bending moments. The hinged rotor was also found to exhibit no tendency to become dynamically unstable, nor were any excessive outboard blade motions about the hinge observed. From an operational point of view, the blades with the

mid-span hinge behaved much like the blades without the hinge.

In addition to testing two-bladed teetering rotor configurations, the GRAM testbed was used in 1975 for testing of a four-bladed flex-hinge rotor configuration (refs. 6 and 43). Figure 14 shows the flex-hinge rotor mounted on the GRAM testbed in the TDT. The flex-hinge rotor was hingeless in the flapping direction, using low bending stiffness flexures to allow blade flapping motions. The blades were hinged in the lead-lag direction with an elastomeric damper used to provide inplane damping and stiffness. This inplane configuration allowed the rotor to behave dynamically as a soft-inplane hingeless rotor. The flex-hinge model had a diameter of 10 feet and was Froude-scaled for operation in air, as opposed to R-12, because the test required a large number of configuration changes. Typically, tests in R-12 required as much as 3 hours of gas handling for each model configuration change. The objectives of the tests were to provide performance, loads, and stability data for the flex-hinge configuration. These data were intended to aid the development and eventual flight test of full-scale hardware by Bell Helicopter Company as part of its internal research and development efforts. Figure 15 shows samples of the flex-hinge rotor performance data obtained at an advance ratio of 0.35. The results in figure 15 are plots of the rotor torque coefficient versus rotor thrust coefficient and rotor lift coefficient versus rotor drag coefficient for three values of rotor shaft angle of attack. Similar performance results were obtained over the intended operational envelope to determine how the flex-hinge rotor could be expected to perform.

A concern for testing of the flex-hinge rotor was whether the configuration would experience the air resonance phenomenon that can occur for soft-inplane hingeless rotors. Air resonance involves coupling between the first blade inplane mode and fuselage pitch and roll modes. In order to examine the stability characteristics of the flex-hinge rotor, an on-line subcritical testing technique (ref. 44-45) was used to determine the frequency and damping in the mode of interest at each test condition. By monitoring the damping as a function of the test parameters the stability boundary may be defined. Although no instabilities were experienced during testing of the flex-hinge rotor, damping trends were obtained to determine an optimum level of damping from both a stability and blade response point of view. Figure 16 shows the trend of damping for the blade lead-lag mode as a function of advance ratio for the nominal damper configuration.

Tests Utilizing the ARES Testbed

In 1977, the ARES testbed (fig. 2d) was put into service at the TDT and has been used since then for all

studies of aeroelastically scaled main-rotor systems. A description of the ARES and associated instrumentation can be found in references 7 and 8. Initial use of the ARES testbed was accompanied by a change in emphasis from the testing of two-bladed teetering rotor configurations to the testing of four-bladed articulated rotor configurations. The initial series of articulated rotor tests was conducted in the late 1970's and early 1980's to investigate conformable rotor configurations. A conformable rotor (refs. 46-50) is intended to use passive means of inducing dynamic twist along a rotor blade to alter unfavorable blade spanwise and azimuthal load distributions to improve rotor performance and reduce vibratory loads. The tests in the TDT investigated the use of tip geometry as a means of inducing rotor blade dynamic twist.

1977

Reference 51 documents the initial TDT test that investigated the use of blade tip geometry to improve rotor performance and reduce loads. This test used model rotor blades that were aeroelastically designed but did not represent any full-scale rotor in production. The blades were originally designed to be Mach-scaled for operation in air, but were converted for operation in R-12 by adding ballast weights that produced the proper Lock number. The tests were conducted at combinations of rotor shaft angle of attack, rotor lift, and rotor advance ratio to evaluate the effects of tip geometries incorporating sweep, taper, and anhedral. Tip geometry changes were made through the use of interchangeable blade tips. Results from this test indicated that the use of tip sweep reduced blade flapwise and chordwise bending moments and torsional moments as well as control system loads, while improving rotor forward flight performance above an advance ratio of 0.30. The use of blade tip anhedral was found to increase blade bending moments while reducing torsional moments. Anhedral was found to improve rotor performance in hover as well as in forward flight up to an advance ratio of 0.30.

1978

In 1978 a test was conducted in the TDT as a follow-up to the 1977 test. The follow-up test used the same model rotor blades as the 1977 test, and was conducted to evaluate the impact of additional tip geometries on the interaction between blade torsional loads and rotor performance. This test is documented in reference 52. The data acquired were evaluated to determine if the tip geometries tested produced the torsional moments required for a successful conformable rotor, i.e., reducing nose-down twist on the advancing side of the rotor disk while avoiding stall on the retreating side of the disk. Results from the test indicated that there

does not appear to be a strong correlation between blade torsional loads and the prediction of rotor performance. It was also determined that reducing the nose-down twist on the advancing blade appeared to be more important to rotor forward flight performance than increasing the nose-down twist on the retreating blade. Reference 52 also includes analytical results that addressed the effect of using uniform and non-uniform inflow models on the correlation between measured rotor torsional loads and performance. It was shown in reference 52 that the nonuniform inflow model more accurately predicted the angle-of-attack environment that would result in the blade torsional moments needed for a successful conformable rotor.

1979

Based on the results of the 1977 and 1978 tests, tests were conducted at the TDT to investigate additional conformable rotor configurations. The 1979 test was conducted to investigate the effects of blade torsional stiffness, tip sweep, and camber on blade dynamic twist as suggested by the analysis described in reference 49. This test (refs. 53-54) used two sets of aeroelastically scaled model rotor blades. The baseline blade set was generally based on the full-scale UH-60A blade design. Blade weight, torsional inertia and flapwise, chordwise and torsional stiffnesses were scaled from UH-60A blade properties although no attempt was made to match the detailed distributions of the full-scale blades. The second blade set was geometrically identical to the baseline blade but incorporated a nominal 4-to-1 reduction in torsional stiffness outboard of the fifty-percent radius station. The blade set with reduced torsional stiffness is referred to as the aeroelastically conformable rotor, or ACR. Each blade set incorporated adjustable trailing edge tabs to allow changes in local pitching moment, as well as the capability to vary the tip geometry outboard of the 89% radial station by using interchangeable blade tips. Data were obtained in R-12 at a nominal density of 0.006 slugs/ft³ at advance ratios from 0.2 to 0.45 and at hover tip Mach numbers of 0.62, 0.65, and 0.68. The results of this test indicated that blade dynamic twist is controllable through blade design. It was shown (fig. 17) that the use of the blade trailing edge tabs produced more elastic twist than either tip sweep or tip anhedral. Blade flapwise, chordwise and torsion loads were found to be reduced, and rotor performance improved for configurations that reduced advancing blade twist. This result is in agreement with results obtained during the 1978 test documented in reference 52. One concern of using blades with reduced torsional stiffness is the possible effect on aircraft stability and control characteristics. The variation of blade torsional response with the application of controls or with airspeed, for example, can affect the rotor contribution to

aircraft stability and control derivatives. However, test results showed that the control inputs required to achieve trim (fig. 18) and the control derivatives of the reduced torsional stiffness configuration were not significantly different from those of the baseline rotor.

1980 to 1983

A second test of an ACR configuration was conducted in the TDT in 1980 (ref. 55). This test used a new set of baseline and ACR model blades. The characteristics of both sets of blades were based on the rotor system of the U.S. Army YAH-64 helicopter, however, the ACR blade torsional stiffness was reduced by a factor of 6, compared to the baseline blade, from 23% radial station to the tip.. The model blades had a chord of 4.24 inches with -8 deg of linear twist over the full blade span and used a NACA 23012 airfoil section. The blade mass and elastic properties had mean values such that Mach, Froude, and Lock scaling from the full-scale blade were correct when tested in an R-12 environment. The test was conducted in R-12 at a density of 0.007134 slugs/ft³, three times standard air density. Both the baseline and ACR blades used a rectangular planform, however, the ACR blade had an interchangeable tip that could be used to introduce 20 deg of sweep over the outboard 8% of the blade span.

The test was conducted to evaluate potential benefits of the ACR concept over a range of advance ratios and rotor thrust conditions. The test was conducted by "flying" the model to an analytically pre-determined trim condition that represented loadings a rotor system must develop in flight to trim a helicopter for steady-state operation. This procedure was followed for both the baseline and ACR blade sets. Sample results from this test are shown in figures 19-20. The results show the performance improvements offered by the ACR configuration with a swept tip at high blade loading values (fig. 19). Figure 20 also indicates reduced flapwise oscillatory bending loads for the ACR configuration compared to the baseline configuration. However, data not presented here indicates that this trend of reduced oscillatory bending loads for the ACR configuration is not always the case at higher advance ratios.

During the conformable rotor tests conducted in the TDT, the aeroelastic mechanism linking rotor configuration performance and loads to blade deflection wasn't always easy to determine. Therefore, tests were conducted in 1981 and 1982 in an effort to understand the coupling between configuration response and the resulting rotor aeroelastic environment. Because earlier conformable rotor studies had indicated the importance of the rotor blade tip geometry in producing the necessary dynamic twist, emphasis was given to parameter changes in this area. Seven blade tip shapes were

tested (ref. 56) on a four-bladed articulated hub using the baseline and ACR blade sets used in the 1979 test (refs. 53-54). The different tip shapes coupled with the different blade torsional stiffnesses of the two blade sets produced significant differences in both performance and loads. Configurations that exhibited low oscillatory loads also had the best performance, while the configurations with poor performance generated the highest loads. Another interesting result of these tests was the strong correlation between azimuthal variation of elastic twist and rotor behavior. As noted in reference 52, the configurations that exhibited small azimuthal activity in elastic twist were the best performers.

The utilization of a conformable rotor concept should be evaluated not only for how successfully it achieves improved performance and reduced loads, but also how well it can be "fielded". That is, how much change, if any, in current installation, maintenance, and rotor tuning is necessary for the rotor concept to be employed. One aspect of this "fielding" process is rotor tracking sensitivity and its implications to rotor and fuselage loads. As part of the conformable rotor studies in the TDT, a rotor track sensitivity investigation was conducted, again using the same blade set as in the 1979 test (refs. 53-54). The blades were subjected to a test matrix that included a perturbation in the track on one blade. This perturbation was accomplished by a deflection of the blade trailing edge tabs. The elastic response of the baseline and ACR torsionally soft blades to tab deflection was correlated with fixed-system loads (ref. 57). The torsionally soft blades were found to respond very differently than the baseline blades to the same tab deflection. As shown in figure 21, the torsional moments for both stiff and soft blades, due to tab deflection, resulted in different blade flapping magnitudes, flapwise loads, and fixed-system vibration. These results indicate a potential coupling of blade torsional deflection, blade oscillatory loads, and fixed-system vibration which results from a high sensitivity of the conformable rotor to practical tracking procedures.

The interest in reducing helicopter fixed-system vibration led to the investigation of the use of active as well as passive means of controlling rotor vibratory loads. These active control tests were conducted in conjunction with the conformable rotor studies and involved the higher harmonic control (HHC) concept of references 58-63. The approach combined HHC experimental studies with the development of control algorithms suitable for real-time implementation of the required control inputs, and presented the first opportunity to evaluate an adaptive control system using optimal control theory for model helicopter vibration re-

duction. The HHC concept involves superimposing fixed-system swashplate motions at the blade passage frequency on the basic collective and cyclic requirements. The phase and amplitude of the HHC inputs are chosen to minimize the blade passage responses transmitted to the fixed-system. Details of the choice of electronic control designs and software can be found in references 60 and 61.

Experimental verification of the HHC concept was conducted during two tests in 1980 using a four-bladed articulated model rotor tested over a range of advance ratios simulating 1g flight with the rotor first harmonic flapping trimmed to the shaft. Data were recorded to quantify the vibratory load levels without the HHC operating. The HHC closed-loop system was then activated and allowed to stabilize. With the controller still operating at its stabilized condition, data were recorded to establish the vibratory responses with higher harmonic control. The success of the HHC in reducing fixed-system vibratory responses is shown in figure 22. Variations in the fixed-system signals with and without the HHC operating indicated substantial control of the fixed-system vibration levels. It should be noted that although the required control inputs are small (less than one degree) the blade and control system loads usually increase with the HHC system operating as shown in figure 23. These experimental studies helped to accelerate the successful application of the HHC concept in a full-scale helicopter flight test described in references 62 and 63.

It has already been noted that the initial helicopter tests in the TDT were conducted to investigate hingeless rotor configurations. Soft in-plane hingeless rotors were of primary interest when two tests, combined with analytical studies, were conducted in 1982 and 1983 to investigate the ground resonance characteristics of these configurations (refs. 64 - 65). These efforts were intended to aid in the identification of an analysis that can be used in both the design and testing phases of hingeless and bearingless rotor development.

The rotor model used for these tests was a soft in-plane hingeless rotor that was not a dynamically scaled representation of a specific aircraft hub, but rather was representative of a typical full-scale design based on Mach number, Lock number, and frequency simulation. The model blades used were fabricated specifically for testing in R-12. The rotor hub (fig. 24) consisted of metal flap and lead-lag flexures each strain-gaged and calibrated to measure motion in those directions. The hub also utilized a mechanical feathering hinge to allow blade pitch motion.

The first generation Comprehensive Analytical Model of Rotorcraft Aerodynamics and Dynamics (CAMRAD) (refs. 66 – 67) computer program was used as the analytical tool for these tests. The structural dynamic model of the rotor included elastic degrees of freedom in flap bending, lead-lag bending, torsion, and a rigid pitch degree of freedom. The blade was represented by a spanwise distribution of mass, flapwise and chordwise bending stiffness and torsion stiffness, and moment of inertia. An estimated structural damping was also included in the rotor data and body characteristics were also included in the CAMRAD model. The rotor blade aerodynamic forces were calculated using lifting line theory and steady two-dimensional airfoil characteristics with corrections for unsteady and three-dimensional flow effects. The degrees of freedom used in the stability analysis were the blade flap and lag motions, the body pitch and roll motions, and rotor dynamic inflow.

Testing was conducted in both hover and forward flight. A sample of the predicted and measured hover results is shown in figure 25 for a blade collective pitch of eight degrees. The predicted and experimental lead-lag frequencies are seen to be in good agreement. The regressing lag mode damping in the fixed-system is also well predicted. An unstable region is indicated near the regressing lag-roll coalescence rotor speed. Due to rotor stress level limitations, the test could not be carried out for rotor speeds above 650 rpm. Figures 26 and 27 present analytical and experimental lead-lag damping results that show the effect of blade droop and pre-cone angles on the damping levels in forward flight. These wind-tunnel tests of a hingeless rotor configuration aided the further development of a satisfactory technique for aeromechanical stability testing at the TDT, as well as identifying an analysis that produced good correlation with experimental results.

1985

In the mid – 1980s the emphasis of helicopter testing in the TDT changed once again to an area referred to as “advanced rotor design studies.” Testing in this area has been continued up to the present time. These tests, like others previously discussed, have focused on improving rotor performance and reducing vibratory loads. The first of these tests was conducted in 1985 in support of a U.S. Army program that was intended to upgrade the UH-60 Blackhawk helicopter. This planned upgrade involved the design and qualification of new main-rotor blades to improve aircraft performance. In support of this effort, the aerodynamic characteristics (airfoil section, planform, twist, and solidity) of an advanced rotor blade were analytically designed at the U.S. Army Aerostructures Directorate, located at Langley Research Center, using the approach described

in reference 68. The advanced blade planform geometry is shown in figure 28. The baseline blades for this investigation were models of the UH-60A rotor (fig. 29) that were used in the conformable rotor studies conducted in 1979. Both the baseline and advanced blade sets were nominally 1/6-size and aeroelastically scaled. The tests were conducted to reduce the risk of full-scale development by providing comparative data between a candidate advanced rotor design and the baseline rotor.

The purpose of this test (ref. 69-70) was to compare the performance and loads characteristics of the baseline and advanced rotor systems. Therefore, each rotor was evaluated at the same nominal test conditions defined by advance ratio, hover tip Mach number, and rotor lift and drag coefficients. The range of advance ratio covered in these tests was from 0.0 to 0.40. Some illustrative rotor performance and fixed-system vibratory loads results are shown in figures 30 and 31, respectively. These results are for a nominal design condition used by the Army, namely, 4000 feet geometric altitude and 95 deg F ambient temperature. The data in figure 30 show the improvement in performance provided by the advanced rotor throughout the speed range for two simulated gross weight conditions. Similar results were obtained for the other simulated gross weight conditions tested. Although the data are not presented here, the advanced rotor also showed performance improvements in hover. Figure 31 shows the 4-per-rev fixed-system vertical loads produced by the baseline and advanced rotor. The data show that the 4-per-rev fixed system loads produced by the advanced rotor are higher than those produced by the baseline rotor throughout the speed range. This trend was consistent for all gross weight conditions tested.

1987

The first helicopter rotor test using a bearingless rotor hub configuration was conducted in the TDT in 1987. The objective of the test described in reference 71 was to investigate the use of a Bell Helicopter Textron rotor structural tailoring concept known as rotor nodalization (refs. 72 - 73) in conjunction with advanced blade aerodynamics and to evaluate rotor blade aerodynamic design methodologies. A nodalized rotor design is intended to cancel the inertial and aerodynamic loads at the rotor hub at a frequency equal to the blade passage frequency (ref. 72). This test was a part of ongoing programs of the U.S. Army and NASA to improve the aerodynamic performance of helicopters and to reduce helicopter vibrations. The model rotor hub used in this investigation was a 1/5-size, four-bladed bearingless hub (fig. 32). Rotor flap, lag, and pitch motions are accommodated by flexural arms that are constructed of fiberglass, extend outward from the

center of rotation, and are pre-coned 2.75 deg upward at their inboard end. Five sets of 1/5-size model blades designed to represent those of an intermediate-weight civil helicopter were used during these tests. Two of the five blade sets were Froude scaled for testing in air at standard density. The remaining three blade sets were Mach scaled for testing in R-12 at a density of 0.006 slugs/ft³, and included a rectangular planform blade and two tapered planform blades. The Froude scale blades tested in air were used to evaluate structural tailoring, while the blades tested in R-12 were used to evaluate the use of structural tailoring in conjunction with advanced blade aerodynamics. The planforms of the Froude scaled blade sets are shown in figure 33 and the planforms of the Mach scaled blades are shown in figure 34.

Each blade set was evaluated at the same nominal test conditions defined by advance ratio, rotor rpm, and rotor lift and drag. The rotor rpm used for all of the test points was 780 rpm. The values of rotor lift and drag used for all five blade sets were chosen to represent an aircraft of 7850 lbs gross weight with an equivalent parasite area of 20.65 ft² operating at 4000 ft geometric altitude and an ambient temperature of 95 deg F. The range of advance ratio covered in this test was from 0.06 to 0.35, which includes the region from transition to high-speed forward flight. Reference 71 documents this test and presents a tabulation of the data pertaining to the evaluation of the structural tailoring concept. These data consist of fixed-system and rotating system vibratory loads measured during the test. No results are presented in reference 71 pertaining to an evaluation of the aerodynamic design methodologies used to create the model rotor blades used in the test.

1988

At the conclusion of the 1987 test, it was determined that insufficient rotor performance data were acquired for the evaluation of the aerodynamic design methodologies. To obtain the required data a test was conducted in 1988 using the Mach scaled model rotor blade sets (fig. 34) tested in 1987. Because structural tailoring was not an issue during this test, the rotor performance data were obtained using an articulated rotor hub instead of the bearingless rotor hub used during the 1987 test. The test was conducted in R-12 and data were acquired in hover and forward flight at advance ratios from 0.10 to 0.45.

Sample hover and forward flight performance results from this test are shown in figures 35 and 36. The hover data presented in figure 35, for a condition of 4000 ft geometric altitude and an ambient temperature of 95 deg F, show that the tapered planform blade re-

quired less rotor torque coefficient over the entire range of rotor lift coefficient than did the rectangular planform blade. Similar results not shown here, for the tapered and rectangular planform blades were also obtained at a condition representative of sea level standard conditions. Figure 36 shows the rotor torque coefficient required versus advance ratio for both the tapered and rectangular planform blades. These data were obtained at rotor lift and drag coefficients representative of a 7850 lb gross weight aircraft with an equivalent parasite area of 20.65 ft² operating at sea level standard conditions. The data in figure 36 show little difference in rotor torque required between the two blade configurations except at advance ratios of 0.15 and 0.35. Although not shown here, it was also determined that as advance ratio was increased to 0.40 and 0.425 the rectangular planform blades attained higher lift and propulsive force coefficients than the tapered blades before encountering high blade loads. However, the tapered planform blades were designed for a maximum advance ratio of 0.36. It should be noted that at this time none of these results have been documented in a formal report.

In 1988, another test of the advanced rotor design developed and tested in 1985 was conducted to investigate a passive method of reducing the 4-per-rev fixed-system vibratory loads. The passive method makes use of concentrated non-structural masses to "tune" the blade, similar to the approach used in reference 74, so that vibratory shear loads transmitted to the fixed-system are reduced. The model blades were aerodynamically identical to the previously tested advanced blades, and were comprised of two major components: an airfoil glove, which had an internal channel centered about its quarter chord; and a steel spar which could be inserted in the channel (fig. 37). The steel spar had 13 cutouts located every 5% of span beginning at the 30% radial station. A tungsten or steel mass could be mounted in any of the cutouts on the steel spar that was then mated with the airfoil glove to form the complete blade assembly. Testing was conducted at advance ratios up to 0.35 at several rotor thrust levels while maintaining constant rotor rotational speed. A sample of the results obtained during these tests is shown in figure 38. Each data point represents the effect of adding a mass equivalent to approximately 10% of the total blade mass at the radial location specified by the abscissa. The results show the 4-per-rev vertical fixed-system loads for a simulated 1g thrust condition (Thrust = 285 lbs model scale) at an advance ratio of 0.35. The results may be compared directly with the baseline condition, in which no insertable masses were installed in the blades, represented by the horizontal line in figure 38. A more thorough description of this

research as well as additional results may be found in references 75 and 76.

1989

A test conducted in 1989, while not dealing strictly with “advanced rotor designs”, evaluated an “advanced” method of addressing rotor blade vortex interaction (BVI) noise. Impulsive BVI noise, due to blade interaction with shed vortices of preceding blades, has been a major focus of rotorcraft acoustics research for a number of years. One noise reduction concept (ref. 77) purported that decreases in blade lift and/or vortex strength at the blade-vortex encounters should reduce the intensity of the interactions and thus the noise produced by the interaction. This idea involves the application of higher harmonic pitch (HHP) to the rotor blades to modify the strengths of the shed vortices and alter the location of the blade vortex interactions (fig. 39). The amplitude and phase of such HHP inputs are important since the strongest BVI occurrences tend to be located within a limited rotor azimuth angle range roughly between 45 deg and 75 deg (ref. 78).

The test was conducted using an articulated, 4-bladed rotor with rectangular blades having NACA 0012 airfoil sections. Because this was the first acoustics test to be conducted in an R-12 test medium, detail flow-noise calibrations were performed in the TDT for both air and R-12. The results reinforced the conclusions that acoustic pressures are readily scaled between test media. Microphone sensitivity questions for R-12 were also addressed by conducting calibrations prior to conducting the wind-tunnel test. The results of these calibrations showed that the microphone response at specific harmonics of blade passage frequency is the same whether the tests were to be conducted in air or R-12. A total of 12 microphones were used for this test, and because of the reverberant character of the TDT test section it was decided not to attempt directivity measurements but to determine only sound power spectra.

Open-loop HHP inputs were superimposed on top of the rotor trim values of collective and cyclic pitch for a broad range of rotor operating conditions while maintaining a constant rotor thrust coefficient. The HHP inputs included 4-per-rev collective pitch inputs, as well as inputs developed to simulate individual blade control. It was found that the application of the HHP inputs could increase or decrease the intensity of the BVI noise depending on the amplitude and phase of the inputs. A sample of the results obtained during these tests is presented in figure 40, showing the potential of using HHP inputs for reducing BVI noise levels. A complete documentation of this effort is presented in reference 79.

1992

Between 1990 and 1992 there were no rotorcraft tests conducted in the TDT because of a moratorium on the use of R-12 due to environmental concerns. When the moratorium was lifted in 1992, a test was conducted to evaluate two advanced rotor blade design concepts that were under development prior to the moratorium. The first concept involved the use of paddle-type tip technology (refs. 80-83) that could be used in future U.S. advanced rotor designs. During this test, data were obtained, using a 4-bladed articulated hub, for both a baseline main-rotor blade and a main-rotor blade with a paddle-type tip. The main-rotor blade with the paddle-type tip has the same planform as that developed under the British Experimental Rotor Program (BERP) but uses different airfoils, and so is referred to as a “BERP-type” blade. The intent of using these two blade sets was to evaluate the effect of the BERP planform geometry on performance and loads, not to conduct an exhaustive study of the BERP concept. The baseline and BERP-type blades (fig. 41) were compared with regard to rotor performance, oscillatory pitch-link loads, and 4-per-rev vertical fixed-system loads. Data were obtained in hover and forward flight over a nominal range of advance ratios from 0.15 to 0.425. Sample performance and loads results are presented in figures 42-45. Results from this test indicate that the BERP-type blade offers no performance improvements in either hover or forward flight, when compared to the baseline rotor. Pitch link oscillatory loads for the BERP-type blade were found to be higher than for the baseline blade, whereas 4-per-rev vertical fixed-system loads are generally lower. A complete documentation of this test is presented in reference 84.

The second concept evaluated during the 1992 test was a configuration that used slotted airfoils in the rotor blade tip region (85% - 100% radius). This configuration, known as the HIMARCS - I (first generation High Maneuverability and Agility Rotor and Control System) was of interest because of the U.S. Army's need for increased helicopter mission effectiveness and improved safety and survivability. The test was conducted using a 4-bladed articulated hub. Four rotor configurations were tested in forward flight at advance ratios from 0.15 to 0.45 and in hover in ground effect. The rotor hover tip Mach number was 0.627, which is representative of a design point of 4000 ft. geometric altitude and an ambient temperature of 95 deg F. The baseline rotor configuration had a conventional single-element airfoil in the tip region. A second rotor configuration had a forward-slotted airfoil with a -6 deg slat, a third configuration had a forward-slotted airfoil with a -10 deg slat, and a fourth configuration had an

aft-slotted airfoil with a 3 deg flap (trailing edge down). These rotor blade configurations are shown in figure 46. Sample performance and normalized loads results from this test are presented in figures 47-50 and indicate that the -6 deg slat configuration offers some performance and loads benefits over the other three configurations at higher rotor lift coefficients. A complete documentation of this test is presented in reference 85.

1995

During the moratorium on the use of R-12 that was imposed between 1990 and 1992 no new research efforts for model hardware development were initiated. Further, declining budgets permitted little latitude for the development of new model hardware. For this reason, in 1995 an in-house model rotor development program was started. The purpose of this program was to determine if elementary, basic research rotor blades could be designed by personnel at the TDT and built in the model shops at Langley. These blades were designed to acquire loads data for correlation with analyses. The design utilized for these blades involved uniform mass and stiffness distributions with values representative of aeroelastically scaled model blades typically tested in heavy gas at the TDT. The blades were rectangular in planform, used NACA 0012 airfoils, and were untwisted. Blade construction used an aluminum spar as the primary load carrying member, foam for the airfoil shape, and a fiberglass outer skin. The aluminum spar was particularly attractive for the attachment of strain-gages for the measurement of blade bending moments and torsion moments. These blades were tested in October 1995 on a 4-bladed articulated hub in both air and R-134a using the ARES testbed. Data were acquired at advance ratios up to 0.35 at moderate rotor lift coefficients before encountering stall problems attributable to the untwisted design. Additional measurements were made in air at higher advance ratios and rotor lift coefficients specifically for the purpose of acquiring rotor stall data for correlation with analyses. While none of these research results have been published, the entire effort was considered useful due to the experience gained in the design and fabrication of aeroelastically scaled model blades. This effort also helped to bridge the gap between the end of testing with R-12 and the initiation of testing in R-134a.

1999

The most recent TDT test of an advanced rotor design concept involved hover testing of a prototype active twist rotor (ATR) blade. Recent analytical and experimental investigations have indicated that piezoelectric active fiber composites (AFC) imbedded in composite rotor blade structures may be capable of

meeting the performance requirements necessary for a useful individual blade control (IBC) system (refs. 86-92). The use of rotor IBC is of interest because active control concepts can be used to address multiple helicopter problem areas such as vibrations, acoustics, and performance. The ATR blade design employs embedded piezoelectric AFC plies to generate dynamic blade twisting. Mathematical models indicate that from one to two degrees of twisting amplitude over a relatively wide frequency bandwidth is possible using the high strain actuation capabilities of AFC plies. Such levels of twist actuation authority are also possible with only modest increases in blade weight and low levels of power consumption. For these reasons, AFC twist actuated helicopter rotor systems have become an important area of research at the TDT.

Investigation of the potential of AFC rotors was initiated with two ATR mathematical modeling efforts. The first of these modeling efforts was performed in collaboration with researchers at the University of Colorado and focused on the development of a simple mathematical model for helicopter rotor blades incorporating active fiber composite plies. The resulting computer implementation of this mathematical model is the Piezoelectric Twist Rotor Analysis (PETRA) (ref. 88), which is ideally suited for conceptual active twist rotor design and optimization studies. The second mathematical modeling effort used the second generation of the Comprehensive Analytical Model of Rotorcraft Aerodynamics and Dynamics (CAMRAD-II) (ref. 93) code. The use of the CAMRAD-II code allowed detailed active twist rotor numerical studies to be conducted using a state-of-the-art rotorcraft aerodynamics and dynamics computer analysis.

The model prototype ATR blade was dynamically scaled and was designed and constructed in a cooperative effort with the Massachusetts Institute of Technology Active Materials and Structures Laboratory (refs. 91-92). The prototype ATR blade utilizes low weight active fiber composites embedded along the blade, which under appropriate electric fields produce controllable twisting in the blade. The prototype ATR blade was tested using a four-bladed articulated hub with three passive structure blades, identical in twist and planform to the prototype ATR blade, mounted on the hub for balance. This rotor configuration was tested at 688 rpm, at collective pitch settings of 0 and 8 degrees in both air and R-134a. Blade actuation was accomplished by sine-dwell signals at a fixed 1kV amplitude. Peak torsional magnitudes were extracted from FFTs of blade strain gage signal time histories. The torsional load amplitude induced by the piezoelectric actuators was found to be essentially the same for both collective pitch values. This indicates that blade

actuation frequency response remains relatively unaffected by rotor thrust conditions; a trend predicted in pretest analytical studies.

Preliminary results of the prototype ATR blade hover test indicate that peak twist magnitudes of about one degree were attainable at full design rotor speed, test medium density, and collective pitch. This level of twist actuation performance is sufficient to produce 70% reductions in fixed-system vibration amplitudes based on CAMRAD-II active twist simulation studies (ref. 92). Endurance of the active fiber composite actuator plies was also found to be acceptable, with only one actuator electrical failure, out of 19 original actuators, encountered over the course of the testing. A complete evaluation of data obtained during this test is underway. A set of four model ATR blades, based on the prototype blade design, is being fabricated with forward flight testing planned for the summer of calendar year 2000.

The final test to be described, also conducted in 1999, was a test intended to acquire data for correlation with analysis. Throughout the descriptions of the helicopter tests conducted in the TDT there has been the recurring theme of reducing fixed-system vibrations. The primary contributor to helicopter vibration is the main rotor. Accurate prediction of main-rotor vibratory loads enables researchers to develop an understanding of the roles played by various design parameters with regard to helicopter vibration (refs. 94 - 95). The prediction of rotor vibratory loads has produced less than satisfactory results over the years. References 96-98 indicate that throughout the 1970s and 1980s the state-of-the-art of rotor loads analyses made successful prediction of rotor loads difficult, particularly for the higher frequency loads which are of primary interest when addressing helicopter vibrations. Reference 99 indicates that the prediction capability of current analyses has not improved greatly from that of 1970's and 1980's technology. The search for analyses that can accurately predict rotor vibratory loads will continue until an analysis is identified that can give a designer confidence that the goal of lower vibration can be met before committing to a costly fabrication process. To aid in the identification of such an analysis, a test was conducted in the TDT to acquire data for comparison with the CAMRAD-II computer code to evaluate the capability of this code to predict rotor performance and vibratory loads.

The model blades used in this test were 0.16-size, aeroelastically scaled representations of advanced main-rotor blades intended as an upgrade for Sikorsky S-61 helicopters used in commercial applications. The blades incorporate a swept, tapered tip and RC-series

airfoils designed at NASA-Langley Research Center (refs. 100 - 101). Figure 51 shows a planform view of the model blades. Unlike the helicopter tests conducted in previous years at the TDT, this test was conducted in the new R-134a test medium using a 5-bladed rotor system. Rotor performance and loads data were acquired in hover and forward flight up to an advance ratio of 0.375. The data were obtained by trimming the model to rotor lift and drag coefficients representative of a 20,000 lb S-61 helicopter operating at sea level standard conditions. The model was operated at a constant rotor speed that produced the nominal required tip Mach number. Experimental data were compared to CAMRAD-II results obtained at the same conditions. Samples of the comparison between experimental and analytical results are shown in figures 52-53. Figure 52 presents the rotor forward flight performance comparison in terms of rotor torque coefficient required versus advance ratio. It should be noted that experimental and analytical results were obtained at advance ratios beyond the capabilities of the full-scale S-61. This was done in order to obtain information on the advanced S-61 blade design over as wide a range of test conditions as possible. Figure 52 shows that the CAMRAD-II results indicate less rotor torque required than the experimental results at advance ratios above 0.125. The reduced rotor torque coefficient indicated by the analysis can be attributed to the use of airfoil data obtained at full-scale values of Reynolds number, while the experimental results were obtained at less than full-scale Reynolds numbers even though a heavy gas test medium was utilized. The analytical results in figure 52 below an advance ratio of 0.125 are attributed to the free-wake model in the analysis not being fully representative of the experimental environment. Figure 53 shows a comparison of the mean flapwise and chordwise blade bending moments and the mean blade torsional moments versus blade radial station at an advance ratio of 0.25. The results in figure 53 indicate the analysis captures the mean bending moment trends along the blade span at this advance ratio, but is not as successful at predicting the mean blade torsional moments. Results not presented here indicate the analysis, using the free wake model, does a good job of predicting the 5-per-rev fixed-system vibratory loads up to an advance ratio of 0.15, but above that advance ratio the correlation between experimental and analytical results is poor. Reduction and analysis of the experimental results from this test will continue along with continued correlation of the experimental and analytical results.

Current/Planned Helicopter Research

Helicopter research in the TDT/AB continues to involve testing of both passive and active rotor configurations, with comprehensive analyses being used in the

design of models and planning of tests. Currently, the emphasis is on continued testing and development of the active twist rotor (ATR) concept with research on additional active controls concepts under consideration. For example, the use of smart materials in the development of a "swashplate-less" rotor system will be of interest in the next few years. Testing of additional high-lift rotor configurations using slotted airfoils is planned for 2001. Continued analysis using CAMRAD-II will be conducted to investigate the role played by various rotor parameters in the reduction of fixed-system vibration. It is hoped that additional testing will also be conducted in support of the efforts using CAMRAD-II.

Tiltrotor Research Contributions

The Bell/Boeing V-22 Osprey (fig. 54) which is being built for the U. S. Military is a tiltrotor aircraft combining the versatility of a helicopter with the range and speed of a turboprop airplane. The V-22 represents a tiltrotor lineage that goes back fifty years, during which time contributions to the technology base needed for its development were made by both government and industry. NASA-Langley Research Center has made substantial contributions to tiltrotor technology and development in several areas, in particular in the area of aeroelasticity. The purpose of this section of the paper is to present a chronological summary of the tiltrotor aeroelastic research conducted in the TDT by the Aeroelasticity Branch that has contributed to that technology.

Tiltrotor aeroelastic research in the TDT formally began in 1968, but its roots actually extend back to 1960 when an extensive test program was initiated to study the phenomenon of propeller whirl flutter. A brief review of these early studies that are relevant to the subject area is presented first. This work includes the whirl flutter studies conducted initially for conventional propellers, then for propellers having blades with flapping hinges, and finally for high-bypass-ratio ducted fan-jet engines. The major portion of this section addresses the tiltrotor aeroelastic studies which were conducted later, first (1968-1974) in support of the program which led to the XV-15 tiltrotor research aircraft, then (1984-1985) in support of the V-22 tiltrotor aircraft development program, and finally (1994-present) as part of Langley's base research in tiltrotor aeroelasticity. The development of essential computer programs for aeroelastic stability and response analyses of tiltrotor aircraft was initiated in 1970 and has proceeded concurrently with the experimental studies (table 2). Illustrative results obtained from these wind-tunnel tests as well as companion analyses are pre-

sented and discussed. The section concludes with a résumé of current and planned research activities in tiltrotor aeroelasticity.

Relevant Early Work

Propeller Whirl Flutter

Propeller whirl flutter is a self-excited whirling instability that can occur in a flexibly-mounted aircraft propeller-engine combination. The possibility that such an instability might occur was first mentioned as early as 1938. However, the very large margins of safety prevalent at that time and in later years resulted in the phenomenon being accorded only academic interest. In particular, the instability was studied extensively at Rensselaer Polytechnic Institute in the early 1950s by Professor Robert H. Scanlan and his group. The instability remained of academic interest until 1960 when it became of practical concern following the loss of two Lockheed Electra aircraft in fatal accidents. Extensive studies were conducted in the TDT on a 1/8-scale, full-span, dynamic aeroelastic model of the subject aircraft (fig. 55) as part of a national investigation into identifying the cause of the accidents. The TDT studies showed that propeller whirl flutter was possible if the engine support stiffnesses were sufficiently reduced, say due to damage (refs. 102-103). The initial propeller whirl flutter analyses were also developed at this time (refs. 104-105). Following wind-tunnel tests of the Electra model, a more general investigation of propeller whirl flutter was initiated with the aim of identifying and studying the pertinent parameters influencing the phenomenon and to obtain data for verifying analyses. The first study (ref. 106) involved a model of an isolated propeller/pylon/engine system mounted with flexibility in pitch and yaw on a rigid sting support structure (fig. 56). The second study (ref. 107) employed the propeller of reference 106 mounted on a cantilever semispan wing (fig. 57) to determine the effects of a flexible wing on whirl flutter. Reference 107 also extended the analyses of references 104-105 to include the fundamental bending and torsion degrees of freedom of the wing.

Tests of the Electra model, and the ensuing whirl flutter tests of propeller/pylon and propeller/pylon/wing components from the complete model, were the first significant series of flutter tests of a real aircraft to be conducted in the newly-constructed TDT. The experimental studies on the Electra model clearly identified propeller whirl flutter as the most likely culprit in the accidents and pointed the way to the necessary structural changes that needed to be made in the aircraft to preclude whirl flutter. These studies also established the initial credibility of the TDT as a

unique national facility for testing large flutter models. The experimental and analytical studies conducted on isolated components from the Electra model resulted in a wealth of new information on important design parameters influencing the whirl flutter phenomenon and established in the open literature a large database for validation of analyses.

Whirl Flutter of Flapping-Blade Propellers

Several V/STOL aircraft concepts based on the use of propellers having blades which had a hinge at their root to permit flapping motion out of the plane of rotation were proposed as research vehicles in the 1960s, some reaching flight test status. These included the Grumman proposal in the Tri-Service VTOL Transport Competition, the Vertol VZ-2 built for the Army, and the Kaman K-16B amphibian built for the Navy. Because of the attention that was being directed to propeller whirl flutter, it became of interest to consider the manner in which whirl flutter might be altered by the use of hinged blades (ref. 108). Experimental studies using small models (all having propeller diameters of about one foot) were conducted by researchers in government, industry, and academia. These studies showed that either backward or forward whirl flutter could occur for propellers having blades with flapping hinges, in contrast to propellers with fixed blades that flutter only in the backward whirl mode. In parallel with these experimental studies, several researchers extended conventional propeller whirl flutter analyses to include the blade flapping degree of freedom. The whirl flutter equations for propellers with hinged blades developed by Richardson and Naylor (ref. 109) appeared in the open literature at about this time and were used by several researchers, including those in AB. However, none of the analyses that were developed was able to successfully predict the forward whirl instabilities that were obtained experimentally (ref. 110).

The low-speed model tested and studied by AB researchers is shown in figure 58. It consisted of a windmilling propeller mounted on a spring-restrained rod that could rotate in pitch and yaw about a set of gimbal axes behind the propeller. The (symmetric) stiffness could be controlled by varying the tension in a spring connected axially at the other end of the rod. Each blade was attached to the hub by means of two pins, such that when both pins were in position the blades were fixed (fig. 58a); and when one of the pins was removed the other pin became a flapping hinge (fig. 58b). The hub geometry was such that hinge offsets of 8% and 13% could be set. Testing was conducted in both a working model of the Langley Full-Scale Tunnel and the Langley 12-foot Low-Speed Wind Tunnel. Analysis predicted the backward whirl

flutter that occurred for the fixed and 13% hinge offset cases but failed to predict the forward whirl flutter that occurred for the 8% hinge offset case. Similar difficulties were being experienced by other researchers in predicting forward whirl flutter on their models. The inability of analyses to predict the forward whirl flutter behavior observed in tests of these model propellers caused considerable dismay in the analysis community. This concern was formally expressed by Eugene Baird of Grumman Aircraft at a meeting of the Aerospace Flutter and Dynamics Council in November 1969. In prepared comments made to the Council summarizing the state of affairs, Baird questioned whether prop rotor whirl flutter could be predicted with confidence and asked that NASA-Langley look into the issue. The predictability question was settled in 1971 by tests conducted in the TDT using a research configuration of a Grumman tiltrotor model, the results of which are discussed in a later section.

Whirl Flutter of Turbofan Engines

In the mid-1960s, high-bypass-ratio turbofan jet engines were being developed for the Boeing 747 and Lockheed C-5A. These engines are characterized by a large-diameter ducted fan ahead of the engine nacelle. Because of the large gyroscopic and aerodynamic forces acting on the fan, it was thought that a flexibly mounted engine could be susceptible to whirl-type instability analogous to propeller whirl flutter. Preliminary studies to explore the possibility of whirl flutter in such engines were conducted by AB researchers in 1966-68. The initial studies used the low-speed model shown in figure 59. The model employed a windmilling fan inside a duct that was mounted on a sting and elastically restrained with freedom to oscillate in pitch and yaw about a set of gimbal axes located behind the fan. A range of duct chord-to-diameter ratios, restraint stiffnesses, and gimbal axis locations were investigated experimentally (in the Langley 12-foot Low-Speed Wind Tunnel) and the results compared with analysis. Static and dynamic stability derivatives of importance to whirl flutter were also measured. An existing three-dimensional theory for computing the static derivatives of ducted propellers at angle of attack was extended under contract to include the calculation of the important dynamic derivatives. The resulting quasi-static analysis using measured derivatives was found to give good agreement with the measured instability boundaries. The results of this investigation are summarized in a Langley internal report (Rao, K. V. K.: *A Preliminary Investigation of Whirl-Flutter Characteristics of High By-Pass Ratio Ducted Fan-Jet Engines*. LWP 523, 1967).

Some limited testing was conducted later by the second author in the Langley 8-foot Transonic Pressure

Tunnel using the high-speed engine model shown in figure 60 to measure the static stability derivatives at full-scale Mach numbers. The engine was mounted on a six-component balance that was attached to the end of a cantilevered wing. A balsa wood aerodynamic fairing fixed to the wing tip surrounded the balance and its fittings. The extended theory mentioned above and the derivatives measured on the high-speed model were applied to a typical set of full-scale nacelle parameters but using a reduced value of nacelle-pylon support stiffness to approximate a partially failed structural condition. The calculated stability boundaries, taken from reference 111, are shown in figure 61. The velocities associated with the two instability boundaries, whirl flutter and static divergence, are shown in the figure as a function of cowl-length-to-diameter ratio. In spite of the lowered support stiffness assumed in the calculations, both stability boundaries are at relatively high velocities. These results suggested that whirl flutter of high-bypass-ratio fan-jet engines as (then) being planned for the 747 and C-5A should not be a serious problem. The results also indicated that relatively simple whirl flutter analyses using measured stability derivatives are probably adequate.

Tiltrotor Aeroelastic Research

Preparatory Remarks

A number of essential aeroelastic analyses have been developed and implemented into computer programs by Aeroelasticity Branch researchers, either in support of the tiltrotor testing in the TDT or as part of broader studies being conducted by the Branch. Because several of these programs will be mentioned by name and results obtained from them will be shown in this section of the paper, a brief summary of these aeroelastic analyses is appropriate before beginning discussion of the tests. In addition, due to the significant role played by proprotor-induced aerodynamic forces on all facets of tiltrotor aircraft stability, a brief comment on these forces here would aid in understanding the stability results to be presented.

Aeroelastic Analysis Development: The development of tiltrotor aeroelastic analyses at AB has proceeded along the lines indicated in table 2. Most of the analytical work encompassed the periods during which testing was being conducted in the TDT. The initial phase of the analytical development (1970-72) was intended to support the experimental work being done in the TDT at that time in support of what would become the XV-15, as well as to serve as part of a Ph.D. dissertation (ref. 112). The second phase (1973-74) involved some enhancements and extensions to the codes developed during the initial phase as a prelude to the

phasing out of this research area by the Branch. Several major extensions and enhancements to the stability code were made in the period 1984-85 to provide analysis support both during and after the tests conducted on a V-22 flutter model in the TDT. The latest phase of aeroelastic analysis development began in 1991. The development during 1991-93 was primarily intended for a Ph.D. dissertation (ref. 113). However, this analytical work was continued, and several other analyses were initiated later, in support of the new tiltrotor research program initiated within the AB in 1994.

Programs PRSTAB1 - PRSTAB9 are a series of linear stability analysis codes of increasing dynamic and aerodynamic complexity in the rotor modeling, all of which are based on a lumped mass-spring-damper representation of the wing structure. The analysis on which PRSTAB6 is based is described in reference 112. HFORCE1 is a code for computing rotor oscillatory force and moment derivatives due to shaft pitching oscillations. GUST1 is a version of HFORCE1 that includes a vertical sinusoidal gust in the computation of the rotor hub oscillatory inplane shear forces. ROTDER1 - ROTDER4 are codes for computing rotor oscillatory flapping derivatives due to shaft pitching oscillations. The analytical bases of programs HFORCE1 and ROTDER4 are described in reference 112. The lumped parameter model of the wing in PRSTAB9 was replaced by a modal model in 1984 and the new program called PASTA1 (Proprotor Aeroelastic STability Analysis, version 1.0). PASTA2 and 3 were extensions of PASTA1 to include first a blade coning hinge (1984) and then an airplane rigid-body stability analysis capability (1985). A PC version of PASTA3 was developed in 1987. Several upgrades of the PC version of the code were made in 1995-96. Major enhancements made at that time include: engine gyroscopic effects, improved treatment of airframe support springs for representing spring-supported wind-tunnel models, addition of a five-degree-of-freedom drive system dynamic model, provision for reading in externally-computed (MSC/NASTRAN) quasi-steady generalized aerodynamic force matrices for the wing elastic modes, and the QZ algorithm for solving the generalized matrix eigenvalue problem. PASTA4.1 is the most recent version of the code that is available for public distribution. This is also the version that is typically used in AB. A MATLAB version of PASTA4.1 was developed in 1998.

PASTA4.1 is a code for the aeroelastic and rigid-body stability analysis of a tiltrotor aircraft in the airplane mode of flight. The analysis is based on a ten-degree-of-freedom linear mathematical model of the rotor and drive system. The rotor is assumed to be

windmilling (i.e., non-thrusting) but perturbations in the rotor rotational speed can be mechanically coupled to the airframe through the torsional dynamics of the drive system. The blades are assumed to undergo rigid flapping motion due to both the gimbal action of the hub and an offset coning hinge. The blades are also assumed to execute rigid lead-lag motion about a virtual lag hinge. Quasi-steady strip-theory aerodynamics is employed for the blade airloading. Compressibility effects are introduced using a Ribner Mach number correction that is applied to the blade lift curve slope. A modal representation is employed for the airframe (up to ten modes). Either full-span or semi-span configurations can be treated. The aerodynamic forces acting on the airframe rigid-body modes are expressed in terms of stability derivatives. No airloads are assumed to be acting on the wing elastic modes. Stability is determined by examining the eigenvalues that are obtained by solving the system equations as a matrix eigenvalue problem.

UMARC/G is a general-purpose aeroelastic analysis applicable to tiltrotor aircraft operating in the helicopter, conversion and airplane modes of flight that was the subject of a Ph.D. dissertation (ref. 113). It is an extensive modification of a helicopter analysis called UMARC (University of Maryland Advanced Rotorcraft Code) developed at the University of Maryland. A finite-element methodology using anisotropic beam elements is employed for structurally modeling the rotor blades and the wings. Quasi-steady aerodynamics are assumed for the wing airloading. Either quasi-steady or Leishman unsteady aerodynamics can be employed for the blade airloads. The rotor wake can either be prescribed or treated as a free-wake using either the Scully or Baigai wake models. The resulting nonlinear equations are linearized about a trim solution that is calculated using a time-finite-element method. Stability is determined by solving for the eigenvalues of the matrix that results by applying either the constant coefficient approximation or Floquet theory to the linear perturbation equations with periodic coefficients. Blade loads can also be calculated as part of the trim solution. UMARC/G is currently being extended as part of a Ph.D. investigation to include aerodynamic interaction effects between the rotor and the wing, and a drive train dynamics model including the rotor speed perturbation (ref. 114). UMARC/S is the Sikorsky Aircraft version of UMARC/G that has been modified to analyze the variable diameter tiltrotor (VDTR), a Sikorsky concept aimed at improving the tiltrotor's performance in the helicopter and airplane modes of flight (refs. 115-116).

MBDyn is a multi-body code that is under development at the *Dipartimento di Ingegneria Aero-*

spaziale of the Politecnico di Milano, Italy. MBDyn is intended to be a general-purpose tool for the multidisciplinary analysis of complex aerospace systems. Extensions of the analysis and the code to tiltrotor configurations were begun by a Ph.D. candidate from the university while he was in residence at AB during the summer of 1998. Since that time, a number of applications of that code have been made to the Wing and Rotor Aeroelastic Testing System (WRATS) testbed (refs. 117-119).

Rotor-Induced Aerodynamic Forces: Disturbances occurring in flight can, depending on their frequency content, excite either the elastic or rigid-body modes of an aircraft in an oscillatory manner. For a tiltrotor aircraft, any motions of this type effectively represent oscillatory motions of the prop rotor shaft in space. This leads to prop rotor-generated forces and moments that are a function of these oscillatory motions (ref. 112). Figure 62 shows the perturbation rotor aerodynamic forces acting on an aircraft executing small pitching and yawing motions when operating in an airplane mode of flight. From the position of these forces on the aircraft, it is clear that the forces shown can influence aircraft longitudinal and lateral-directional stability. However, the shear forces H and Y can, quite independently of any rigid-body motions, also destabilize the prop rotor-pylon-wing system aeroelastically. In fact, it is precisely these forces that are the drivers for prop rotor-pylon whirl flutter. Propeller whirl flutter, on the other hand, is driven by aerodynamic cross-stiffness moments. A discussion of these and other important differences in the aeromechanical behavior of propellers and prop rotors is given in reference 112.

Bell Model 266

In 1965, the U. S. Army started the Composite Aircraft Program with the objective of producing a rotary-wing research vehicle combining the characteristics of an airplane and a helicopter. Bell Helicopter Company proposed a tiltrotor design designated the Model 266 (fig. 63) and was awarded one of the two exploratory definition contracts which were let under the program. The design features a three-bladed prop rotor with highly-twisted blades that are rigidly attached to a hub assembly that is gimbal-mounted to the mast. Hub flapping restraint is employed to increase control power when operating in the helicopter mode. Three degrees of precone is built into the pitch axis of each blade to ensure blade pitch-lag stability. The prop rotor is designed so that the blade lowest inplane natural frequency remains well above the rotor rpm over the entire operating range, thus precluding mechanical (ground resonance) instability. The blades have a built-in structural twist of -27.7° . A blade root cuff

extending from the hub to 30% blade radius results in an overall aerodynamic twist of -43.5° . Blade kinematic (mechanical) pitch-flap coupling (δ_3) is employed to reduce flapping in maneuvers and gusts when operating in the airplane mode of flight. Positive pitch-flap coupling (negative δ_3) was selected for the Model 266 rather than the more conventional use of negative pitch-flap coupling (positive δ_3) to preclude blade flap-lag instability (ref. 120). The value of positive pitch-flap coupling used on the Model 266 ($\delta_3 = -22.5^\circ$) lowers the blade rigid-body flapping frequency below one-per-rev (1P), and as the inflow angle increases with airspeed the frequency is further decreased. This ensures an adequate separation of this mode from the blade inplane mode whose frequency is also decreasing with airspeed, thus preventing the coupling necessary for a flap-lag instability. The Model 266 wing is designed to be soft in bending (the fundamental cantilevered vertical and fore-and-aft bending (beam and chord) mode frequencies are below 1P) but stiff in torsion (torsion mode frequency is above 1P).

A 1/7.5-scale semi-span model that is a dynamic and aeroelastic representation of the Model 266 proprotor, pylon and wing was built by Bell in support of their studies. When the program was terminated in 1967, the model was given to the Aeroelasticity Branch by the Army. Both NASA and Bell were interested in continuing the experimental work initiated by Bell with the model to further define the aeroelastic and dynamic characteristics of proprotor-type aircraft. This common interest led to a joint NASA/Bell investigation in the TDT of proprotor stability, dynamics, and loads using the model in September 1968. The model is shown in airplane and conversion modes in figures 64 and 65, respectively. The model was Froude-scaled for operation in air and could be run with the proprotor either powered or windmilling. The model proprotor has a diameter of 5.1 feet. For windmilling operation the rotor rpm was controlled remotely by adjusting blade collective pitch. The rotor was disconnected from the drive train when windmilling to reduce wear on the bearings. A close-up view of the pylon with its spinner and aerodynamic fairings removed is shown in figure 66. Scale factors pertinent to the model are given in table 3. Since the high-speed (airplane) mode of flight is critical insofar as proprotor-ptylon instability is concerned, most of the effort was devoted to investigating the airplane mode of flight with the pylon fully converted forward and the airflow passing axially through the rotor.

Some results pertaining to stability and gust response while operating in an airplane mode with a windmilling proprotor are shown in figures 67-71,

where equivalent full-scale values are given. The effects of several system parameters on stability over the design rpm range of the Model 266 are shown in figure 67. The calculated stability boundaries shown were obtained using program PRSTAB6. Figure 67 shows that, with respect to the stability boundary of the reference configuration, altitude is stabilizing, increased pylon yaw flexibility is destabilizing, and both hub flapping restraint and wing aerodynamics are stabilizing. The wing beam mode (consisting primarily of wing vertical bending) was the system mode that went unstable in all of the cases shown. Figures 68 and 69 provide an indication of the relative degree to which stability of the wing beam mode is affected by rotor-induced aerodynamic forces and wing aerodynamics. The calculated results were computed using program PRSTAB8. Figure 68 illustrates the dominant role played by rotor aerodynamic forces in the balance of forces leading to flutter of the proprotor-ptylon-wing system. Figures 68 and 69 show that wing aerodynamic forces have only a slight stabilizing effect. The calculated results in figure 69 also show the stabilizing effects of blade inplane flexibility. The sharp rise in the damping at about 170 kt in figure 69 is associated with the coupling of the blade inplane (lag) bending mode with the wing vertical bending (beam) mode. The dynamic response characteristics of the model due to excitation by a vertical sinusoidal gust that was generated by the TDT airstream oscillator (fig. 5) were also studied. The measured variation of gust-induced angle of attack versus vane oscillation frequency is shown in figure 70, where the quantities have been normalized as indicated to make them independent of vane amplitude and airspeed. These data were measured using a flow direction transmitter that was mounted at the upstream end of a boom extending from the nose of the model as seen in figure 65. Some results showing the variation of wing vertical bending moment with gust frequency for the rotor-on and rotor-off conditions are shown in figure 71. Calculated results were obtained with program GUST1 using the gust curve of figure 70. It is clear that proprotors operating at advance ratios typical of airplane mode flight are quite sensitive to vertical gusts.

The results of this wind tunnel investigation as well as companion analytical studies that were conducted are described in references 112, 121, and 122. Reference 112, in particular, contains the results of an extensive analytical parametric investigation into the effects of several important system design parameters on stability.

Bell Model 266 - Folding Proprotor Variant

A joint NASA/Bell/Air Force test was conducted in the TDT in January 1970 to investigate any potential

problem areas associated with the folding proprotor variant of the tiltrotor concept. The model used in this study was the same model employed in the previous investigation, but modified to include a collective drive motor that permitted rapid feathering and unfeathering of the proprotor and a manually adjustable blade folding hinge (figs. 72 and 73). The main objectives of the test were to investigate stability in the airplane mode of flight at low (including zero) rotor rotational speeds, during rotor stopping and starting, and during blade folding. The rotor was unpowered for this test. The stability boundary obtained for one of the configurations tested is shown in figure 74, where equivalent full-scale values are shown. The variation of flutter airspeed with rotor rpm as rpm is reduced from its maximum design value to zero is shown. As indicated in the figure, the model experienced several different modes of instability as rpm was reduced. The instability experienced at low and zero rpm was unexpected as no pretest predictions were made at those rpm. Based on analytical studies conducted after the test to gain an understanding of the phenomenon, it was concluded that blade precone was the primary cause of the instability (refs. 112, 122). The subcritical response through flutter for the 172 rpm condition is shown in figure 75 where, in addition to the measured wing beam mode damping and frequency, the calculated variation of both the wing beam and low-frequency rotor flapping modes is shown. These results indicate a changeover from a dominant (least stable) wing beam mode to a dominant (least stable) rotor flapping mode as airspeed is increased. The effect of the blade flapping degree of freedom on stability is illustrated in figure 76, which compares the wing beam mode damping versus airspeed at 300 rpm for flapping locked and unlocked. Stability calculations were made using program PRSTAB6.

The variation of steady-state one-per-rev blade flapping response with rotor rotational speed for a (nominally) constant shaft angle-of-attack is shown in figure 77. These data were taken to establish a steady-state flapping response baseline for evaluating the transient flapping response during the rotor feathering portion of the test (ref. 123). The calculated results shown were obtained using program ROTDER4. The peak in the flapping response occurs when the rotor rotational speed is in resonance with the blade flapping natural frequency in the rotating system.

Bell Model 300-A1A

In 1968, Bell Helicopter initiated an in-house development program for a tiltrotor aircraft designated the Model 300 that would ultimately evolve into the XV-15. This design, like the Model 266, features a three-bladed proprotor with highly-twisted blades that

are rigidly attached to a hub assembly that is gimbal-mounted to the mast. Hub flapping restraint is employed to increase control power when operating in the helicopter mode. Blade precone is 2.5° and $\delta_3 = -15^\circ$.

The blade first inplane natural frequency again is well above the rotor rpm, thus precluding ground resonance instability. The cantilevered wing beam and chord mode frequencies are well below 1P but the torsion mode frequency is only slightly below 1P. In support of this aircraft design activity, Bell designed and built a 1/5-scale, full-span dynamic aeroelastic model for testing on a vertical rod mount in the TDT. The model was Froude scaled for air because of testing that was to be conducted in the LTV Low-Speed Wind Tunnel before coming to the TDT for flutter clearance testing. However, the model was sized so that it would also be Mach scaled when tested in R-12 (recall discussion in Model Scaling Considerations section). The model proprotor had a diameter of five feet. Scale factors for the model are given in table 4.

The Bell Model 300-A1A was tested in the TDT in August 1970 (fig. 78). This test was intended to be the required flutter clearance demonstration for the aircraft over its simulated flight envelope. However, unexpectedly poor lateral-directional flying qualities exhibited by the model during the test precluded the conduct of a flutter clearance test. The test convinced Bell to change the design of the tail from a single-vertical-tail configuration to an H-tail configuration (ref. 124).

Grumman Helicat

A joint NASA/Grumman investigation of a 1/4.5-scale semi-span model (fig. 79) of a Grumman tiltrotor design called Helicat was conducted in two entries in the TDT during February/March 1971. The Helicat design featured a stiff (strut-supported) wing that resulted in the wing beam, chord and torsion mode frequencies all being well above 1P. The three-bladed proprotor had blades with 5% offset flapping hinges and positive δ_3 (30°). The blades were also stiff-inplane so that their first inplane natural frequency was well above rotor rpm. The model was targeted for flutter clearance testing in the TDT and thus was Mach scaled for R-12. However, the model was sized so that it would also be Froude scaled if tested in R-12 (recall discussion in Model Scaling Considerations section). The model proprotor had a diameter of 4.9 feet. Scale factors for the model are listed in table 5.

A blade flap-lag instability that destroyed one blade and damaged another occurred unexpectedly during an early checkout run of the model in air. It was found that the model blades were considerably softer inplane than expected and this, in combination with the value

of positive δ_3 used, led to a coalescence of the blade flap and lag natural frequencies with increasing airspeed and the resulting instability (ref. 120). The model was repaired, the design value of δ_3 reduced from $+30^\circ$ to $+20^\circ$, and a flutter clearance test conducted in the second (March) entry without incident (ref. 125).

During the second entry, an off-design research configuration of the model (fig. 80) was employed in an extensive investigation of prop rotor whirl flutter. This portion of the test was aimed at establishing the whirl flutter database needed to respond to Gene Baird's 1969 challenge of resolving the whirl flutter predictability issue. A range of pylon pitch and yaw stiffnesses, blade hinge offsets, and blade kinematic pitch-flap couplings were investigated over a wide range of windmilling advance ratios in air. To obtain flutter at low tunnel speeds, a reduced-stiffness pylon-to-wing-tip restraint mechanism (fig. 81) that permitted independent variations in pylon pitch and yaw stiffness was employed. The restraint was sufficiently soft so that the wing was effectively rigid. Fifty cases of forward whirl flutter and 26 cases of backward whirl flutter were clearly identified (ref. 126). Some whirl flutter results from reference 126 showing the effect of pitch-flap coupling (δ_3) on stability of a symmetric pylon configuration are given in figure 82, where the flutter advance ratio, $V_F / \Omega R$, is plotted versus pylon frequency nondimensionalized by the rotor speed. For the cases shown, all flutter occurred in the forward whirl mode, except for the two points denoted by the solid symbols, which were in the backward whirl mode. The calculated results were obtained using program PRSTAB5. The measured whirl flutter characteristics (flutter speed and frequency, direction of pylon whirl, and pylon yaw-to-pitch amplitude ratio and phase angle) were in excellent agreement with predictions from two different four-degree-of-freedom linear stability analyses (PRSTAB5 and ref. 109) for all of the configurations tested (ref. 126). This study clearly demonstrated that prop rotor whirl flutter, both backward and forward, can be predicted with confidence using linear analyses based on relatively simple math models and quasi-steady strip-theory aerodynamics for the blade airloads.

Aerodynamic Test of Bell Model 300-A2A

A joint NASA/Bell investigation employing a 1/5-scale full-span sting-mounted aerodynamic (force) model of the Bell Model 300 with the new H-tail (designated the Model 300-A2A) was conducted in the TDT in August 1971 for the purpose of determining the longitudinal and lateral static stability and control characteristics and establishing the effect of the prop rotors

(windmilling only) on the basic airframe characteristics. The model is shown in figure 83. The rotors used on this model were the same ones used on the aeroelastic model. Use of R-12 permitted testing at full-scale Mach numbers and near full-scale Reynolds numbers (ref. 124). Blade flapping was measured in both air and R-12 for several values of tunnel airspeed over a range of sting pitch angles. The resulting flapping derivatives are shown in figure 84. Since the range of inflow (advance) ratios over which the derivatives were measured was the same in air and R-12, and the test medium density at the simulated condition was about the same, an indication of the effects of Mach number on the flapping derivatives can be obtained by comparing the air and R-12 results. The drag rise associated with operating at high Mach numbers is seen to reduce flapping as Mach number is increased. The calculated results shown were obtained using program ROTDER4.

Flutter Clearance Test of Bell Model 300-A2A

The 1/5-scale full-span rod-mounted aeroelastic model of the Bell Model 300 with the new H-tail was tested in the TDT in March 1972 (fig. 85). The objective of the test was to demonstrate that the design had the required flutter margin of safety and to confirm that the aircraft rigid-body modes were adequately damped over the simulated flight envelope (ref. 127). Aeroelastic and flight mode stability were assessed in both R-12 and air over the simulated flight envelope with windmilling prop rotors. The Model 300 was shown to be flutter free up through the $1.2 V_L$ requirement of the aircraft and to exhibit good flight mode stability beyond the V_L requirement of the aircraft. A cursory investigation of the autorotational characteristics of the model was also conducted (fig. 86).

During this test, the importance of rotor "thrust damping" (forces T in figure 62) on stability of the Dutch Roll mode was dramatically demonstrated when the rotor interconnect shaft broke and the model went into a violent Dutch Roll instability. Tiltrotor aircraft employ an interconnect shaft between the two rotor/engine systems so that in the event of an engine failure either engine may drive both rotors. The interconnect shaft also maintains synchronization of the rotor speeds during any aircraft motions. This means that yawing motions of the aircraft generate perturbation lift forces that tend to damp the yawing motion, as indicated in figure 62. If this synchronization is lost due to a failed interconnect shaft this damping is lost. The Dutch Roll stability boundary of the model was mapped in air with the interconnect shaft engaged and disengaged to assess the effect of thrust damping. The results are illustrated in figure 87, which shows the variation in the damping of that mode with tunnel air-

speed for each of those two cases. The substantial contribution of thrust damping to total damping is quite apparent.

In 1973, NASA and the Army selected Bell to design and build two tiltrotor research aircraft (to be later named the XV-15) based on the Model 300-A2A design. Roll out of the first aircraft occurred in 1976. First flight took place in 1977. The XV-15 (fig. 88) has been an extremely successful research aircraft. Both aircraft are still being used extensively today. The long-term success of the XV-15 tiltrotor, both as a technology demonstrator and as a flight research aircraft, went a long way toward establishing the technical confidence and expertise for proceeding with the development of the V-22. Indeed, it is probably fair to say that if there had not been an XV-15, there would not now be a V-22.

Bell/Boeing JVX (V-22)

A 1/5-scale dynamically and aeroelastically scaled semi-span model (fig. 89) of first a preliminary design and then an updated version of the Bell/Boeing JVX (V-22) was tested in two entries in the TDT during February and June of 1984. The V-22 design features a three-bladed proprotor with highly-twisted blades that are attached via coning flexures to a hub assembly that is mounted to the mast with a constant-velocity joint that eliminates two-per-rev torque oscillations of the drive shaft. Hub flapping restraint is employed to increase control power when operating in the helicopter mode. Blade precone is 2.5° and $\delta_3 = -15^\circ$. The blades are stiff inplane so that their lowest inplane natural frequency is above the rotor rpm and remains well separated from the first and second harmonics of the rotor rotational speed. The cantilevered wing beam and chord mode frequencies are well below 1P while the torsion mode frequency is only slightly above 1P. The semi-span model was the right half of the full-span model that was designed and built by Bell for testing in the Boeing V/STOL Wind Tunnel. For this reason, the model was Froude scaled for air. However, like the earlier model of the XV-15, the V-22 model was sized so that it would also be Mach scaled when tested in R-12 (recall discussion in Model Scaling Considerations section). The model proprotor has a diameter of 7.6 feet. Scale factors for the model are listed in table 6.

The main objective of the TDT tests was to confirm predicted stability in the high-speed airplane mode of flight and to provide data for correlation with the aeroelastic stability analyses being used by the contractors in their preliminary design work. Testing was conducted in both R-12 and air. The model was tested in

both powered and unpowered conditions. However, most of the testing in the airplane mode of flight was done with a windmilling proprotor. A variety of configurations were tested and analyzed. Parameters which were varied included pylon-to-wing locking (on and off downstop), rotor rpm, blade pitch-flap coupling (δ_3), hub flapping restraint, and wing and blade stiffness distributions. Several configurations of the model with an updated hub design that had offset coning hinges in addition to the gimbal were tested in the second entry. Some illustrative results from the first entry are presented in figures 90 and 91 as the variation with airspeed of the calculated and measured damping and frequency of the three lowest wing modes which are of importance to stability of the rotor-pylon-wing system. The wing beam mode (primarily wing vertical bending) is seen to be critical (lowest flutter speed) for the case shown in figure 90 while the wing chord mode (primarily fore-and-aft wing bending) is critical for the case shown in figure 91. The wing torsion mode was not critical for any of the configurations tested in either of the entries. The "peaks" which are evident in the calculated damping curves for the wing beam and chord modes in both of the cases shown are due to the coupling of those modes with the blade lag (inplane bending) mode as velocity is increased, as can be seen by inspection of the plots showing the variation of the modal frequencies with airspeed. The calculated results shown were obtained with PASTA1.

Data of the type shown in figures 90 and 91 were obtained for all of the configurations tested in both of the entries. The PASTA code (initially version 1.0 and later 2.0) was used extensively during the tests and comparisons made with measured subcritical damping variation with airspeed up to instability. The demonstrated accuracy of the PASTA code in these comparisons prompted Bell to use the program extensively during the preliminary design phase of the V-22. Since that time, the code has been used in government, industry, and academia for a variety of tiltrotor studies.

The experimental results obtained during the V-22 model tests are documented in internal company reports. A concise summary of the tests may be found in reference 128.

WRATS Tiltrotor Testbed (1995-)

The 1/5-scale aeroelastic model, which was used by the V-22 contractors to support the preliminary and full-scale design phases of the aircraft, had a long and distinguished test history (ref. 129). Upon completion of that series of tests, the Navy transferred the components for the right-half semi-span configuration of the model to NASA-Langley under an indefinite-loan

agreement to be used as the experimental testbed for a new tiltrotor aeroelastic research program that was initiated at AB in 1994. The tiltrotor testbed (fig. 92) was designated the Wing and Rotor Aeroelastic Testing System (WRATS).

The focus, general scope, and initial elements of the new AB tiltrotor research program were laid out in collaboration with Bell Helicopter Textron, Inc. (BHTI), with due regard to NASA's Short Haul Civil Tiltrotor Program that was being planned at the time. It was agreed that the program would focus on those aeroelastic areas that were identified as having the potential for enhancing the commercial viability of tiltrotor aircraft. In particular, considerable emphasis was to be directed to the development and evaluation of modern adaptive control techniques for active vibration control and stability augmentation of tiltrotor aircraft. Attention was also to be given to the use of passive design techniques to enhance aeroelastic stability and aerodynamic performance.

A shakedown test of the WRATS tiltrotor testbed was conducted in the TDT in April 1995. A chronological summary of the tests conducted to-date on the testbed following the shakedown test is given below. BHTI, under a Memorandum of Agreement with NASA, was a partner in all of these tests.

August 1995: This was the first WRATS test conducted in the TDT. The objectives of the test were twofold: (1) to establish the stability characteristics of the baseline configuration; and (2) to evaluate a higher harmonic control (HHC) algorithm for reducing aircraft vibrations by actively controlling the wing flaperon. The test was conducted in air with a wind-milling rotor.

The first objective of this test was to establish the stability characteristics of the baseline model, which had a wing spar representing the untailored wing design of the V-22. Stability boundaries measured on the baseline model for two different values of the wing torsion natural frequency are presented in figure 93 as the variation of rotor speed with tunnel airspeed. The wing torsion frequencies were varied by changing a connection spring that represented the stiffness of the pylon/wing downstop locking mechanism. The figure indicates that stability is strongly influenced by wing torsion frequency, with a difference of only 0.2 Hz producing a shift of about 12 knots at constant rpm.

The second objective of this test was to evaluate a higher harmonic control algorithm called MAVSS (Multipoint Adaptive Vibration Suppression System) for its effectiveness in reducing vibrations in the air-

plane mode of flight by actively controlling the wing flaperon. MAVSS was developed by BHTI for reducing rotor-induced aircraft vibrations occurring at integer multiples of the rotor speed. The MAVSS algorithm, which operates in the frequency domain, assumes that changes in aircraft vibratory responses are linearly related to changes in control inputs through a system transfer matrix that is identified on line. The deterministic controller on which MAVSS is based is obtained by minimizing a scalar performance index which includes the harmonic vibratory responses to be reduced, the HHC inputs necessary to effect the reduction, and the transfer matrix describing the dynamics of the system. The active flaperon model hardware consisted of a new, stiffer flaperon assembly which replaced the baseline dynamically scaled flaperons and hangers (fig. 94). The active flaperon was driven by a single hydraulic actuator that was mounted on the model splitter-plate inside the fuselage shell. The drive shaft between the actuator and the active flaperon ran along the wing conversion axis where the interconnect drive shaft would be when the model is configured for powered operation. Typical results obtained are illustrated in figure 95, which shows the 3-per-rev vibratory wing torsion loads as a function of tunnel airspeed for the cases in which MAVSS is off and on. The significant reduction in response is evident. The corresponding motions of the flaperon to achieve the load reductions are indicated by the open circles next to the bars. Based on the results of this investigation (ref. 130) it was concluded that active control of an aerodynamic surface (e.g., a flaperon) can produce the forces required for significant vibration reduction in the mode directly influenced by that surface. Multiple responses in different modes are not controlled as well by a single actuator, as might be expected. In all cases, the required motions of the flaperon were found to be quite modest (± 3 -deg maximum) and no degradation of aeroelastic stability was noted during activation of MAVSS. The success of the active flaperon test led the way for a 1997 flight test of a MAVSS-controlled active elevator on the XV-15 tiltrotor research aircraft.

December 1995: The objective of this test was to demonstrate that composite wing tailoring could be used to improve proprotor stability. The V-22 has a 23% wing thickness-to-chord (t/c) ratio to provide the wing torsional stiffness required to ensure an adequate level of proprotor-ylon-wing aeroelastic stability within its operating envelope. Studies conducted by Bell as part of a full-scale composite tailored wing study (ref. 131) indicated that by using composite tailoring techniques in the design of tiltrotor wings, a reduction in wing thickness ratio is possible while maintaining acceptable proprotor aeroelastic stability. A reduction in wing thickness would permit higher cruise

speeds and/or increased range when operating in the airplane mode of flight. The WRATS testbed was selected for the wind-tunnel evaluation of the composite tailored-wing concept. To this end, Bell designed and fabricated a composite, elastically-tailored graphite-epoxy model wing spar that had the scaled dynamics of a full-scale tailored-wing design having an 18% t/c ratio (ref. 131) and would be interchangeable with the untailored spar of the baseline model (which has a 23% t/c ratio) tested in August 1995. Structural tailoring of the model wing torque box was accomplished by using unbalanced composite laminates in the model wing spar to modify wing bending-torsion coupling. All testing was conducted in air with an unpowered rotor. Some measured and predicted stability boundaries for the baseline and tailored wings over the normal rpm operating range of the model are shown in figure 96. Comparison of the boundaries shows an increase of about 30 KEAS (58 KEAS full scale) in the instability airspeed for the tailored wing. This represents a significant improvement in stability for a full-scale design. Figure 97 shows a typical variation of wing beam mode frequency and damping with tunnel airspeed for the tailored wing in an off-downstop configuration corresponding to the 84% rpm condition of figure 96. The calculated stability boundaries shown in both of these figures were obtained using Bell's ASAP (Aeroelastic Stability Analysis of Proprotors) program. A complete summary of this test may be found in references 132-133.

The tests of the baseline and tailored wings demonstrated that proprotor aeroelastic stability can be increased while reducing the t/c ratio of a wing using composite tailoring techniques. From a broader perspective, this means that composite tailoring can be employed by the designer to increase stability, reduce wing thickness for higher cruise speeds and improved performance, or a combination of these.

January 1996: The August 1995 test was a successful wind-tunnel demonstration of a MAVSS-controlled active flaperon for reducing airframe vibrations. However, it was recognized that a broader evaluation of MAVSS was required to validate the algorithm for use as an HHC system in tiltrotor applications. The purpose of this January test was to effect this broader evaluation of the MAVSS algorithm. All testing was conducted in air with an unpowered rotor.

The WRATS model was modified to incorporate an HHC system employing both the swashplate and the wing flaperon. The major mechanical modifications made to the baseline model for this test included the replacement of the electric control actuators with high-frequency hydraulic servo-actuators to drive the

swashplate, a new servo-controlled wing flaperon (the same one used on the active flaperon test), and the hydraulic lines associated with these actuators. Some of the new components are indicated in figure 98. For convenience, the elastically tailored wing spar from the previous test was retained. The effectiveness of the swashplate and the flaperon acting either singly or in combination in reducing one-per-rev (1P) and three-per-rev (3P) wing vibrations over a wide range of tunnel airspeeds and rotor rotational speeds was demonstrated (ref. 134). The MAVSS algorithm was found robust to variations in tunnel airspeed and rotor speed, requiring only occasional on-line recalculations of the system transfer function. No degradation in aeroelastic stability was noted for any of the conditions tested. The MAVSS control system, when configured to reduce 3P harmonics of the wing loads, was generally able to reduce the wing beam, chord, and torsion load components simultaneously by 85 to 95 percent over the entire range of rotor speeds and tunnel airspeeds considered. Representative results are shown in figure 99. The effectiveness of MAVSS in reducing 1P vibrations was also assessed. For example, figure 100 shows the effect of MAVSS on reducing the 1P vibrations associated with the small inherent imbalance in the rotor. Based on the success of this wind-tunnel demonstration of MAVSS, Bell is currently preparing to test an active vibration suppression system based on MAVSS on the V-22.

May 1998: In 1997, a NASA/Bell team initiated a study of Generalized Predictive Control (ref. 135) to evaluate that method's suitability for implementation as an active stability augmentation system on the WRATS model. GPC is a time-domain predictive control method that uses an ARX representation for the input/output map of the system. The ARX model is used for both system identification and control design. The coefficient matrices of the ARX equation are the quantities determined by the identification algorithm. Closed-loop feedback control is enhanced by performing the system identification in the presence of external disturbances acting on the system. The coefficients of the ARX model are assembled into a multi-step output prediction equation, the desired (target) response is specified, and the resulting expression is used to form a cost function. Minimization of the cost function leads to an expression for the control to be applied to the system.

As part of the GPC study, the team began evaluating a suite of MATLAB m-files for system identification and control that were written by Dr. Jer-Nan Juang of NASA-Langley based on the theory of references 136-138. Following extensive numerical simulations conducted on simple math models, and bench tests on

the "Cobra stick model" (a 36-inch, 50-lb multiple-degree-of-freedom lumped-mass dynamic system that approximates the dynamics of a Cobra helicopter), the relevant m-files were assembled into a computer program system for active controls testing of the WRATS model.

The initial evaluation of GPC on the WRATS model was conducted in May 1998 during a one-week test conducted in the AB tiltrotor hover facility in a building adjacent to the TDT. Emphasis of this test was on active control of vibration using only the collective control. To provide a rigorous test of the GPC algorithm, the open-loop response of the model was exaggerated by running the rotor at an rpm that nearly coincided with the natural frequency of the wing beam mode. Additional excitation was provided by the downwash associated with running the rotor at a high thrust level. Some results illustrating the effectiveness of GPC in reducing vibrations are shown in figure 101.

August 1998: The objectives of this test were two-fold: (1) to establish new baseline stability boundaries for the WRATS model that included the hydraulic components that had been added for active controls testing; and (2) begin an investigation into the use of active δ_3 as a means for augmenting mechanical δ_3 . Most of the test was conducted in air but some limited testing was carried out in R-134a. All testing was done with the model in an airplane mode and a windmilling prop rotor.

Definitive stability boundaries could not be identified for the model. The subcritical damping in the wing beam mode varied with airspeed as expected for speeds up to about 110 knots. However, as tunnel airspeed was increased further the damping did not decrease to zero as usual but rather leveled out at about 1% and held this value up through the maximum safe operating speed of the model (200 knots). This behavior occurred for all configurations of the model tested. Because the observed behavior had the character of a limit cycle, it was thought that there might be some mechanical interference or rubbing that was introducing nonlinearity into the model. However, examination of the model in-situ during the test failed to identify the cause for this unusual behavior. A closer examination of the model after the test identified the cause of the problem: a loose bolt in the bracket that holds the pylon to the downstop spring. The baseline stability will be determined in the next scheduled entry of WRATS into the TDT.

The use of so-called "active δ_3 " is being investigated as a means for augmenting mechanical δ_3 in

proprotors. Active δ_3 is implemented electronically by introducing cyclic inputs to the swashplate in a manner that introduces blade pitch-flap coupling of the appropriate magnitude and sign. An electronic δ_3 scheme developed by Bell was investigated on the WRATS model during this entry. The measured flapping response associated with the active δ_3 met design requirements. However, the stability augmentation associated with using active δ_3 could not be defined with confidence because of the problem noted above with the model. This study will be completed in the next scheduled entry of the model into the TDT.

October 1999: A brief investigation of the use of GPC to actively control the ground resonance behavior of a soft inplane tiltrotor was conducted in the tiltrotor hover facility in October 1999. For this test, the model blades were modified by replacing the stiff inplane flexure at the root of each blade with a spindle incorporating a lag hinge and an adjustable viscous damper and spring. The open-loop behavior (frequency and damping versus rotor rpm) of the modified model was compared with its closed-loop behavior for several values of collective pitch and settings of the lag hinge damping and stiffness. A GPC-based algorithm was used to actively control the cyclic inputs to the swashplate in a manner which produced a whirl of the rotor tip-path-plane in the direction and at the frequency needed to stabilize the critical body mode. For the open-loop configuration of the model in which a definitive ground resonance instability was observed, use of GPC was found to be strongly stabilizing. In particular, damping levels of about 2% critical were noted in the rpm range where the open-loop system was unstable. While these results are quite encouraging with respect to the viability of the method, it is recognized that a broader evaluation of the methodology is needed to validate GPC-based algorithms for active stability augmentation of tiltrotor aircraft. This evaluation will be continued in the next scheduled entry of the model into the TDT.

Other Work

The Variable Diameter Tilt Rotor (VDTR) is a Sikorsky Aircraft concept for improving tiltrotor aerodynamic performance in hover and cruise. Over the years, Sikorsky has performed analytical studies and conducted wind-tunnel tests on several models to validate their concept. In support of these studies, UMARC/S (Sikorsky's version of UMARC/G) was modified to allow modeling of blades with multiple load paths, such as those associated with the bearingless rotor design of the VDTR. An example of the ability of the code to predict torque tube and blade

loads measured on a 1/6-scale model of the VDTR is indicated in figure 102 (ref. 115).

Some Closing Remarks on Tiltrotor Research

The AB/TDT has a long history of propeller and proprotor aeroelastic research. The research has included a broad range of experimental and analytical studies that have made creditable contributions to the technology base which has led to the successful development of the XV-15 and V-22 tiltrotor aircraft. These studies have also contributed substantially to increased understanding of the aeroelastic and dynamic characteristics that are unique to tiltrotor aircraft. The current tiltrotor research program in AB is continuing this tradition and is expected to play an important role in the development of future tiltrotor aircraft such as the Bell/Augusta BA-609 (fig. 103) and the Bell Quad Tilt Rotor (fig. 104).

Current/Planned Tiltrotor Aeroelastic Research

Tiltrotor research in AB/TDT continues to consist of a mixture of experimental and analytical activities. On the experimental side, current plans call for several tests in the TDT over the next few years. Those currently on the tunnel schedule include: (1) A WRATS investigation of the use of GPC for augmenting stability in the airplane mode of flight and a further study of active δ_3 ; (2) A high-speed study of the stability and loads of the Sikorsky VDTR rotor model on the WRATS testbed; (3) Stability and active control testing of a soft inplane gimbaled rotor; and (4) A semi-span model of the Bell QTR.

On the analytical side, work is nearly completed on the extension of UMARC/G to include rotor/airframe interactional aerodynamics and a drive system model. The use of Generalized Predictive Control techniques for vibration reduction and stability augmentation will continue to be studied. Work will continue on improving the GPC program that is currently being used with WRATS, and on developing a recursive version of the program to speed up on-line calculations. It is expected that enhancements will continue to be made to the UMARC/G and PASTA codes as appropriate to support the in-house studies. Development of the MBDyn code and its application to the WRATS model is also expected to continue in cooperation with the University of Milan.

Concluding Remarks

This paper has presented a historical overview of the contributions of the Langley Transonic Dynamics Tunnel and its associated Aeroelasticity Branch to ro-

torcraft technology and development since the tunnel's inception in 1960. That research has included a broad range of experimental investigations using a variety of testbeds and scale models, and the development and application of essential analyses. Based on the overview, it is fair to say that the TDT has had a long and creditable history of rotorcraft aeroelastic research that has contributed to the technology base needed by the industry for designing and building advanced rotorcraft systems. In particular, studies conducted in the TDT have contributed substantially to supporting rotorcraft research and development programs, to identifying and investigating aeroelastic phenomena unique to rotorcraft systems, and to the resolution of aeroelastic anomalies. Building on this foundation, and with due regard for current and planned research activities in helicopter and tiltrotor aeroelasticity, it is expected that this tradition of service to the nation will continue well into the 21st century.

Acknowledgements

The authors wish to acknowledge the work of the research staff of the Aeroelasticity Branch at NASA Langley Research Center and our partners from government, industry, and academia whose research has been reviewed in this paper.

References

1. Reed, W. H., III: *Aeroelasticity Matters: Some Reflections on Two Decades of Testing in the NASA Langley Transonic Dynamics Tunnel*. NASA TM-83210, September 1981.
2. Doggett, R. V., Jr.; and Cazier, F. W., Jr.: *Aircraft Aeroelasticity and Structural Dynamics Research at the NASA Langley Research Center - Some Illustrative Results*. NASA TM 100627, May 1988.
3. Ricketts, R. H.: *Experimental Aeroelasticity History, Status and Future in Brief*. NASA TM 102651, April 1990.
4. Perry, B., III; and Noll, T. E.: Activities in Aeroelasticity at NASA Langley Research Center. Fourth International Symposium on Fluid-Structure Interactions, Aeroelasticity, Flow-Induced Vibration and Noise, ASME, Dallas, TX, November 16-21, 1997.
5. Kvaternik, R. G.: A Review of Some Tilt-Rotor Aeroelastic Research at NASA-Langley. *Journal*

- of Aircraft, Vol. 13, No. 5, May 1976, pp.357-363.
6. Hammond, C. E.; and Weller, W. H.: Wind-Tunnel Testing of Aeroelastically Scaled Helicopter Rotor Blades. *Army Science Conference*, West Point, NY, June 1976.
 7. Mantay, W. R.; Yeager, W. T., Jr.; Hamouda, M. N.; Cramer, R. G., Jr.; and Langston, C. W.: *Aeroelastic Model Helicopter Rotor Testing in the Langley TDT*. NASA TM 86440 (USA AVSCOM Technical Memorandum 85-B-5), June 1985.
 8. Yeager, W. T., Jr.; Mirick, P. H.; Hamouda, M. N.; Wilbur, M. L.; Singleton, J. D.; and Wilkie, W. K.: Recent Rotorcraft Aeroelastic Testing in the Langley Transonic Dynamics Tunnel. Presented at the 47th Annual Forum of the American Helicopter Society, Phoenix, AZ, May 1991.
 9. Kvaternik, R. G.: *A Historical Overview of Tilt-rotor Aeroelastic Research at Langley Research Center*. NASA TM 107578, April 1992.
 10. Notes on the Proceedings of the 1939 Meeting of the Aircraft Industry with the National Advisory Committee for Aeronautics. *Journal of the Aeronautical Sciences*, Vol. 6, Number 7, May 1939, pp. 299-301.
 11. Moxey, R. L.: Transonic Dynamics Wind Tunnel. *Compressed Air Magazine*, Vol. 68, Number 10, October 1963, pp. 8-13.
 12. Yates, E. C., Jr.; Land, N. S.; and Foughner, J. T., Jr.: *Measured and Calculated Subsonic and Transonic Flutter Characteristics of a 45° Swept-back Wing Planform in Air and in Freon-12 in the Langley Transonic Dynamics Tunnel*. NASA TN-1616, March 1963.
 13. Lee, C.; Bruce, C.; and Kidd, D.: *Wind-Tunnel Investigation of a Quarter-Scale Two-Bladed High-Performance Rotor in a Freon Atmosphere*. USAAVLABS Tech. Rep. 70-58, U.S. Army, Feb. 1971.
 14. Treon, S. L.; Hofstetter, W. R.; and Abbott, F. T., Jr.: On the Use of Freon-12 for Increasing Reynolds Number in Wind-Tunnel Testing of Three-Dimensional Aircraft Models at Subcritical and Supercritical Mach Numbers. *Facilities and Techniques for Aerodynamic Testing at Transonic Speeds and High Reynolds Number*, AGARD CP No. 83, Aug. 1971, pp. 27-1 – 27-8.
 15. Yeager, W. T., Jr.; and Mantay, W. R.: *Correlation of Full Scale Helicopter Rotor Performance in Air with Model-Scale Freon Data*. NASA TN D-8323, November 1976.
 16. Corliss, J. M.; and Cole, S. R.: Heavy Gas Conversion of the NASA Langley Transonic Dynamics Tunnel. 20th AIAA Advanced Measurement and Ground Testing Technology Conference, June 15-18, 1998, Albuquerque, NM (AIAA Paper 98-2710).
 17. Cole, S. R.; and Garcia, J. L.: Past, Present and Future Capabilities of the Transonic Dynamics Tunnel From an Aeroelasticity Perspective. Presented at the AIAA Dynamics Specialists Conference, Atlanta, GA, April 5-6, 2000 (Paper AIAA-2000-1767).
 18. Murphy, G.: *Similitude in Engineering*. The Ronald Press Co., New York, 1950.
 19. Baker, W. E.; Westine, P. S.; and Dodge, F. T.: *Similarity Methods in Engineering Dynamics*. Hayden Book Company, Rochelle Park, New Jersey, 1973.
 20. USAF/AIA: *Proceedings of Symposium on Aeroelastic & Dynamic Modeling Technology*. Dayton, OH, September 23-25, 1963. (AFFDL Report RTD-TDR-63-4197, Part I, March 1964.)
 21. Regier, A. A.: The Use of Scaled Dynamic Models in Several Aerospace Vehicle Studies. Paper presented at ASME Colloquium on the Use of Models and Scaling in Shock and Vibration, Philadelphia, PA, November 1963, pp. 34-50.
 22. Guyett, P. R.: *The Use of Flexible Models in Aerospace Engineering*. R.A.E. Technical Report No. 66335, November 1966.
 23. Kuntz, W. H.; Wasserman, L. S.; and Alexander, H. R.: Dynamically Similar Model Tests of Rotary Wing and Propeller Types of VTOL Aircraft. *Proceedings of the Air Force V/STOL Technology and Planning Conference*, Las Vegas, NV, September 23-25, 1969.
 24. Brooks, G. W.: The Application of Models to Helicopter Vibration and Flutter Research. *Proceedings of the Ninth Annual Forum of the*

- American Helicopter Society*, Washington, D.C., May 14-17, 1953.
25. Fradenburgh, E. A.; and Kiely, E. F.: Development of Dynamic Model Rotor Blades for High Speed Helicopter Research. *Journal of the American Helicopter Society*, Vol. 9, Jan. 1964, pp. 3-20.
 26. Albrecht, C. O.: Factors in the Design and Fabrication of Powered, Dynamically Similar V/STOL Wind Tunnel Models. *American Helicopter Society Mid-East Region Symposium on the Status of Testing and Modeling Techniques for V/STOL Aircraft*, Essington, PA, Oct. 26-28, 1972.
 27. Ormiston, R. A.: Helicopter Modeling. *Aeronautical Journal*, Vol. 77, Nov. 1973, pp. 579-591.
 28. Rabbott, J. P., Jr.: Model vs. Full Scale Rotor Testing. *Proceedings of the CAL/AVLABS Symposium on Aerodynamics of Rotary Wing and V/STOL Aircraft* (Vol. II - Wind Tunnel Testing), June 18-20, 1969, Buffalo, NY.
 29. Kelly, M. W.: The Role of Wind Tunnel Testing in the Development of Advanced Rotary-Wing Aircraft. Prepared comments made as panel member, Wind tunnel Testing Panel Discussion at the *AHS Mideast Region Symposium on Status of Testing and Modeling Techniques for V/STOL Aircraft*, Essington, PA, Oct. 26-28, 1972.
 30. Langhaar, H. L.: *Dimensional Analysis and Theory of Models*. John Wiley and Sons, Inc., 1956.
 31. Templeton, H.: *Models for Aero-Elastic Investigations*. Aeronautical Research Council, Technical Report C.P. No. 255, Great Britain, 1956.
 32. Molyneux, W. G.: *Aeroelastic Modeling*. RAE Tech Note Structures 353, March 1964.
 33. Hunt, G. K.: *Similarity Requirements for Aeroelastic Models of Helicopter Rotors*. RAE Technical Report 72005, January 1972.
 34. Lee, C: Weight Considerations in Dynamically Similar Model Rotor Design. Presented at the *27th Annual Conference of the Society of Aeronautical Weight Engineers, Inc.*, New Orleans, LA, May 13-16, 1968 (Paper No. 659).
 35. Hanson, P. W.: *An Assessment of the Future Roles of the National Transonic Facility and the Langley Transonic Dynamics Tunnel in Aeroelastic and Unsteady Aerodynamic Testing*. NASA TM 81839, June 1980.
 36. Singleton, J. D.; and Yeager, W. T., Jr.: Important Scaling Parameters for Testing Model-Scale Helicopter Rotors. *20th AIAA Advanced Measurement and Ground Testing Technology Conference*, Albuquerque, NM, June 15-18, 1998 (Paper AIAA-98-2881).
 37. Ward, John F.; and Huston, Robert J.: A Summary of Hingeless-Rotor Research at NASA-Langley. Presented at the *20th Annual Forum of the American Helicopter Society*, Washington, D.C., May 13-15, 1964.
 38. Ward, J. F.: A Summary of Hingeless-Rotor Structural Loads and Dynamics Research. *Journal of Sound and Vibration*, Vol. 4, No.3, 1966, pp. 358 - 377.
 39. Hanson, T. F.: *Investigation of Elastic Coupling Phenomena of High-Speed Rigid Rotor Systems*. U. S. Army TRECOM Technical Report 63-75, 1964.
 40. Hanson, T. F.: *Wind-Tunnel Tests of an Optimized, Matched-Stiffness Rigid Rotor*. U. S. Army TRECOM Technical Report 64-56, 1964.
 41. Lee, Charles D.; and White, James A.: *Investigation of the Effect of Hub Support Parameters on Two-Bladed Rotor Oscillatory Loads*. NASA CR-132435, May 1974.
 42. Weller, William H.; and Lee Bill L.: *Wind-Tunnel Tests of Wide-Chord Teetering Rotors With and Without Outboard Flapping Hinges*. NASA Technical Paper 1046, Nov. 1977.
 43. Weller, William H.: *Load and Stability Measurements On a Soft-Inplane Rotor System Incorporating Elastomeric Lead-Lag Dampers*. NASA TN D-8437, July 1977.
 44. Doggett, R.V., Jr.; and Hammond, C.E.: *Application of Interactive Computer Graphics in Wind-Tunnel Dynamic Model Testing. Applications of Computer Graphics in Engineering*, NASA SP-390, 1975, pp. 325-353.
 45. Hammond, Charles E.; and Doggett, Robert V., Jr.: *Determination of Subcritical Damping by Moving-Block/Randomdec. Applications. Flutter Testing Techniques*, NASA SP-415, 1976, pp. 59-76.

46. Lemnios, A. Z.; and Smith, A. F.: *An Analytical Evaluation of the Controllable Twist Rotor Performance and Dynamic Behavior*. USAAMRDL Tech. Rep. 72-16, U.S. Army, May 1972.
47. Lemnios, A. Z.; Nettles, William E.; and Howes, H. E.: Full Scale Wind Tunnel Tests of a Controllable Twist Rotor. *Proceedings of a Symposium on Rotor Technology*, American Helicopter Society, Aug. 1976.
48. Doman, Glidden S.; Tarzanin, Frank J.; and Shaw, John, Jr.: Investigation of Aeroelastically Adaptive Rotor Systems. *Proceedings of a Symposium on Rotor Technology*, American Helicopter Society, Aug. 1976.
49. Blackwell, R. H.: *Investigation of the Compliant Rotor Concept*. Sikorsky Aircraft Division, United Technologies Corporation, USAAMRDL-TR-77-7, Eustis Directorate, USAAMRDL, Fort Eustis, VA. June 1977, AD 1042338.
50. Blackwell, R. H.; and Merkley, D. J.: The Aeroelastically Conformable Rotor Concept. Preprint No. 78-59, *American Helicopter Society*, May 1978.
51. Weller, William H.: *Experimental Investigation of Effects of Blade Tip Geometry on Loads and Performance for an Articulated Rotor System*. NASA Technical Paper 1303, January 1979.
52. Yeager, William T., Jr.; and Mantay, Wayne R.: *Wind-Tunnel Investigation of the Effects of Blade Tip Geometry on the Interaction of Torsional Loads and Performance for an Articulated Helicopter Rotor*. NASA Technical Paper 1926. December 1981.
53. Blackwell, R. H.; Murrill, R. J.; Yeager, William T., Jr.; and Mirick, Paul H.: Wind Tunnel Evaluation of Aeroelastically Conformable Rotors. Preprint 80-23. Presented at the 36th *Annual Forum of the American Helicopter Society*, Washington, D. C., May 1980.
54. Blackwell, R. H.; Murrill, R., J.; Yeager, William T., Jr.; and Mirick, P. H.: Wind-Tunnel Evaluation of Aeroelastically Conformable Rotors. *Journal of the American Helicopter Society*, vol. 26, no. 2, Apr. 1981, pp. 31-39.
55. Sutton, Lawrence R.; White, Richard P., Jr.; and Marker, Robert L.: *Wind-Tunnel Evaluation of an Aeroelastically Conformable Rotor*. USAAVRADCOM-TR-81-D-43, Applied Technology Laboratory, U.S. Army Research and Technology Laboratories, Ft. Eustis, Va., Mar. 1982.
56. Mantay, Wayne R.; and Yeager, William T., Jr.: *Parametric Tip Effects for Conformable Rotor Applications*. NASA Technical Memorandum 85682, August 1983.
57. Mantay, Wayne R.; and Yeager, William T., Jr.: *Aeroelastic Considerations for Torsionally Soft Rotors*. NASA Technical Memorandum 87687, Aug. 1986.
58. Wood, E. R.; and Powers, R. W.: Practical Design Considerations for a Flightworthy Higher Harmonic Control System. Presented at the 36th *Annual Forum of the American Helicopter Society*, Washington, D.C., May 1980.
59. Hammond, C. E.; and Cline, J. H.: On the Use of Active Higher Harmonic Blade Pitch for Helicopter Vibration Reduction. Presented at the 12th *Army Science Conference*, West Point, New York, June 17-20, 1980.
60. Hammond, C.E.: Wind-Tunnel Results Showing Rotor Vibratory Loads Reduction Using Higher Harmonic Blade Pitch. *Journal of the American Helicopter Society*, Jan. 1983, pp. 10-15.
61. Molusis, J. A.; Hammond, C. E.; and Cline, John H.: A Unified Approach to the Optimal Design of Adaptive and Gain Scheduled Controllers to Achieve Minimum Rotor Vibration. *Journal of the American Helicopter Society*, Apr. 1983.
62. Wood, E. R.; Powers, R. W.; Cline, J. H.; and Hammond, C. E.: On Developing and Flight Testing a Higher Harmonic Control System. Presented at the 39th *Annual Forum of the American Helicopter Society*, St. Louis, Missouri, May 1983.
63. Straub, F. K.; and Byrns, E. V., Jr.: *Application of Higher Harmonic Blade Feathering on the OH-6A Helicopter for Vibration Reduction*. NASA CR-4031, December 1986.
64. Yeager, William T., Jr.; Hamouda, M-Nabil; and Mantay, Wayne R.: Aeromechanical Stability of a Hingeless Rotor in Hover and Forward Flight: Analysis and Wind Tunnel Tests. Presented at the *Ninth European Rotorcraft Forum*, Stresa, Italy, Sept. 1983.

65. Yeager, William T., Jr.; Hamouda, M-Nabil; and Mantay, Wayne R.: *An Experimental Investigation of the Aeromechanical Stability of a Hingeless Rotor in Hover and Forward Flight*. NASA TM-89107, USAAVSCOM TM 87-B-5, June 1987.
66. Johnson, W.: *A Comprehensive Analytical Model of Rotorcraft Aerodynamics and Dynamics, Part I – Analysis Development*. NASA TM-81182, 1980.
67. Johnson, W.: *A Comprehensive Analytical Model of Rotorcraft Aerodynamics and Dynamics, Part II – User's Manual*. NASA TM-81183, 1980.
68. Bingham, Gene J.: The Aerodynamic Influences of Rotor Blade Airfoils, Twist, Taper and Solidity on Hover and Forward Flight Performance. Proceedings of the 37th Annual Forum, American Helicopter Society, May 1981, pp. 37-50.
69. Yeager, William T., Jr.; Mantay, Wayne R.; Wilbur, Matthew L.; Cramer, Robert G., Jr.; and Singleton, Jeffrey D.: *Wind-Tunnel Evaluation of an Advanced Main-Rotor Blade Design for a Utility-Class Helicopter*. NASA Technical Memorandum 89129, Sept. 1987.
70. Singleton, Jeffrey D.; Yeager, William T., Jr.; and Wilbur, Matthew L.: *Performance Data From a Wind-Tunnel Test of Two Main-Rotor Blade Designs for a Utility-Class Helicopter*. NASA Technical Memorandum 4183, June 1990.
71. Yeager, William T., Jr.; Hamouda, M-Nabil; Idol, Robert F.; Mirick, Paul H.; Singleton, Jeffrey D.; and Wilbur, Matthew L.: *Vibratory Loads Data From a Wind-Tunnel Test of Structurally Tailored Model Helicopter Rotors*. NASA Technical Memorandum 4265, Aug. 1991.
72. Yen, J. G.: Coupled Aeroelastic Hub Loads Reduction. Proceedings of the *Theoretical Basis of Helicopter Technology Seminar, Part 3*. Nanjing Aeronautical Inst. (Peoples's Republic of China) and American Helicopter Society, Inc., 1985, pp.D4-1-D4-9.
73. Yen, Jing G.; Yuce, Mithat; Chao, Chen-Fu; and Schillings, John: Validation of Rotor Vibratory Airloads and Application to Helicopter Response. *Journal of the American Helicopter Society*, vol. 35, no. 4, Oct. 1990, pp. 63-71.
74. Taylor, Robert B.: Helicopter Vibration Reduction by Modal Shaping. Presented at the 38th Annual Forum of the American Helicopter Society. Anaheim, Calif., May 1982.
75. Wilbur, Matthew L.: Experimental Investigation of Helicopter Vibration Reduction Using Rotor Blade Aeroelastic Tailoring. Presented at the 47th Annual Forum of the American Helicopter Society, Phoenix, Ariz., May 1991.
76. Wilbur, Matthew L.; Yeager, William T., Jr.; Singleton, Jeffrey D.; Mirick, Paul H.; and Wilkie, W. Keats: *Wind-Tunnel Evaluation of the Effect of Blade Nonstructural Mass Distribution on Helicopter Fixed-System Loads*. NASA TM-1998-206281, Jan. 1998.
77. Hardin, J. C.; and Lamkin, S. L.: Concepts for Reduction of Blade/Vortex Interaction Noise. *Journal of Aircraft*, Vol.24, No.2, Feb. 1987, pp. 120-125.
78. Splettstoesser, W.R.; Schultz, K. L.; and Martin Ruth M.: Rotor Blade/Vortex Interaction Noise Source Identification and Correlation with Rotor Wake Predictions. *AIAA 11th Aeroacoustics Conference*, AIAA-87-2744, Oct. 1987.
79. Brooks, Thomas K.; and Booth, Earl R., Jr.: Rotor Blade-Vortex Interaction Noise Reduction and Vibration Using Higher Harmonic Control. *16th European Rotorcraft Forum*, Glasgow, U. K., Paper No.9.3, Sept. 1990.
80. Lowson, Martin Vincent; St. David, Barton; Hawkings, David Leonard; Byham, Geoffrey Malcolm; Perry, Frederick John; and Denham, Corton: Helicopter Rotor Blades. U. S. Pat. 4,077,741. Mar. 7, 1978.
81. White, R. W.: Developments in UK Rotor Blade Technology. *AIAA Aircraft Design, Systems and Technology Meeting*, Oct. 1983. (Available as AIAA-83-2525).
82. Wanstall, Brian: BERP Blades - Key to the 200 kn Helicopter. *INTERAVIA*, vol. 3, 1986, pp. 322 - 324.
83. Perry, F. J.: Aerodynamics of the Helicopter World Speed Record. Proceedings of the 43rd Annual Forum of the American Helicopter Society, May 1987, pp. 3-15.

84. Yeager, William T., Jr.; Noonan, Kevin W.; Singleton, Jeffrey D.; Wilbur, Matthew L.; and Mirick, Paul H.: *Performance and Vibratory Loads Data From a Wind-Tunnel Test of a Model Helicopter Main-Rotor Blade With a Paddle-Type Tip*. NASA Technical Memorandum 4754, ARL Technical Report 1283, ATCOM Technical Report 97-A-006. May 1997.
85. Noonan, Kevin W.; Yeager, William T., Jr.; Singleton, Jeffrey D.; Wilbur, Matthew L.; and Mirick, Paul H.: Evaluation of Model Helicopter Main Rotor with Slotted Airfoils at the Tip. Presented at the *American Helicopter Society 55th Annual Forum*, Montreal, Quebec, Canada, May 25 - 27, 1999.
86. Derham, R.; and Hagood, N.: Rotor Design Using Smart Materials to Actively Twist Blades. *American Helicopter Society 52nd Annual Forum Proceedings*, Vol. 2, Washington, D.C., June 4 - 6, 1996, pp. 1242 - 1252.
87. Wilkie, W. Keats; Belvin, W. Keith; and Park, K. C.: Aeroelastic Analysis of Helicopter Rotor Blades Incorporating Anisotropic Piezoelectric Twist Actuation. *ASME 1996 World Congress and Exposition, Adaptive Structures Symposium*, Proceedings, Aerospace Division. Nov. 1996.
88. Wilkie, W. Keats: *Anisotropic Piezoelectric Twist Actuation of Helicopter Rotor Blades: Aeroelastic Analysis and Design Optimization*. Ph. D. thesis, University of Colorado, Boulder, Colorado, 1997.
89. Wilkie, W. Keats; Park, K. C.; and Belvin, W. Keith: Helicopter Dynamic Stall Suppression Using Active Fiber Composite Rotor Blades. AIAA Paper No. 98-2002, presented at the *AIAA/ASME/AHS Structures, Structural Dynamics, and Materials Conference*, Long Beach, Calif., April 20 -23, 1998.
90. Rodgers, John P.; and Hagood, Nesbitt W.: Preliminary Mach-Scale Hover Testing of an Integral Twist-Actuated Rotor Blade. Presented at the *SPIE 5th Annual International Symposium on Smart Structures and Materials*, San Diego, Calif., March, 1998.
91. Cesnik, Carlos E. S.; Shin, SangJoon; Wilkie, W. Keats; Wilbur, Matthew L.; and Mirick, Paul H.: Modeling, Design, and Testing of the NASA/Army/MIT Active Twist Rotor Prototype Blade. Presented at the *American Helicopter Society 55th Annual Forum*, Montreal, Canada, May 25-27, 1999.
92. Wilkie, W. Keats; Wilbur, Matthew L.; Mirick, Paul H.; Cesnik, Carlos E. S.; and Shin, SangJoon: Aeroelastic Analysis of the NASA/Army/MIT Active Twist Rotor. Presented at the *American Helicopter Society 55th Annual Forum*, Montreal, Canada, May 25-27, 1999.
93. Johnson, Wayne: *CAMRAD-II, Comprehensive Analytical Model of Rotorcraft Aerodynamics and Dynamics*, Johnson Aeronautics, Palo Alto, Calif. 1994.
94. Taylor, Robert B.: *Helicopter Blade Design for Minimum Vibration*. NASA CR-3825, Oct. 1984.
95. He, C.: *A Parametric Study of Harmonic Rotor Hub Loads*. NASA CR-4558, Nov. 1993.
96. Bousman, William G.; and Mantay, Wayne R.: A Review of Research in Rotor Loads. Presented at *NASA/Army Rotorcraft Technology Conference*, Mar. 14 - 16, 1987, NASA - AMES Research Center.
97. Ormiston, Robert A.: Comparison of Several Methods for Predicting Loads on a Hypothetical Helicopter Rotor. *Journal of the American Helicopter Society*, Vol. 19, No. 4, Oct. 1974, pp. 2 - 13.
98. Blackwell, R. H., Jr.: Blade Design for Reduced Helicopter Vibration. *Journal of the American Helicopter Society*, Vol. 28, No. 3, July 1983, pp. 33 - 41.
99. Hansford, R. E.; and Vorwald, J.: Dynamics Workshop on Rotor Vibratory Loads Prediction. *Journal of the American Helicopter Society*, Vol. 43, No. 1, Jan. 1998, pp. 76 - 86.
100. Bingham, Gene J.; and Noonan, Kevin W.: *Two-Dimensional Aerodynamic Characteristics of Three Rotorcraft Airfoils at Mach Numbers From 0.35 to 0.90*. NASA TP-2000, AVRADCOM TR-82-B-2, 1982.
101. Noonan, Kevin W.: *Aerodynamic Characteristics of Two Rotorcraft Airfoils Designed for Application in the In-board Region of a Main Rotor Blade*. NASA TP-3009, AVSCOM TR-90-B-005, 1990.

102. Abbott, F. T., Jr.; Kelly, H. N.; and Hampton, K. D.: *Investigation of 1/8-Size Dynamic-Aeroelastic Model of the Lockheed Electra Airplane in the Langley Transonic Dynamics tunnel*. NASA TM SX-456, November 1960. (Also published as: *Investigation of Propeller-Power-Plant Autoprecession Boundaries for a Dynamic-Aeroelastic Model of a Four-Engine Turboprop Transport Airplane*. NASA TN D-1806, August 1963).
103. Bennett, R. M.; Kelly, H. N.; and Gurley, J. R., Jr.: *Investigation in the Langley Transonic Dynamics Tunnel of a 1/8-Size Aeroelastic-Dynamic Model of the Lockheed Electra Airplane with Modifications in the Wing-Nacelle Region*. NASA TM SX-818, March 1963.
104. Reed, W. H., III; and Bland, S. R.: *An Analytical Treatment of Aircraft Propeller Precession Instability*. NASA TN D-659, November 1960.
105. Houbolt, J. C.; and Reed, W. H., III: Propeller-Nacelle Whirl Flutter. *J. Aeronautical Sci.*, March 1962, pp. 333-345.
106. Bland, S. R.; and Bennett, R. M.: *Wind-Tunnel Measurements of Propeller Whirl-Flutter Speeds and Static-Stability Derivatives and Comparison with Theory*. NASA TN D-1807, August 1963.
107. Bennett, R. M.; and Bland, S. R.: *Experimental and Analytical Investigation of Propeller Whirl Flutter of a Power Plant on a Flexible Wing*. NASA TN D-2399, August 1964.
108. Reed, W. H., III; and Bennett, R. M.: Propeller Whirl Considerations for V/STOL Aircraft. *CAL/TRECOM Symposium Proceedings: Vol. II - Dynamic Load Problems Associated with Helicopters and V/STOL Aircraft*, June 1963.
109. Richardson, J. R.; and Naylor, H. F. W.: *Whirl flutter of Propellers with Hinged Blades*. Report No. 24, Engineering Research Associates, Toronto, Canada, March 1962.
110. Reed, W. H., III: *Review of Propeller-Rotor Whirl Flutter*. NASA TR R-264, July 1967.
111. Rainey, A. G.: Aeroelastic Considerations for Transports of the Future - Subsonic, Supersonic, and Hypersonic. Presented at the *AIAA Aircraft Design for 1980 Operations Meeting*, Washington, D.C., Feb. 12-14, 1968.
112. Kvaternik, R. G.: *Studies in Tilt-Rotor VTOL Aircraft Aeroelasticity*. Ph.D. Dissertation, June 1973, Case-Western Reserve University, Cleveland, Ohio.
113. Nixon, M. W.: *Aeroelastic Response and Stability of Tiltrotors with Elastically-Coupled Composite Rotor Blades*. Ph.D. Dissertation, 1993, University of Maryland, College Park, Maryland. (A synopsis of this work may be found in: *Parametric Studies for Tiltrotor Aeroelastic Stability in High Speed Flight*. *J. Amer. Hel. Soc.*, Vol. 38, Oct. 1993, pp. 71-79.)
114. Singleton, J. D.: *Coupled Rotor-Fuselage Aeroelastic Analysis for Tiltrotor Configurations*. *Eighth ARO Workshop on Aeroelasticity of Rotorcraft Systems*, October 18-20, 1999, State College, PA.
115. Wang, J. M.; Torok, M. S.; and Nixon, M. W.: *Experimental and Theoretical Study of Variable Diameter Tilt Rotor Dynamics*. Presented at the *AHS Vertical Lift Aircraft Design Conference*, San Francisco, CA, January 18-20, 1995.
116. Wang, J. W.; Jones, C. T.; and Nixon, M. W.: *A Variable Diameter Short Haul Civil Tiltrotor*. Presented at the *55th Annual Forum of the American Helicopter Society*, Montreal, Canada, May 25-27, 1999.
117. Ghiringhelli, G. L.; Masarati, P.; Mantegazza, P.; and Nixon, M. W.: *Multi-body Analysis of the 1/5-Scale Wind Tunnel Model of the V-22 Tiltrotor*. Presented at the *55th Annual Forum of the American Helicopter Society*, Montreal, Canada, May 25-27, 1999.
118. Ghiringhelli, G. L.; Masarati, P.; Mantegazza, P.; and Nixon, M. W.: *Multi-Body Analysis of an Active Control for a Tiltrotor*. *CEAS/AIAA/ICASE/NASA Langley Forum on Aeroelasticity and Structural Dynamics 1999*. NASA CP-1999-209136/PT 1, June 1999.
119. Ghiringhelli, G. L.; Masarati, P.; Mantegazza, P.; and Nixon, M. W.: *Multi-Body Analysis of a Tiltrotor Configuration*. *Nonlinear Dynamics*, Vol. 19, 1999, pp. 333-357.
120. Gaffey, T. M.: *The Effect of Positive Pitch-Flap Coupling (Negative δ_3) on Rotor Blade Motion Stability and Flapping*. *Journal of the American Helicopter Society*, Vol. 14, No. 2, April 1969, pp.49-67.

121. Gaffey, T. M.; Yen, J. G.; and Kvaternik, R. G.: Analysis and Model Tests of the Proprotor Dynamics of a Tilt-Proprotor VTOL Aircraft. Presented at the *Air Force V/STOL Technology and Planning Conference*, Las Vegas, NV, September 23-25, 1969.
122. Kvaternik, R. G.: Experimental and Analytical Studies in Tiltrotor Aeroelasticity. *AHS/NASA Ames Specialists' Meeting on Rotorcraft Dynamics*, Moffett Field, CA, Feb. 13-15, 1974 (Proceedings available as *Rotorcraft Dynamics*, NASA SP-352, 1974).
123. Yen, J. G.; Weber, G. E.; and Gaffey, T. M.: *A Study of Folding Proprotor VTOL Aircraft Dynamics*. AFFDL-TR-71-7 (Vol. I), September 1971.
124. Marr, R. L.; and Neal, G. T.: Assessment of Model Testing of a Tilt-Proprotor VTOL Aircraft. Presented at the *AHS Mid-East Region Symposium on the Status of Testing and Modeling Techniques for V/STOL Aircraft*, Essington, PA, Oct. 26-28, 1972.
125. Baird, E. F.; Bauer, E. M.; and Kohn, J. S.: Model Tests and Analysis of Prop-Rotor Dynamics for Tilt-Rotor Aircraft. Presented at the *AHS Mid-East Region Symposium on the Status of Testing and Modeling Techniques for V/STOL Aircraft*, Essington, PA, Oct. 26-28, 1972.
126. Kvaternik, R. G.; and Kohn, J. S.: *An Experimental and Analytical Investigation of Proprotor Whirl Flutter*. NASA TP 1047, December 1977.
127. Edenborough, H. K.; Gaffey, T. M.; and Weiberg, J. A.: Analyses and Tests Confirm Design of Proprotor Aircraft. *AIAA 4th Aircraft Design, Flight Test, and Operations Meeting*, Los Angeles, CA, August 7-9, 1972.
128. Popelka, D.; Sheffler, M.; and Bilger, J.: Correlation of Test and Analysis for the 1/5 Scale V-22 Aeroelastic Model. Presented at the *41st Annual Forum of the American Helicopter Society*, Fort Worth, TX, May 15-17, 1985. (Also, *J. Amer. Hel. Soc.*, Vol. 32, No. 2, April 1987, pp. 21-33).
129. Settle, T. B.; and Kidd, D. L.: Evolution and Test History of the V-22 0.2-Scale Aeroelastic Model. *Journal of the American Helicopter Society*, Vol. 37, No. 1, January 1992, pp. 31-45.
130. Settle, T. B.; and Nixon, M. W.: MAVSS Control of an Active Flaperon for Tiltrotor Vibration Reduction. *53rd Annual Forum of the American Helicopter Society*, Virginia Beach, VA, April 29-May 1, 1997.
131. Popelka, D.; Lindsay, D.; Parham, T.; Berry, V.; and Baker, D.: Results of an Aeroelastic Tailoring Study for a Composite Tiltrotor Wing. *51st Annual Forum of the American Helicopter Society*, Fort Worth, TX, May 9-11, 1995.
132. Corso, L. M.; Popelka, D. A.; and Nixon, M. W.: Design, Analysis, and Test of a Composite Tailored Tiltrotor Wing. Presented at the *53rd Annual Forum of the American Helicopter Society*, Virginia Beach, VA, April 29-May 1, 1997.
133. Nixon, M. W.; Piatak, D. J.; Corso, L. M.; and Popelka, D. A.: Aeroelastic Tailoring for Stability Augmentation and Performance Enhancements of Tiltrotor Aircraft. Presented at the *55th Annual National Forum of the American Helicopter Society*, Montreal, Canada, May 25-27, 1999.
134. Nixon, M. W.; Kvaternik, R. G.; and Settle, T. B.: Tiltrotor Vibration Reduction through Higher Harmonic Control. Presented at the *53rd Annual Forum of the American Helicopter Society*, Virginia Beach, VA, April 29-May 1, 1997. (Also: *Journal of the American Helicopter Society*, July 1998, pp. 235-245).
135. Clarke, D. W.; Mohtadi, C.; and Tuffs, P. S.: Generalized Predictive Control – Parts I and II. *Automatica*, Vol. 23, No. 2, 1987, pp. 137-160.
136. Phan, M. Q.; and Juang, J-N: Predictive Feedback Controllers for Stabilization of Linear Multivariable Systems. *AIAA Guidance, Navigation and Control Conference*, San Diego, CA, July 29-31, 1996.
137. Juang, J-N; and Phan, M. Q.: Deadbeat Predictive Controllers. *Journal of the Chinese (Taiwanese) Society of Mechanical Engineers*, Vol. 19, No. 1, Jan.-Feb. 1998, pp. 25-37.
138. Juang, J-N; and Eure, K. W.: *Predictive Feedback and Feedforward Control for Systems with Unknown Disturbances*. NASA TM-1998-208744, December 1998.

Table 1.- General Aeroelastic Scale Factors Applicable to Rotorcraft Models in TDT for Equal Lock Numbers (Mass Ratios) and Advance Ratios (Reduced Frequencies)

Parameter	Mach Numbers Equal				Froude Numbers Equal			
	General	Air	R-12	R-134a	General	Air	R-12	R-134a
Length	L	L	L	L	L	L	L	L
Mass	$L^3 \rho$	$L^3 \rho$	$L^3 \rho$	$L^3 \rho$	$L^3 \rho$	$L^3 \rho$	$L^3 \rho$	$L^3 \rho$
Time	$L (\gamma RT)^{-1/2}$	$L T^{-1/2}$	$2.23 L T^{-1/2}$	$2.07 L T^{-1/2}$	$L^{1/2} g^{-1/2}$	$L^{1/2}$	$L^{1/2}$	$L^{1/2}$
Mach number	1	1	1	1	$(Lg/\gamma RT)^{1/2}$	$(L/T)^{1/2}$	$2.23(L/T)^{1/2}$	$2.07(L/T)^{1/2}$
Froude number	$(Lg)^{-1} (\gamma RT)$	$L^{-1} T$	$.202 L^{-1} T$	$.234 L^{-1} T$	1	1	1	1
Reynolds number	$L \rho \mu^{-1} (\gamma RT)^{1/2}$	$L \rho T^{-.26}$	$.449 L \rho \mu^{-1} T^{1/2}$	$.484 \rho \mu^{-1} T^{1/2}$	$L^{3/2} \rho \mu^{-1} g^{1/2}$	$L^{3/2} \rho T^{-.76}$	$L^{3/2} \rho \mu^{-1}$	$L^{3/2} \rho \mu^{-1}$
Force	$L^2 \rho (\gamma RT)$	$L^2 \rho T$	$.202 L^2 \rho T$	$.234 L^2 \rho T$	$L^3 \rho g$	$L^3 \rho$	$L^3 \rho$	$L^3 \rho$
Speed	$(\gamma RT)^{1/2}$	$T^{1/2}$	$.449 T^{1/2}$	$.484 T^{1/2}$	$L^{1/2} g^{1/2}$	$L^{1/2}$	$L^{1/2}$	$L^{1/2}$
Acceleration	$L^{-1} (\gamma RT)$	$L^{-1} T$	$.202 L^{-1} T$	$.234 L^{-1} T$	g	1	1	1
Frequency	$L^{-1} (\gamma RT)^{1/2}$	$L^{-1} T^{1/2}$	$.449 L^{-1} T^{1/2}$	$.484 L^{-1} T^{1/2}$	$L^{-1/2} g^{1/2}$	$L^{-1/2}$	$L^{-1/2}$	$L^{-1/2}$
Angular Accel.	$L^{-2} (\gamma RT)$	$L^{-2} T$	$.202 L^{-2} T$	$.234 L^{-2} T$	$L^{-1} g$	L^{-1}	L^{-1}	L^{-1}
Moment, Work	$L^3 \rho (\gamma RT)$	$L^3 \rho T$	$.202 L^3 \rho T$	$.234 L^3 \rho T$	$L^4 \rho g$	$L^4 \rho$	$L^4 \rho$	$L^4 \rho$
Power	$L^2 \rho (\gamma RT)^{3/2}$	$L^2 \rho T^{3/2}$	$.091 L^2 \rho T^{3/2}$	$.113 L^2 \rho T^{3/2}$	$L^{7/2} \rho g^{3/2}$	$L^{7/2} \rho$	$L^{7/2} \rho$	$L^{7/2} \rho$
Moment of Inertia	$L^5 \rho$	$L^5 \rho$	$L^5 \rho$	$L^5 \rho$	$L^5 \rho$	$L^5 \rho$	$L^5 \rho$	$L^5 \rho$
Pressure, Stress	$\rho (\gamma RT)$	ρT	$.202 \rho T$	$.234 \rho T$	$L \rho g$	$L \rho$	$L \rho$	$L \rho$
Stiffness (EI,GJ)	$L^4 \rho (\gamma RT)$	$L^4 \rho T$	$.202 L^4 \rho T$	$.234 L^4 \rho T$	$L^5 \rho g$	$L^5 \rho$	$L^5 \rho$	$L^5 \rho$

Scale factors equal ratio of model to full-scale values of the quantities indicated; e.g., $L = L_M/L_F$, $\gamma RT = (\gamma RT)_M/(\gamma RT)_F$, etc., where T = temperature, ρ = test medium density, R = gas constant, μ = viscosity, γ = specific heat ratio for gas, and g is the acceleration due to gravity.

Air constants based on $\gamma = 1.4$, $R = 1716 \text{ ft}^2/\text{sec}^2 \text{ }^\circ\text{R}$

R-12 constants based on $\gamma = 1.137$, $R = 427.3 \text{ ft}^2/\text{sec}^2 \text{ }^\circ\text{R}$ (95% R-12/air mixture)

R-134a constants based on $\gamma = 1.114$, $R = 505.3 \text{ ft}^2/\text{sec}^2 \text{ }^\circ\text{R}$ (95% R-134a/air mixture)

Table 2.- Chronology of Tiltrotor Aeroelastic Analysis Development at AB/TDT

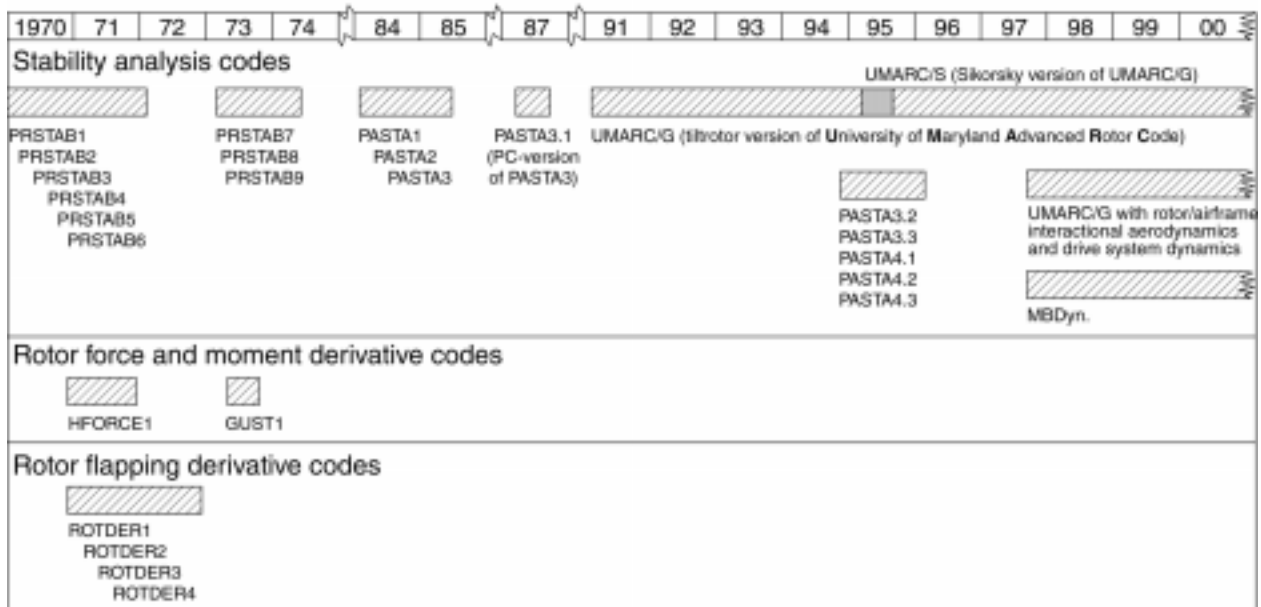


Table 3.- Scale factors for 1/7.5-scale aeroelastic model of Bell Model 266

Parameter	Scale Factor (Model/Airplane)
Froude number	1.00
Lock number	1.00
Mach number	0.365
Advance ratio	1.00
Reynolds number	0.0487
Length	0.1333
Density	1.0
Velocity	0.365
Time	0.365
Mass	0.00237
Frequency	2.738
Force	0.002369
Bending moment	0.0003157
Stiffness	0.000042095
Bending spring rate	0.01777
Torsion spring rate	0.0003157

Table 5.- Scale factors for 1/4.5-scale aeroelastic model of Grumman Helicat

Parameter	Scale Factor (Model/Airplane)
Froude number	1.00
Lock number	1.00
Mach number	1.00
Advance ratio	1.00
Reynolds number	0.1047
Length	0.222
Density	1.0
Velocity	0.471
Time	0.471
Mass	0.01099
Frequency	2.12
Force	0.01099
Bending stiffness	0.0005420
Torsion stiffness	0.0005420
Bending spring rate	0.05
Torsion spring rate	0.002439

Table 4.- Scale factors for 1/5-scale aeroelastic model of Bell Model 300 tiltrotor

Parameter	Scale Factor (Model/Full-Scale)	
	Air	R-12
Froude number	1.0	1.0
Lock number	1.0	1.0
Mach number	0.447	1.016
Advance ratio	1.0	1.0
Reynolds number	0.0894	0.1265
Length	0.2	0.2
Density	1.0	1.0
Velocity	0.447	0.447
Time	0.447	0.447
Mass	0.008	0.008
Frequency	2.24	2.24
Force	0.008	0.008
Bending moment	0.0016	0.0016
Stiffness	0.00032	0.00032
Bending spring rate	0.04	0.04
Torsion spring rate	0.0016	0.0016

Table 6.- Scale factors for 1/5-scale aeroelastic model of Bell/Boeing V-22 tiltrotor

Parameter	Scale Factor (Model/Full-Scale)	
	Air	R-12
Froude number	1.0	1.0
Lock number	1.0	1.0
Mach number	0.447	1.016
Advance ratio	1.0	1.0
Reynolds number	0.0894	0.1265
Length	0.2	0.2
Density	1.0	1.0
Velocity	0.447	0.447
Time	0.447	0.447
Mass	0.008	0.008
Frequency	2.24	2.24
Force	0.008	0.008
Bending moment	0.0016	0.0016
Stiffness	0.00032	0.00032
Bending spring rate	0.04	0.04
Torsion spring rate	0.0016	0.0016



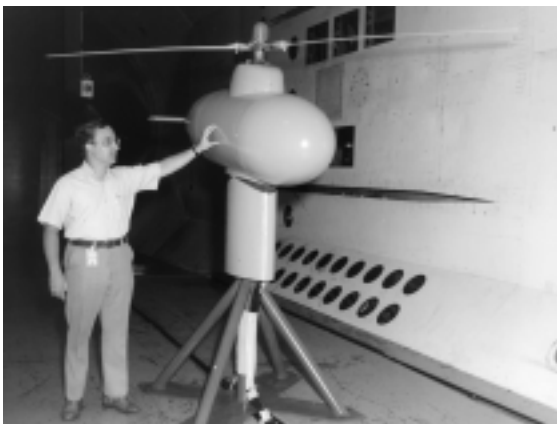
Figure 1.- The Langley Transonic Dynamics Tunnel (TDT).



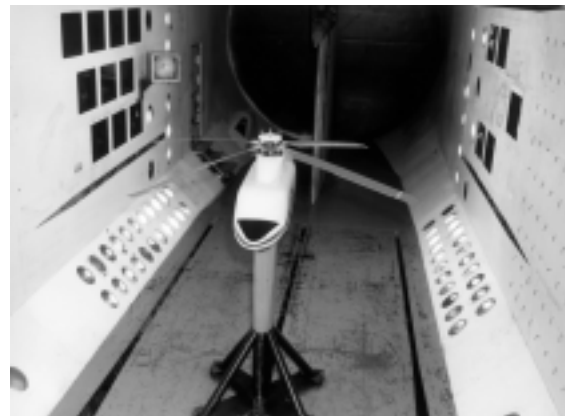
(a) Lockheed Aircraft Company helicopter testbed



(c) Generalized Rotor Aeroelastic Model (GRAM) testbed



(b) Bell Helicopter Company helicopter testbed



(d) Aeroelastic Rotor Experimental System (ARES) testbed

Figure 2.- Helicopter testbeds used in TDT.



Figure 3.- Some tiltrotor models tested in the TDT.

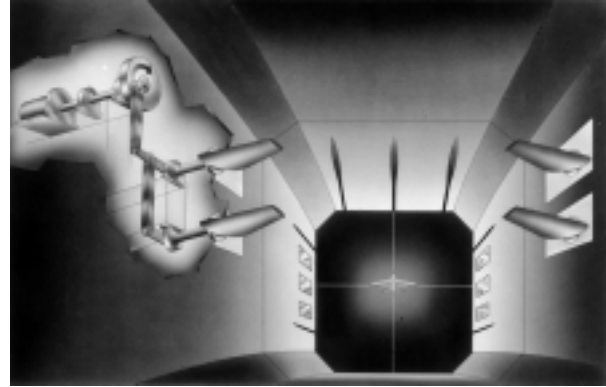
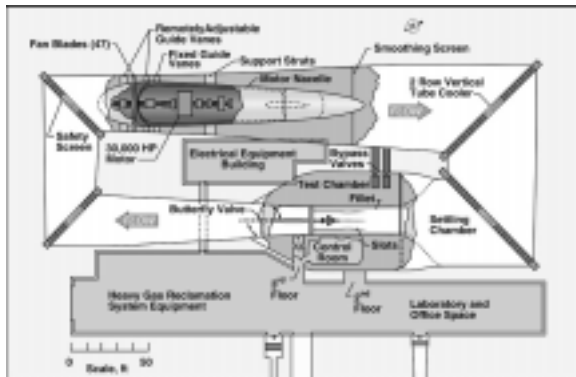
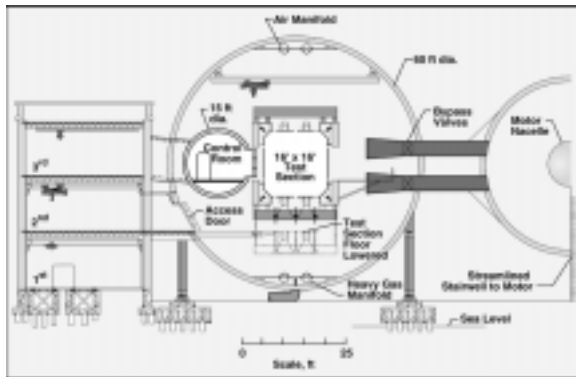


Figure 5.- Sketch of TDT airstream oscillator showing cutaway of driving mechanism.



(a) Plan view



(b) Cross-section through test section

Figure 4.- General arrangement of TDT.

$$\mu = 0.30, M(1.0, 90) = 0.85$$

$$Re_{model} = 4.5 \times 10^6$$

$$Re_{full} = 10 \times 10^6 \text{ scale}$$

- Model (R-12), $\alpha_s = 5^\circ$
- ◐ Full Scale (air), $\alpha_s = 5^\circ$
- Model (R-12), $\alpha_s = 0^\circ$
- ◑ Full Scale (air), $\alpha_s = 0^\circ$
- ◇ Model (R-12), $\alpha_s = -5^\circ$
- ◒ Full Scale (air), $\alpha_s = -5^\circ$
- △ Model (R-12), $\alpha_s = -10^\circ$
- ◕ Full Scale (air), $\alpha_s = -10^\circ$
- ▽ Model (R-12), $\alpha_s = -15^\circ$
- ◔ Full Scale (air), $\alpha_s = -15^\circ$

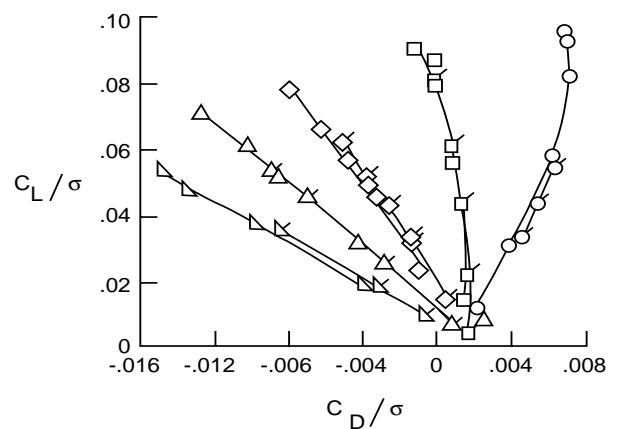


Figure 6.- Full-scale and model rotor performance.

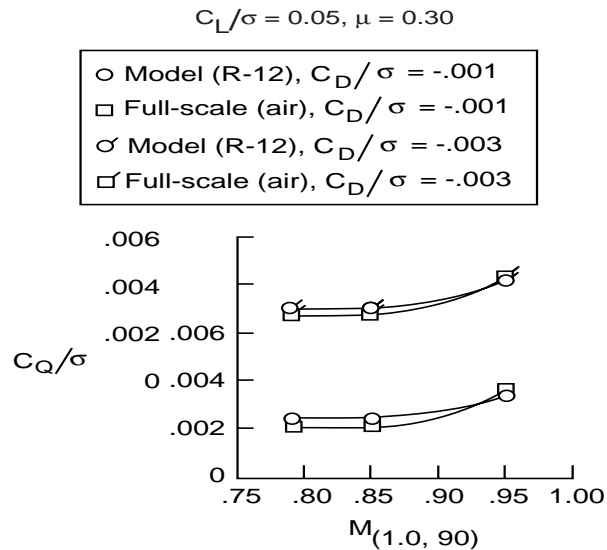


Figure 7.- Full-scale and model rotor performance.

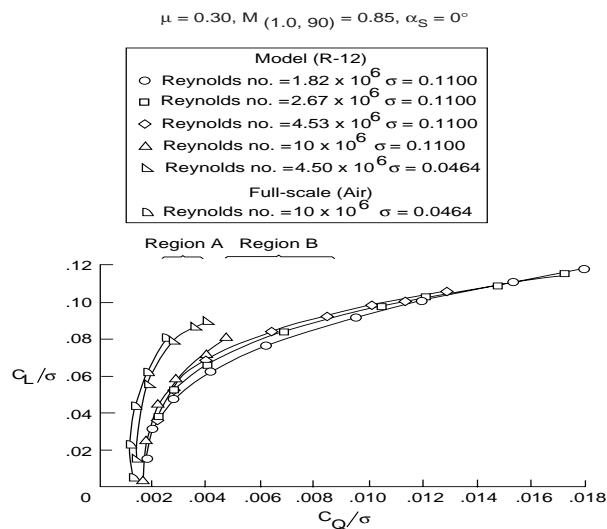


Figure 8.- Effect of scaling parameters on Freon model and full-scale rotor performance.



Figure 9.- GRAM testbed with AH-1G rotor.



Figure 10.- GRAM testbed with hinged wide-chord rotor.



Figure 11.- GRAM testbed with wide-chord rotor (no mid-span flap hinge).

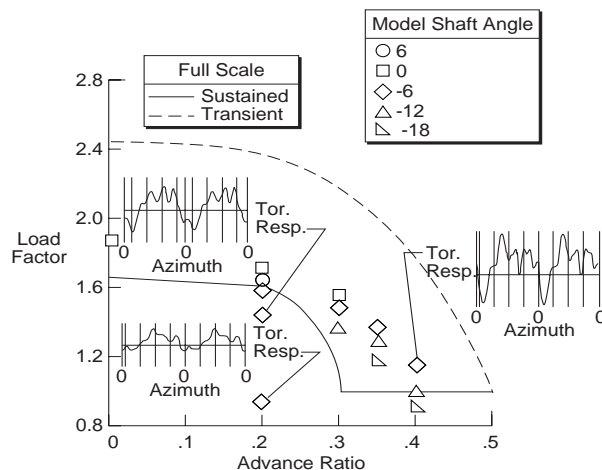


Figure 12.- Model Cobra test conditions compared to full-scale flight envelope with selected blade torsional waveforms.

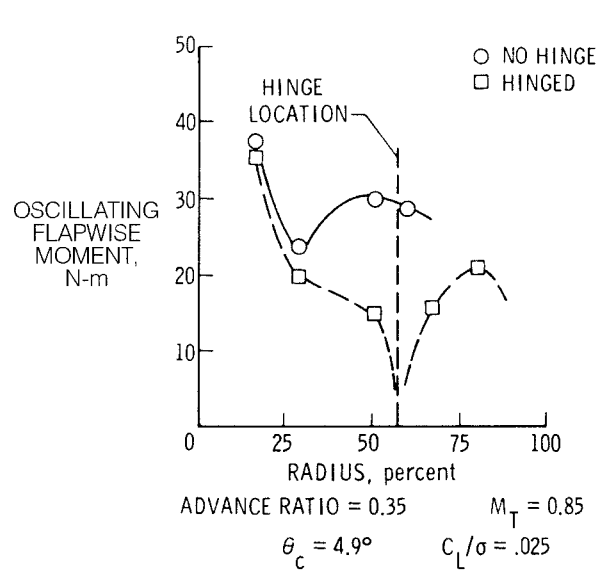


Figure 13.- Comparison of oscillatory blade loadings as a function of span for the wide-chord teetering rotors.

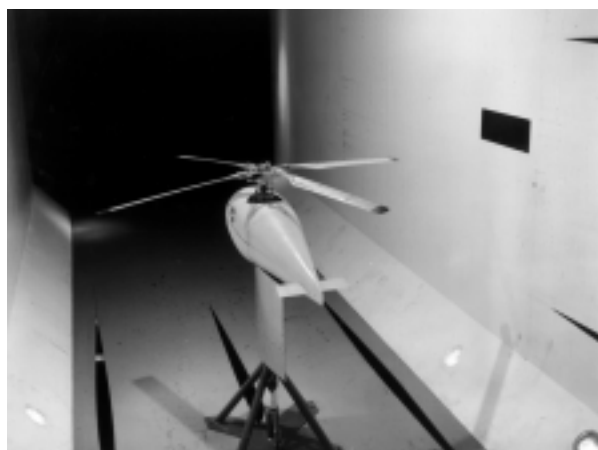


Figure 14.- Flex-hinge rotor mounted on the GRAM testbed.

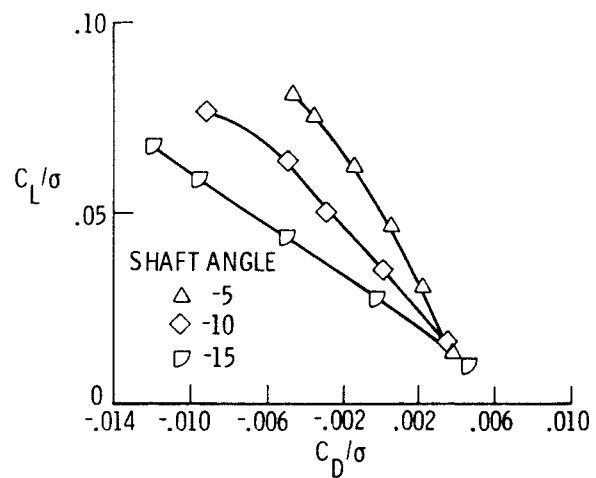
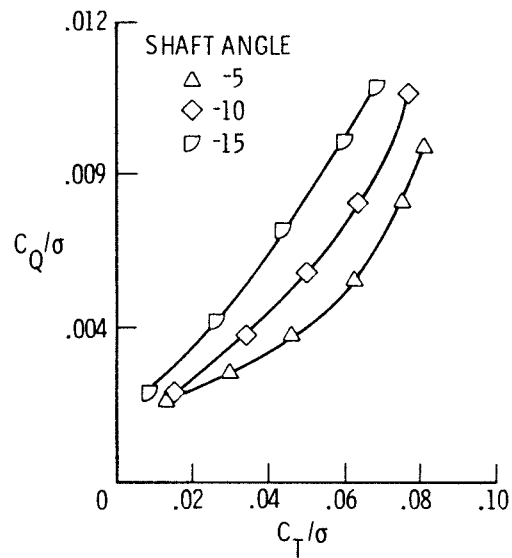


Figure 15.- Rotor performance data for the flex-hinge rotor at an advance ratio of 0.35.

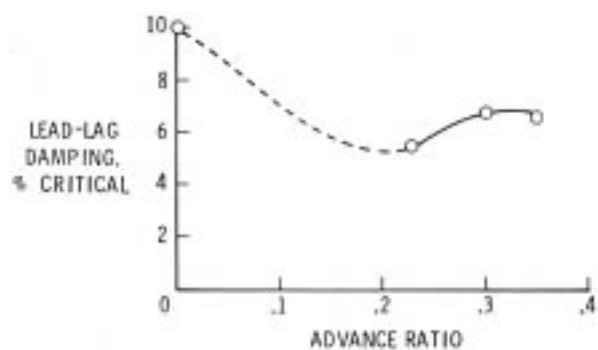


Figure 16.- Blade lead-lag mode damping as a function of advance ratio for the flex-hinge rotor.

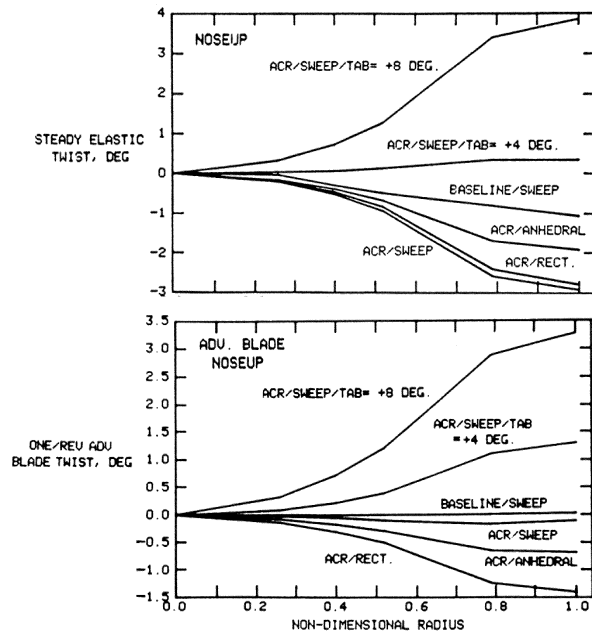


Figure 17.- One/rev lateral twist of ACR configurations and baseline rotor at $\mu = 0.30$, $\alpha_s = -5$ deg, and $C_L / \sigma = 0.08$.

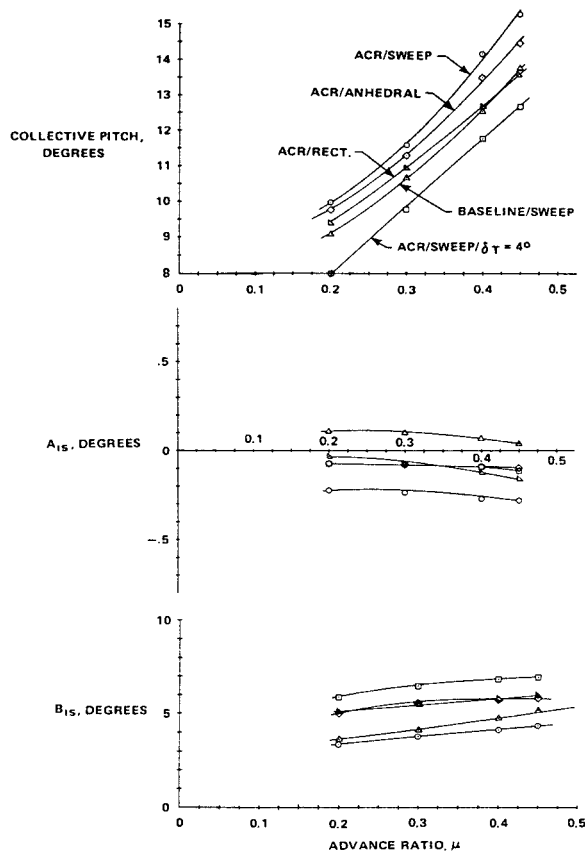


Figure 18.- Trim requirements of ACR and baseline model rotors at $C_L / \sigma = 0.07$ and $f = 30$ ft².

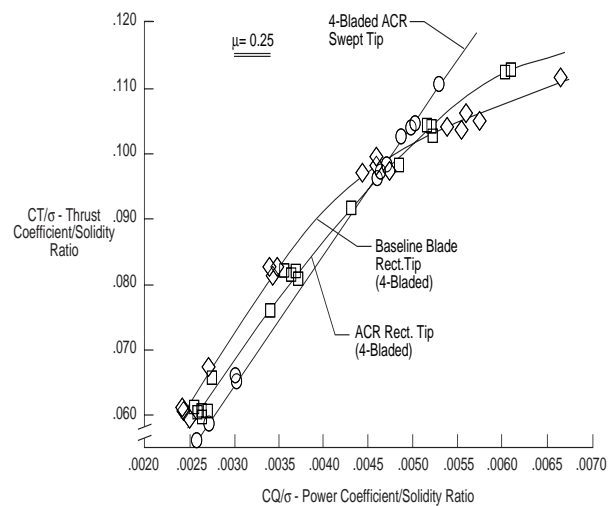


Figure 19.- Coefficient of thrust / solidity ratio vs. coefficient of power / solidity ratio at $\mu = 0.25$.

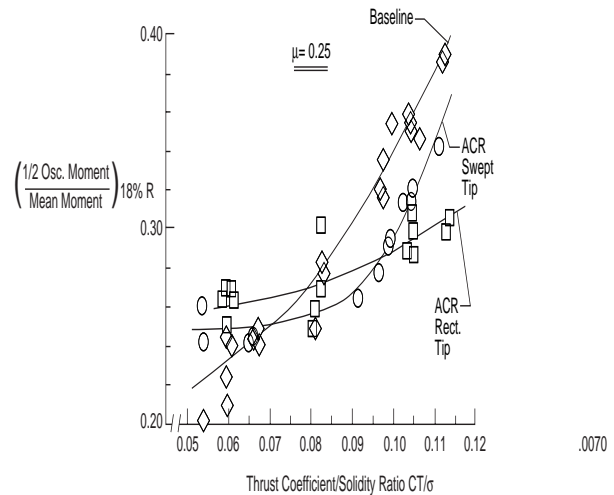


Figure 20.- Nondimensional oscillatory flapwise bending moment at 18% radius vs. thrust coefficient / solidity ratio at $\mu = 0.25$.

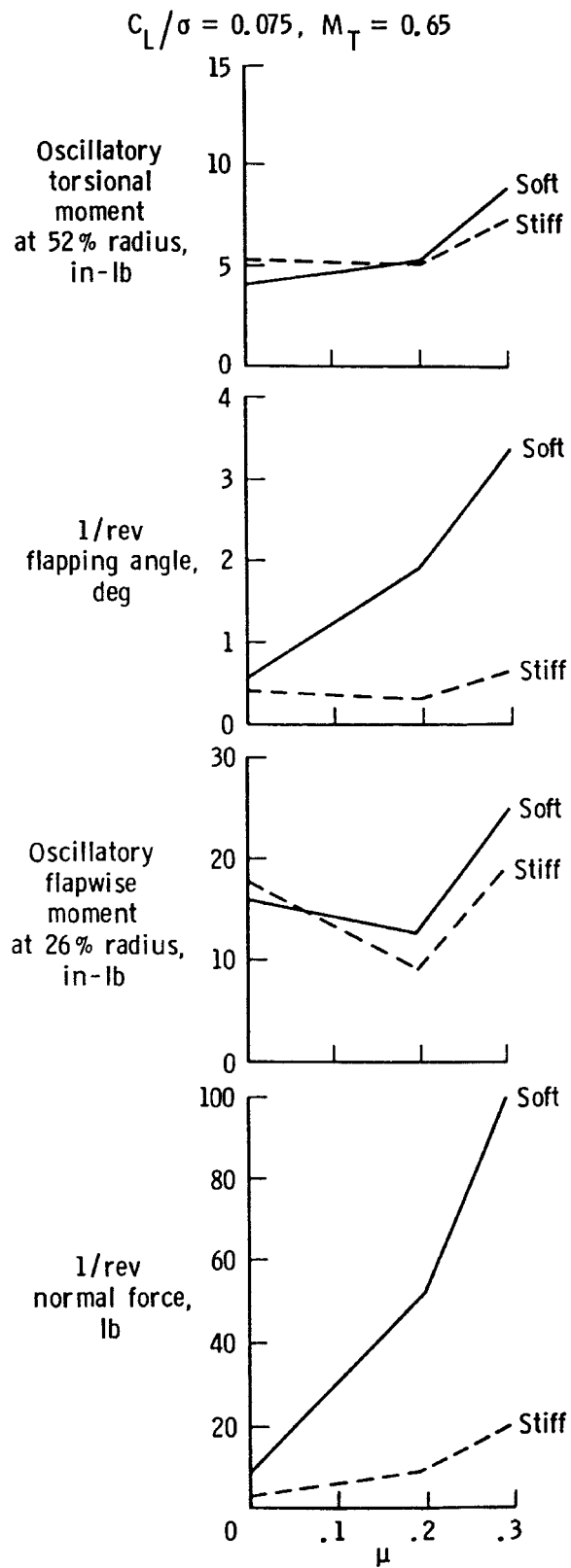


Figure 21.- Effect of 4 deg tab deflection on torsionally soft and stiff blade response.

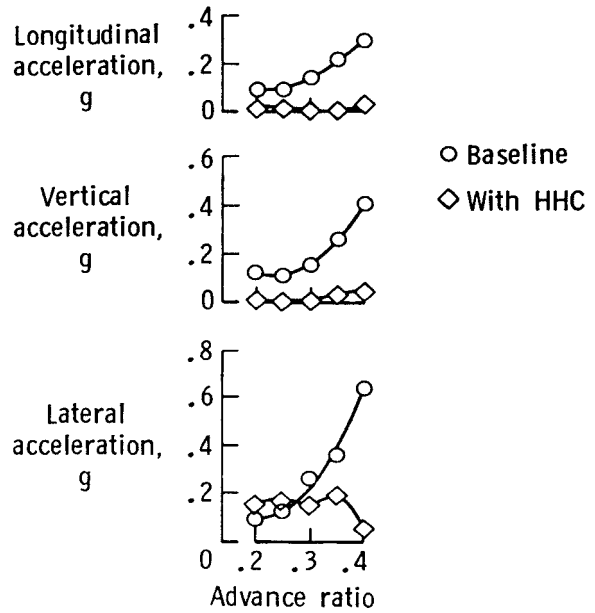


Figure 22.- Effect of higher harmonic control on fixed-system 4-per-rev vibration levels.

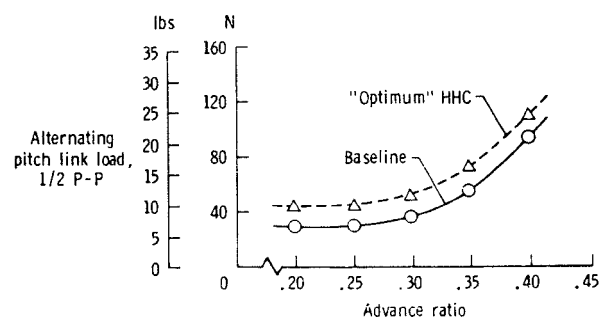


Figure 23.- Variation of alternating pitch link load (1/2 peak-to-peak values) with advance ratio.

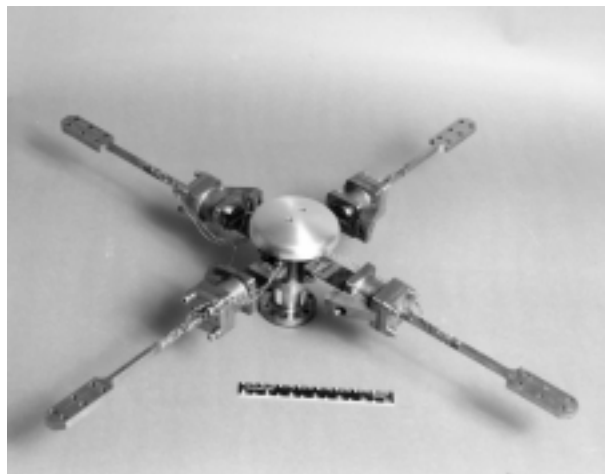


Figure 24.- Model hingeless rotor hub.

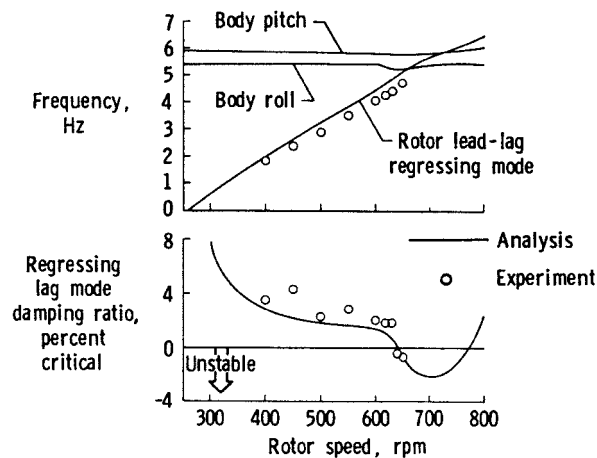


Figure 25.- Comparison of predicted and measured stability as a function of rotor speed in hover.

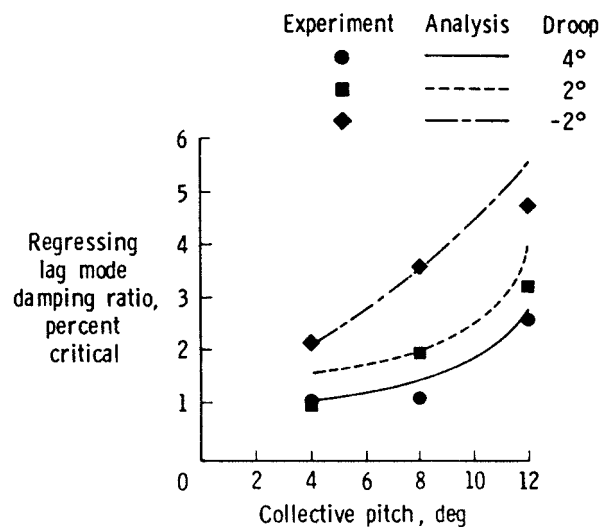


Figure 26.- Effect of blade droop angle on lead-lag damping at advance ratio = 0.30.

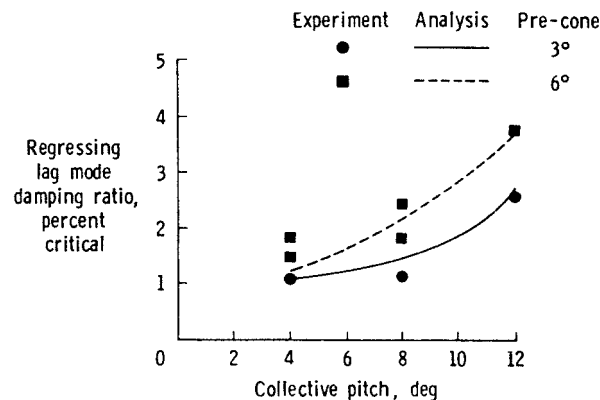


Figure 27. Effect of blade pre-cone angle on lead-lag damping at advance ratio = 0.30.

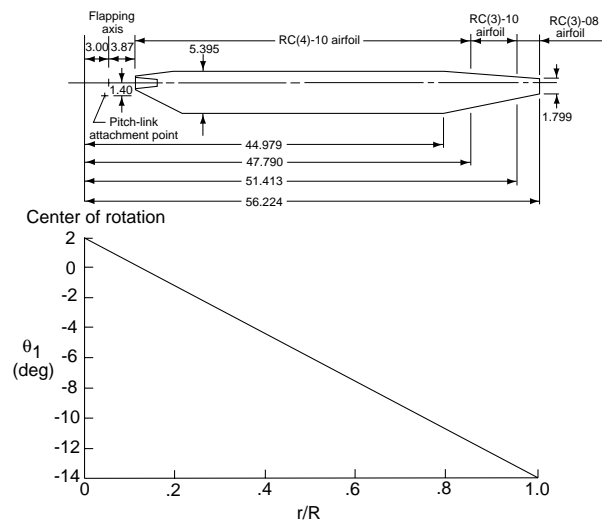


Figure 28.- Advanced rotor blade geometry and built-in twist distribution. Linear dimensions are in inches.

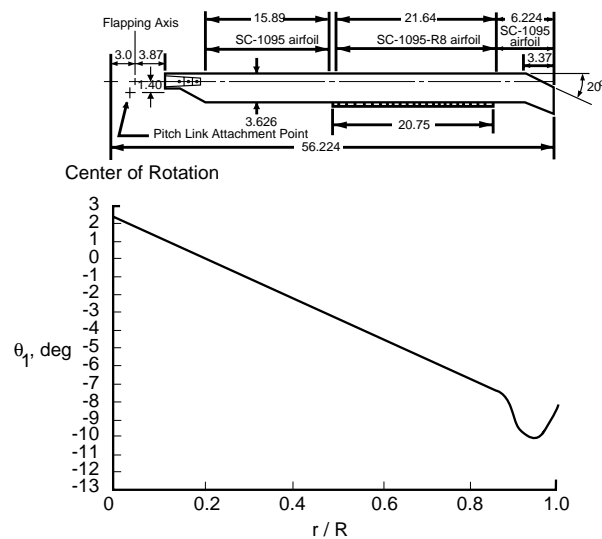


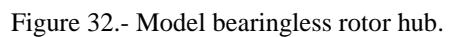
Figure 29.- Baseline rotor blade geometry and built-in twist distribution. Linear dimensions are in inches.



Figure 30.- Comparison of baseline and advanced rotor C_Q for 4000 ft geometric altitude, 95 deg F ambient temperature and vehicle equivalent parasite area of 29.94 ft².



Figure 31.- Comparison of 4-per-rev vertical fixed-system loads for baseline and advanced rotor configurations at 4000 ft geometric altitude, 95 deg F ambient temperature and vehicle equivalent parasite area of 29.94 ft².



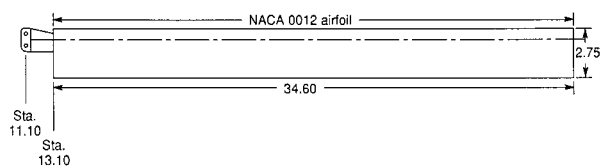


Figure 33.- Geometry of Froude-scaled model rotor blades. All dimensions are in inches.

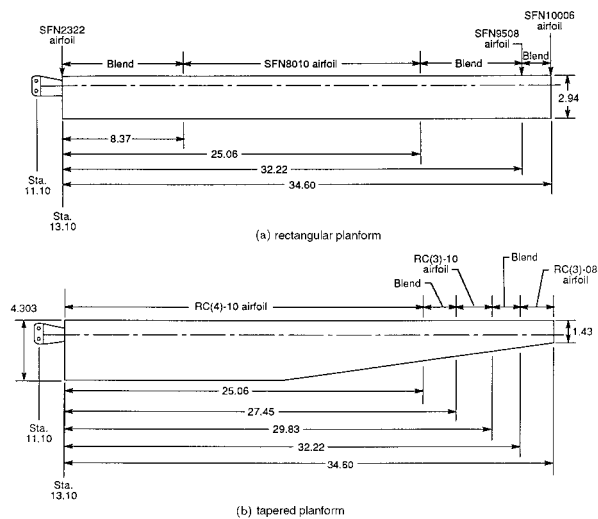


Figure 34.- Geometry of Mach-scaled model rotor blades. All dimensions are in inches.

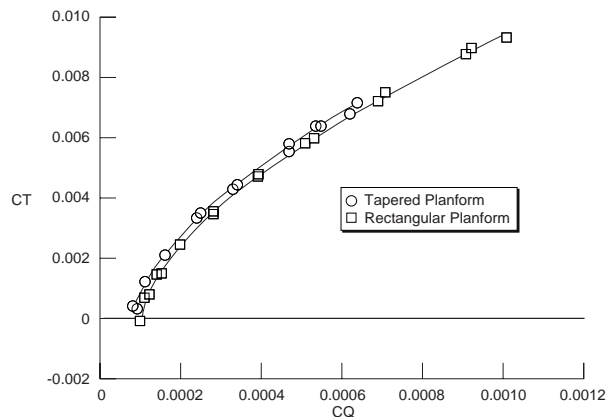


Figure 35.- Comparison of hover performance (IGE, $M_T = 0.626$) of the rectangular and tapered planform blades.

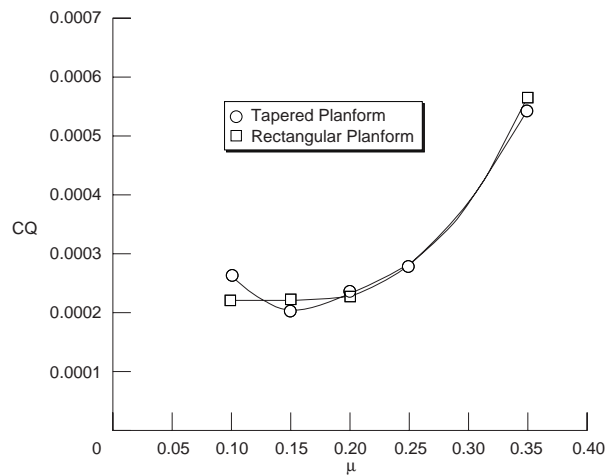


Figure 36.- Comparison of the forward flight performance of the rectangular and tapered planform blades (vehicle equivalent parasite area = 20.65 ft²).

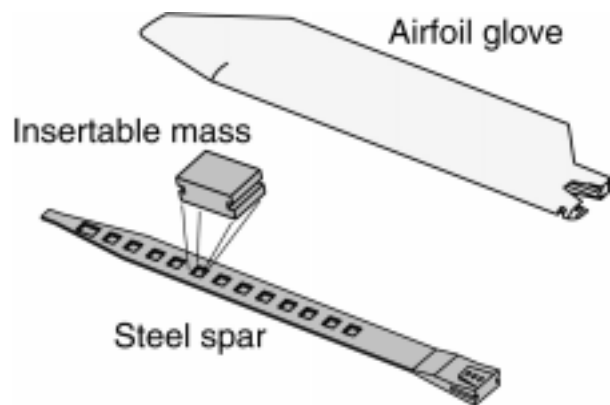


Figure 37.- Components of advanced model rotor blade used for vibration reduction research.

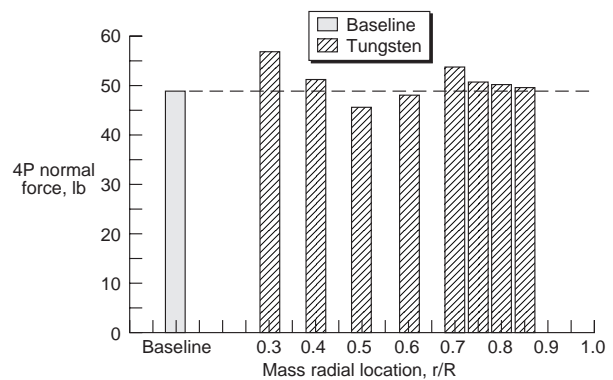


Figure 38.- Effect of non-structural mass on 4-per-rev fixed-system loads for $T = 285$ lbs and $\mu = 0.35$.

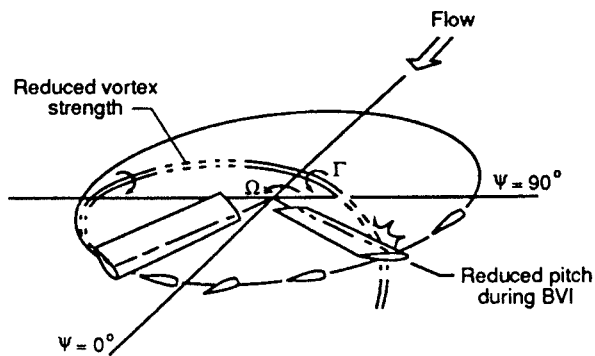


Figure 39.- Illustration of noise reduction concept.

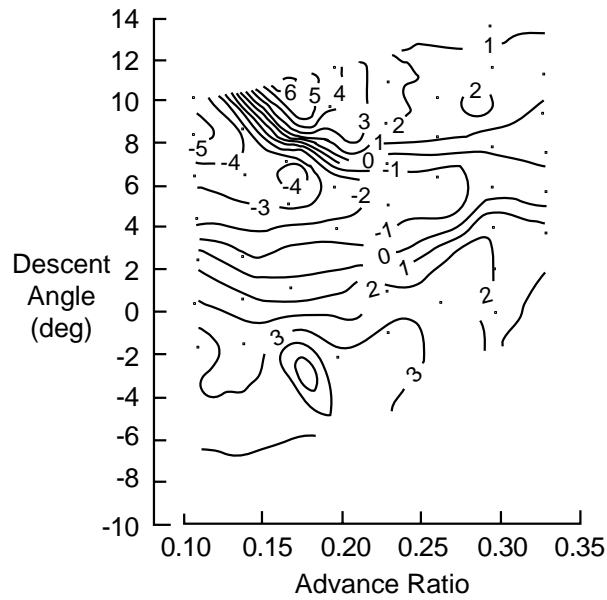


Figure 40.- Effect of higher harmonic pitch (HHP) on rotor noise levels (db).

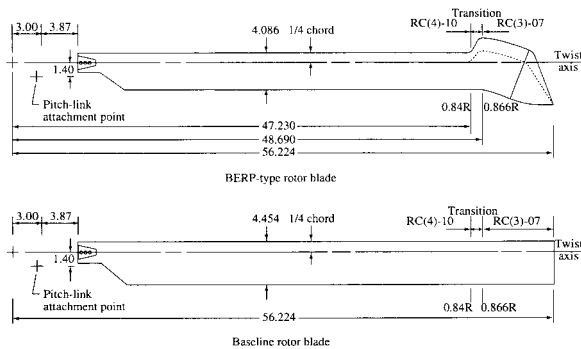


Figure 41.- BERP-type and baseline rotor blade geometries. Linear dimensions are in inches.

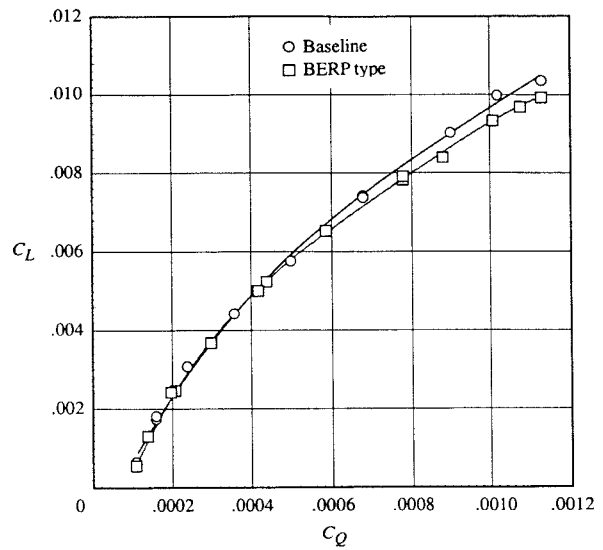


Figure 42.- Rotor hover performance at $M_T = 0.628$ and $z/d = 0.83$.

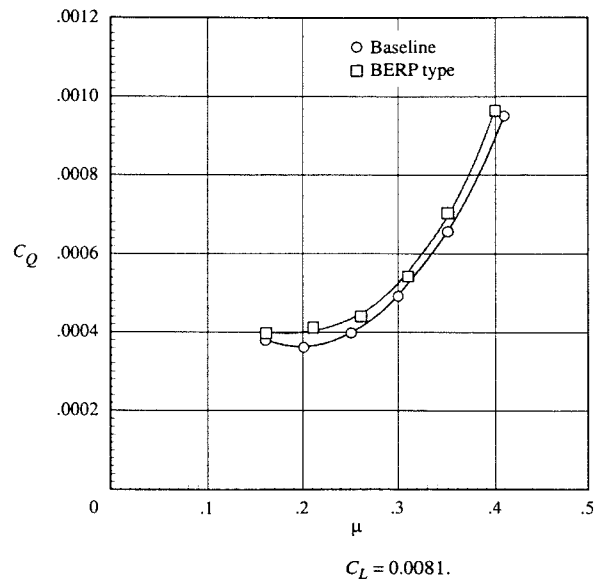


Figure 43.- Variation of rotor torque coefficient with advance ratio for $M_T = 0.628$ and vehicle equivalent parasite area = 29.94 ft².

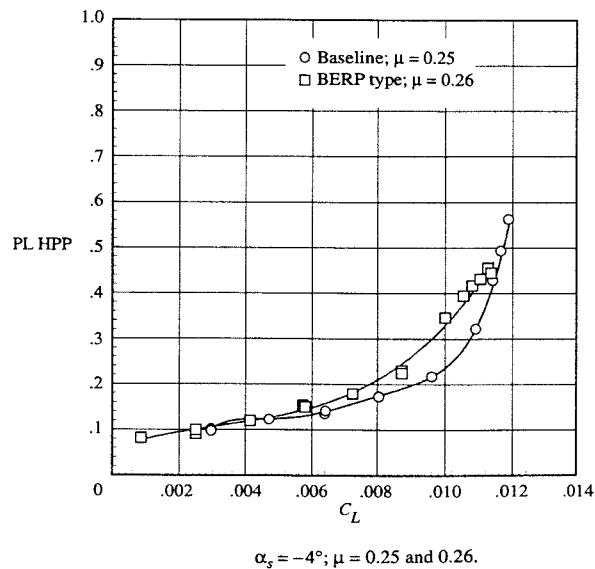


Figure 44.- Pitch-link oscillatory loads for baseline and BERP-type rotors at $\alpha_s = -4$ deg; $\mu = 0.25$ and 0.26 .

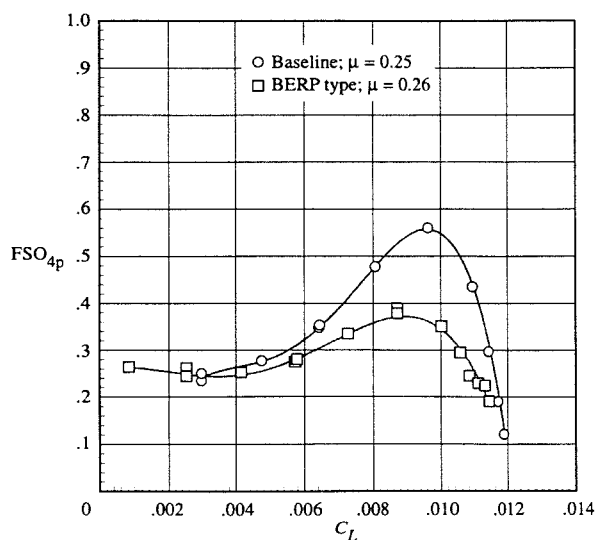


Figure 45.- The 4-per-rev vertical fixed-system loads for baseline and BERP-type rotors at $\alpha_s = -4$ deg; $\mu = 0.25$ and 0.26 .

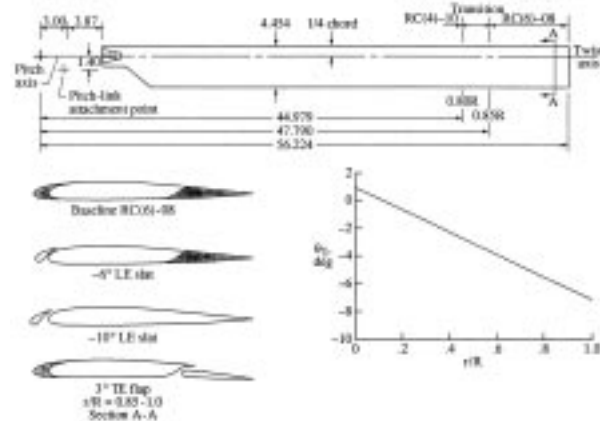


Figure 46.- HIMARCS-I rotor blade geometry and twist distribution. Linear dimensions in inches.

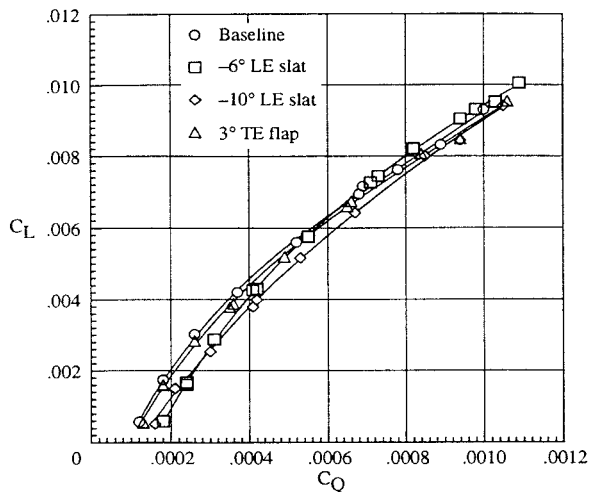


Figure 47.- Rotor hover performance at $M_T=0.627$ and $z/d=0.83$.

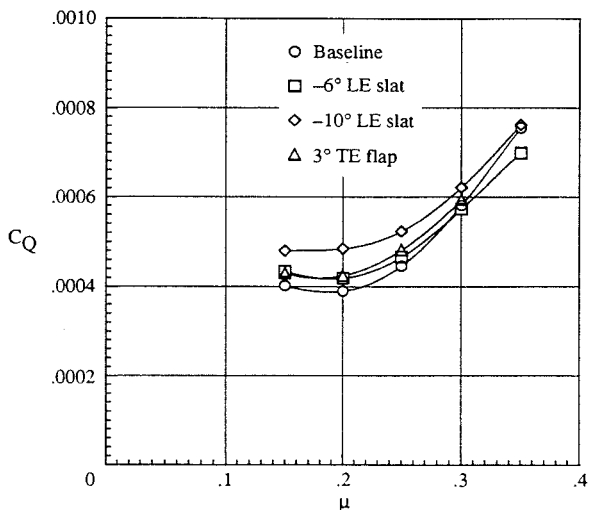


Figure 48.- Variation of rotor torque coefficient with advance ratio for $C_L = 0.0081$, $M_T = 0.627$ and vehicle equivalent parasite area = 29.94 ft^2 .

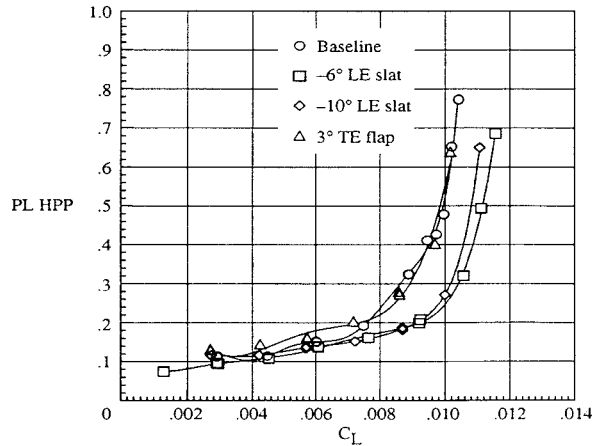


Figure 49.- Variation of pitch-link oscillatory loads with rotor lift coefficient for $M_T = 0.627$, $\mu = 0.25$, and $\alpha_S = -4$ deg.

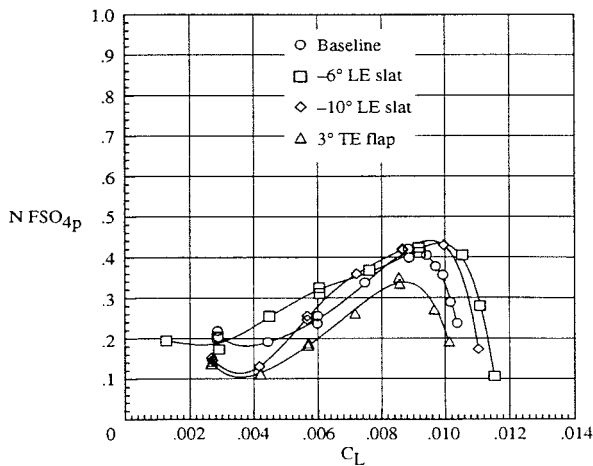


Figure 50.- Variation of 4-per-rev vertical fixed-system loads with rotor lift coefficient for $M_T = 0.627$, and $\alpha_S = -4$ deg.



Figure 51.- Baseline (Advanced S-61) model rotor blade.

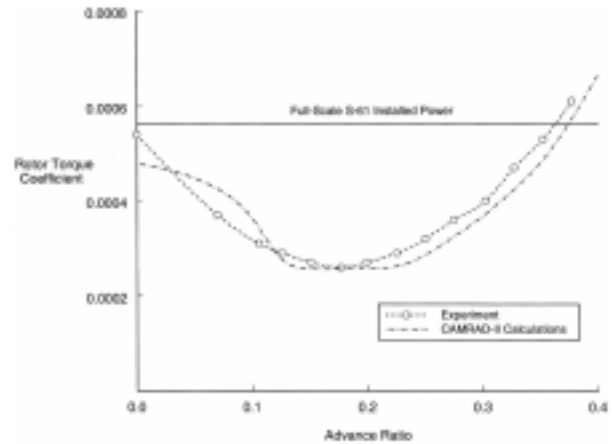


Figure 52.- Comparison of analytical and experimental forward flight rotor performance of advanced S-61 rotor at $GW = 20,000$ lbs, vehicle equivalent parasite area $= 34.55$ ft² and SLS.

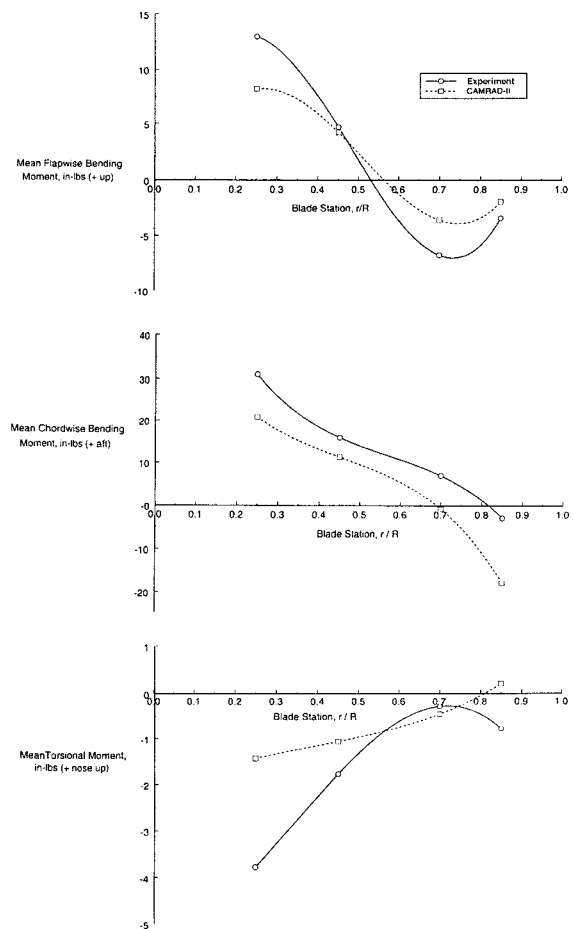


Figure 53.- Comparison of analytical and experimental mean blade bending and torsion moments for advanced S-61 rotor at $GW = 20,000$ lbs, advance ratio $= 0.25$, vehicle equivalent parasite area $= 34.55$ ft², and SLS.



Figure 54.- Bell/Boeing V-22 tiltrotor aircraft.

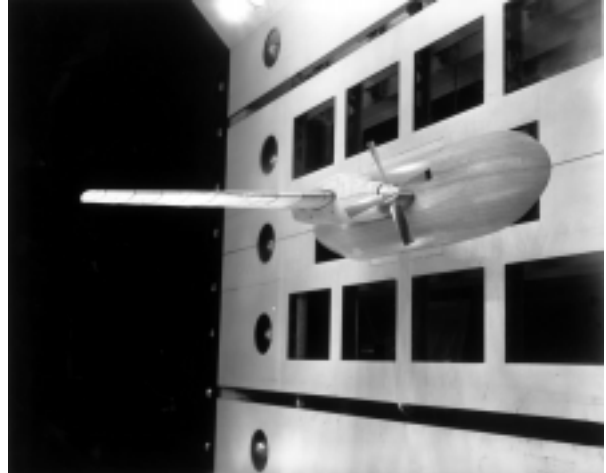


Figure 57.- Wing-mounted propeller/nacelle whirl flutter model.



Figure 55.- 1/8-size Lockheed Electra model in TDT for propeller whirl flutter investigation.



(a) Blades fixed like propeller

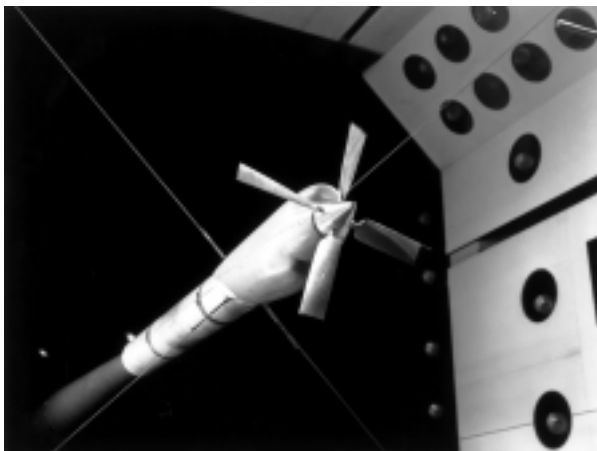


Figure 56.- Sting-mounted propeller/nacelle whirl flutter model.



(b) Blades free to flap

Figure 58.- Flapping-blade propeller whirl flutter model.



Figure 59.- Ducted fan whirl flutter model.

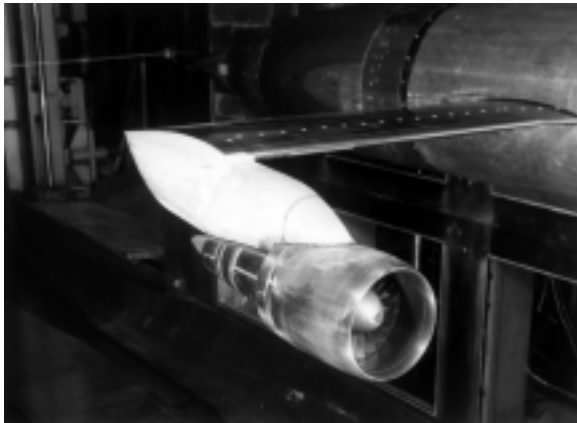


Figure 60.- Model of high bypass ratio fan-jet engine in Langley 8-foot Transonic Pressure Tunnel.

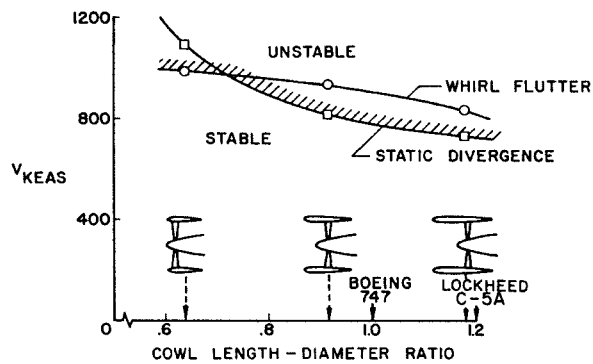


Figure 61.- Estimated stability boundaries for high bypass ratio fan-jet nacelle-pylon.

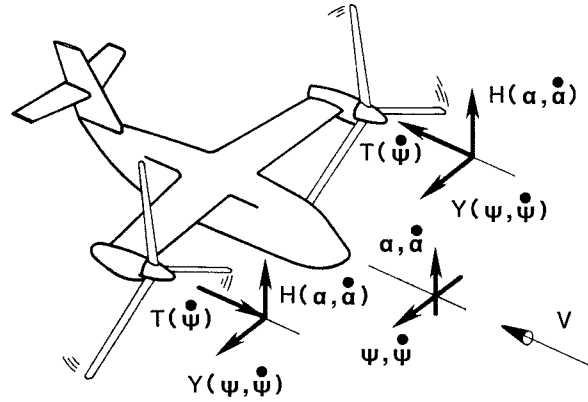


Figure 62.- Perturbation rotor-induced aerodynamic forces acting on a tiltrotor aircraft during pitching and yawing oscillations (rotors interconnected).



Figure 63.- Artist's conception of Bell Model 266 tiltrotor design evolved during the Army Composite Aircraft Program.

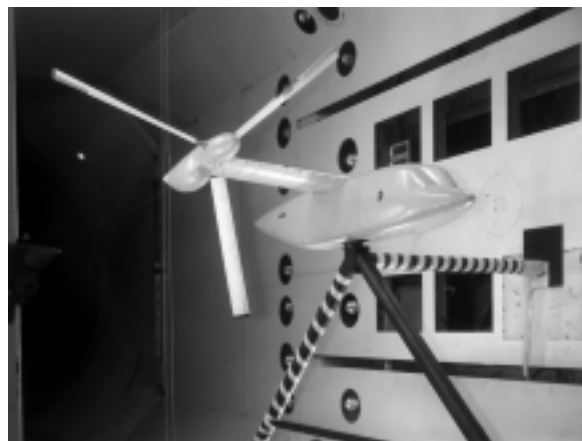


Figure 64.- 1/7.5-scale semispan aeroelastic model of Bell Model 266 in TDT.

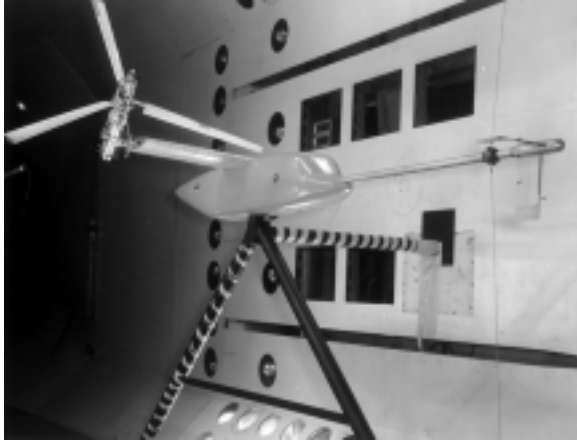


Figure 65.- 1/7.5-scale model in simulated conversion mode.

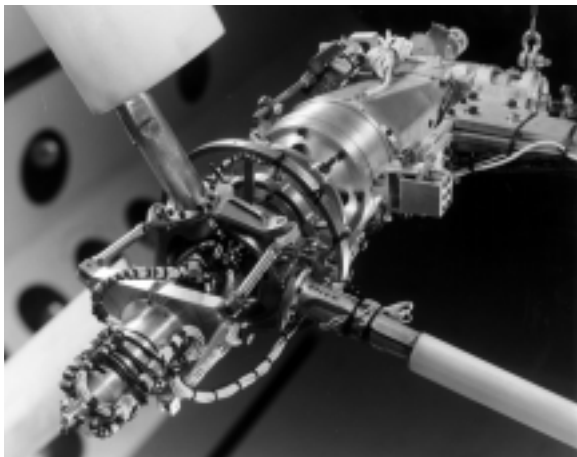


Figure 66.- Close-up view of model pylon with covers removed showing control system used for unpowered testing in airplane mode of flight.

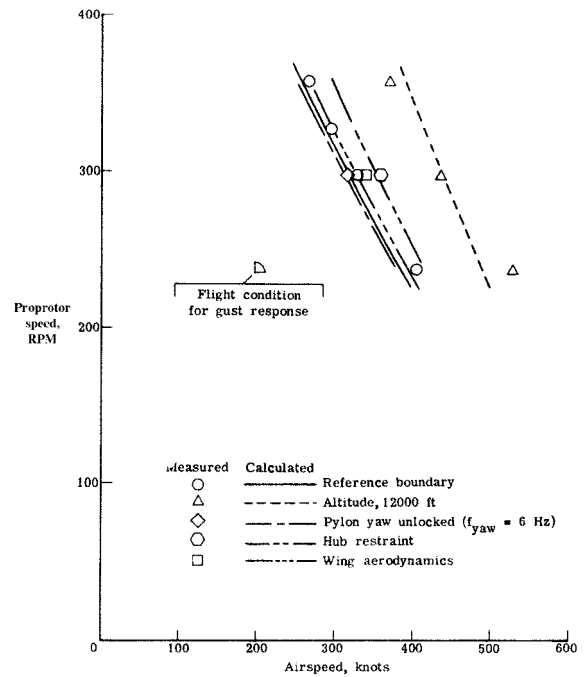


Figure 67.- Effect of some system parameters on proprotor/pylon/wing stability.

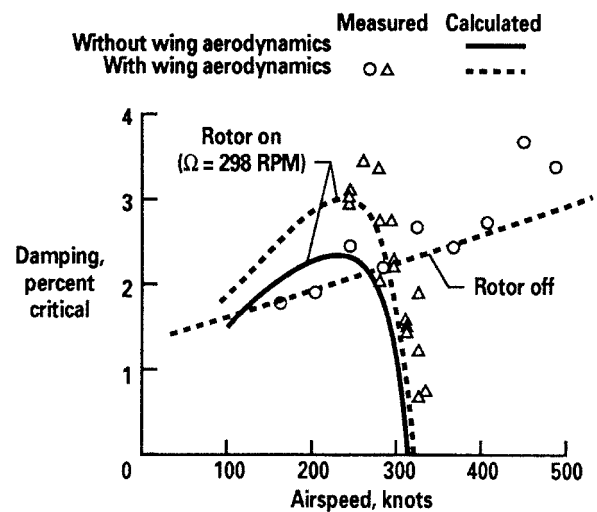


Figure 68.- Effect of proprotor aerodynamics on damping of wing beam mode.

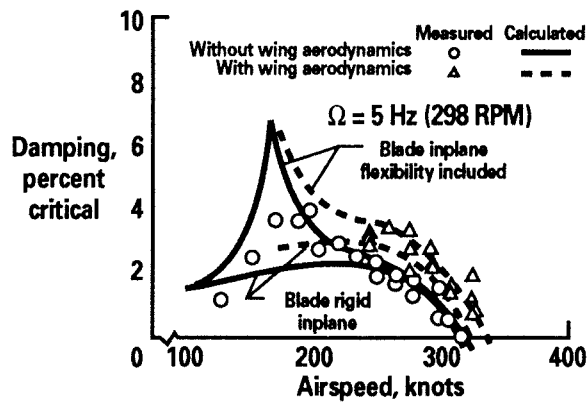


Figure 69.- Effect of wing aerodynamics and blade inplane flexibility on damping of wing beam mode.

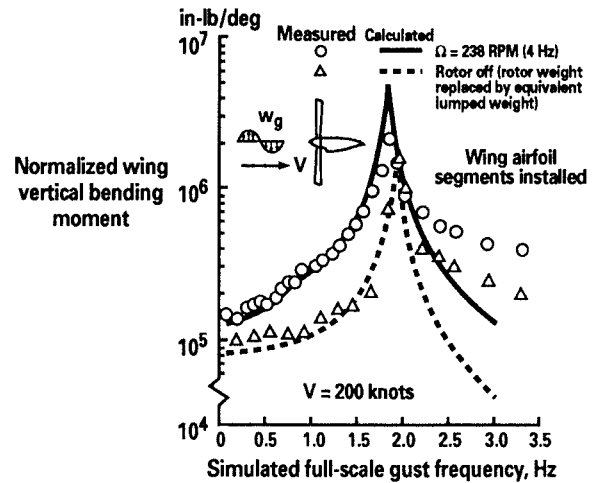


Figure 71.- Effect of propeller aerodynamics on frequency response of wing vertical bending moment during vertical gust excitation.

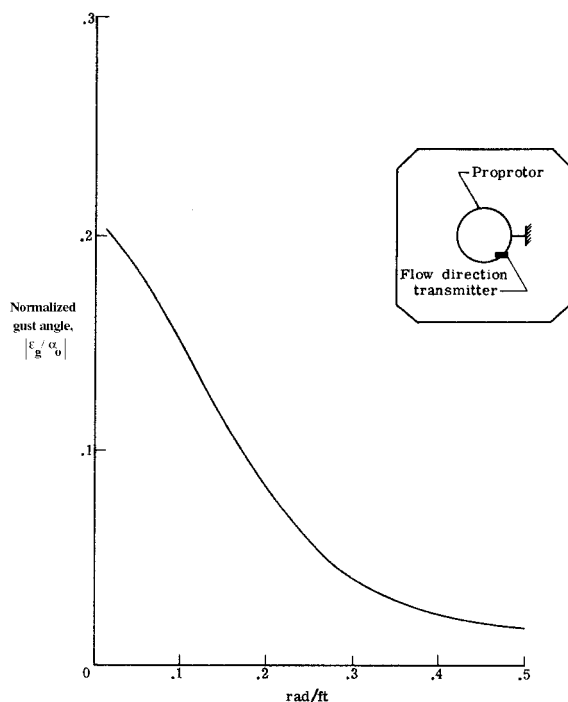


Figure 70.- Measured variation of gust-induced angle of attack with frequency of airstream oscillator.



Figure 72.- Model 266 configured for rotating and stop-start portion of folding propeller investigation.

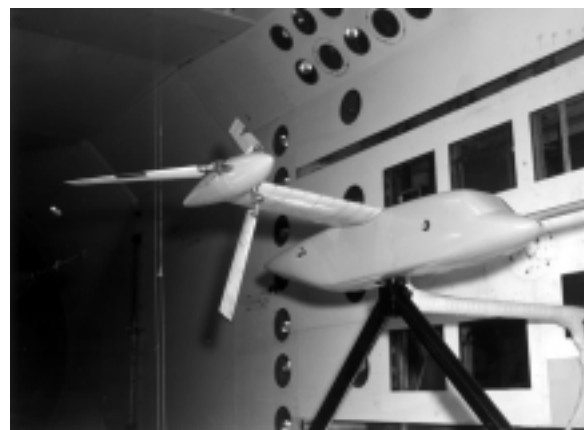


Figure 73.- Model 266 in simulated blade folding configuration.

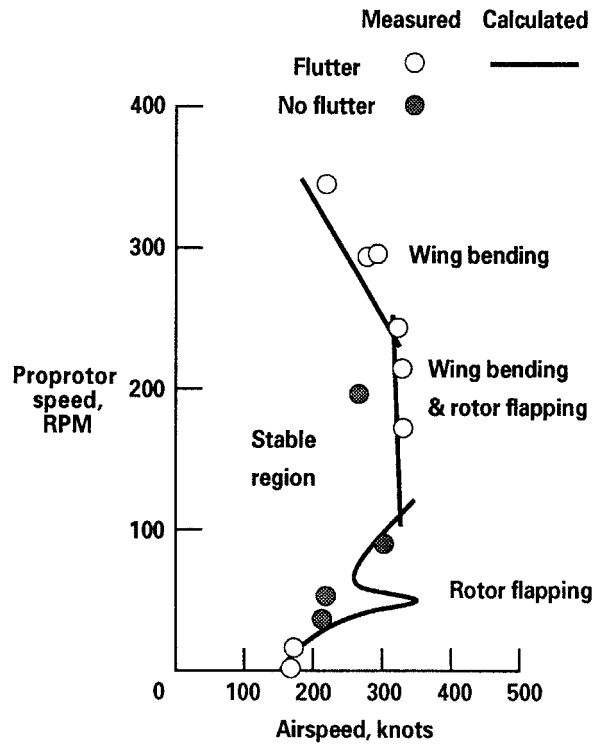


Figure 74.- Model 266 flutter boundaries showing variation in character of flutter modes as rpm is reduced to zero ($\delta_3 = -32^\circ$).

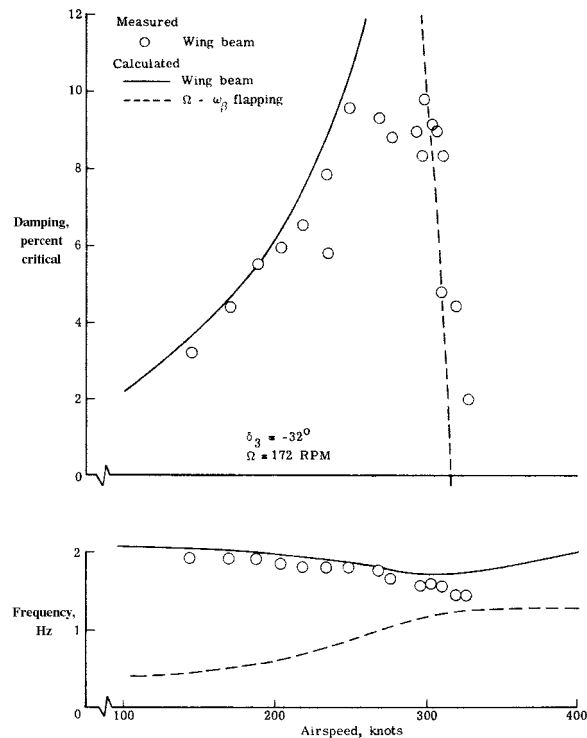


Figure 75.- System subcritical response for $\Omega = 172$ rpm case in figure 77.

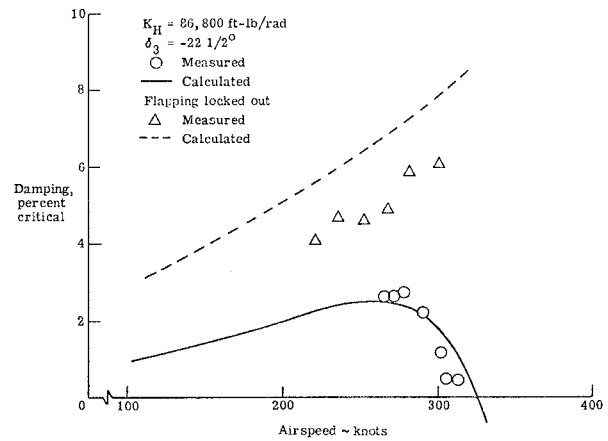


Figure 76.- Effect of blade flapping degree of freedom on wing beam mode damping ($\Omega = 300$ rpm).

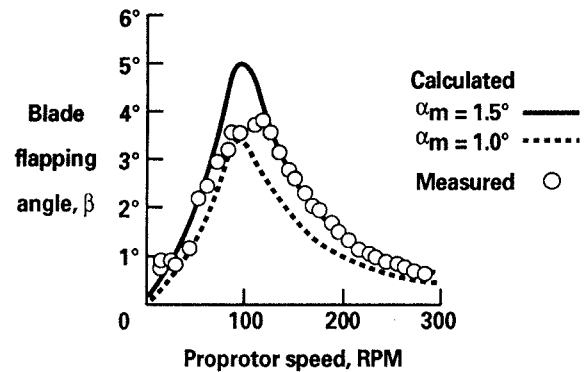


Figure 77.- Variation of blade steady-state flapping with rotor rpm.

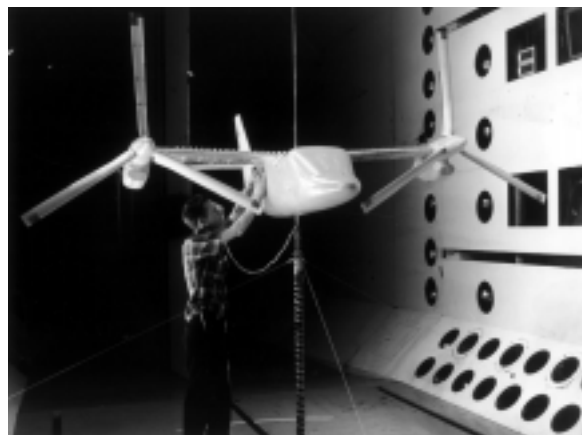


Figure 78.- 1/5-scale aeroelastic model of Bell Model 300-A1A in TDT.

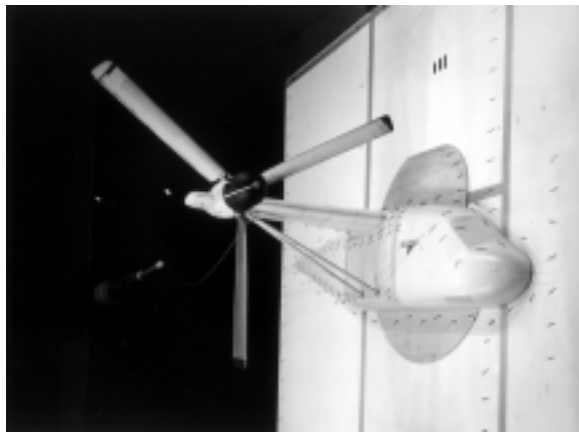


Figure 79.- 1/4.5-scale aeroelastic model of Grumman "Helicat" tiltrotor design in TDT.

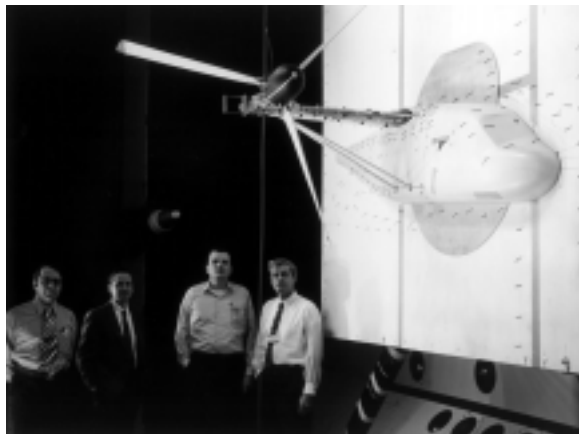


Figure 80.- Grumman tiltrotor model in whirl flutter research configuration.

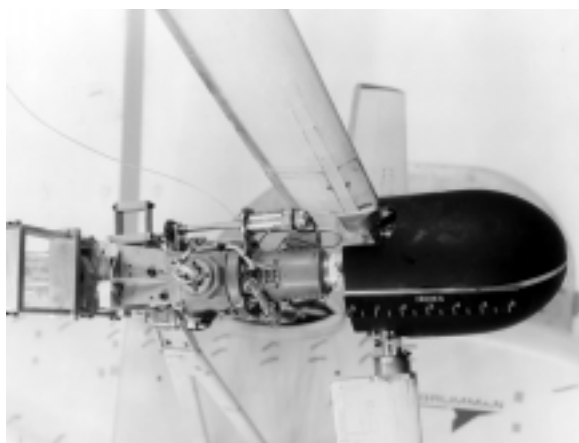


Figure 81.- Close-up view of model pylon in research configuration.

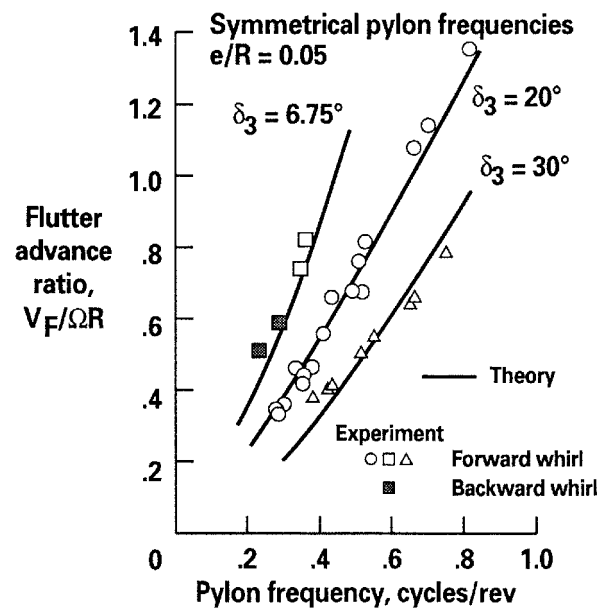


Figure 82.- Effect of blade pitch-flap coupling (δ_3) on whirl flutter.

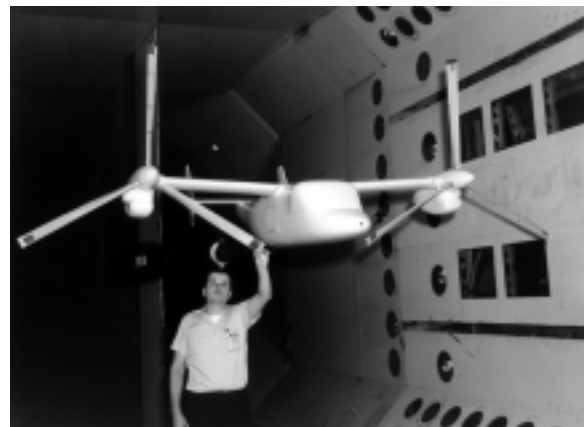


Figure 83.- 1/5-scale rigid aerodynamic force model of Bell Model 300-A2A (XV-15) with rotors from aeroelastic model in TDT.

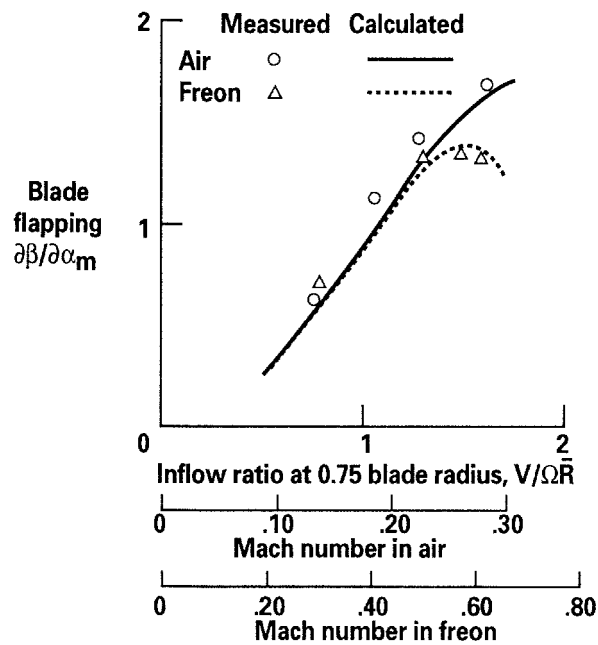


Figure 84.- Effect of Mach number on blade flapping.

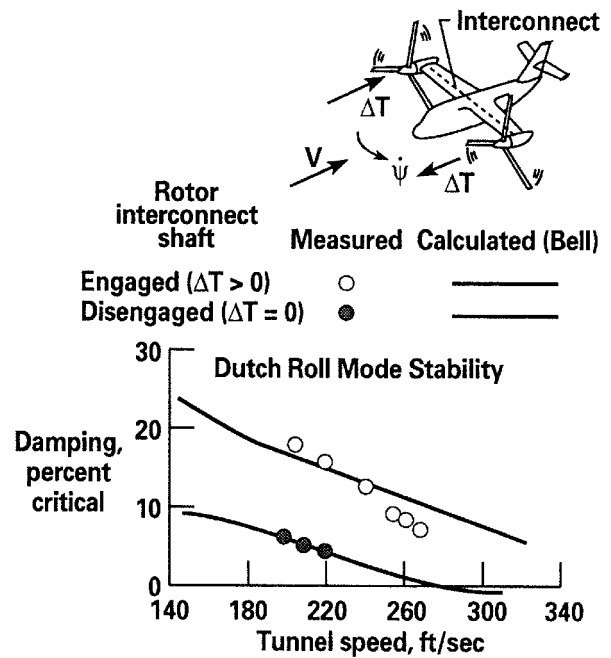


Figure 87.- Proprotor thrust damping effect on model Dutch roll mode stability.

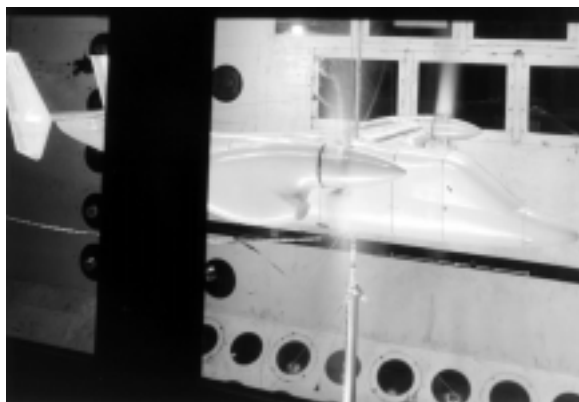


Figure 85.- 1/5-scale aeroelastic model of Bell Model 300-A2A (XV-15) in TDT.



Figure 86.- 1/5-scale model in simulated helicopter autorotational configuration.



Figure 88.- The XV-15 tiltrotor research aircraft.



Figure 89: 1/5-scale semispan aeroelastic model of Bell/Boeing V-22 in TDT.

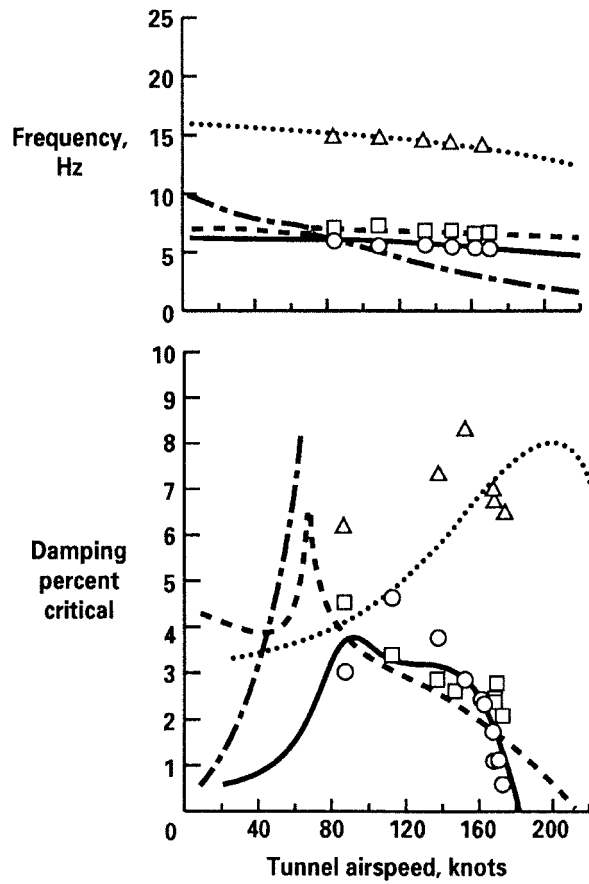


Figure 90.- Stability of wing modes for V-22 model with design stiffness wing spar.

	Measured	Calculated
Wing beam mode	○	——
Wing chord mode	□	- - - -
Wing torsion mode	△
Blade lag mode		- · - ·

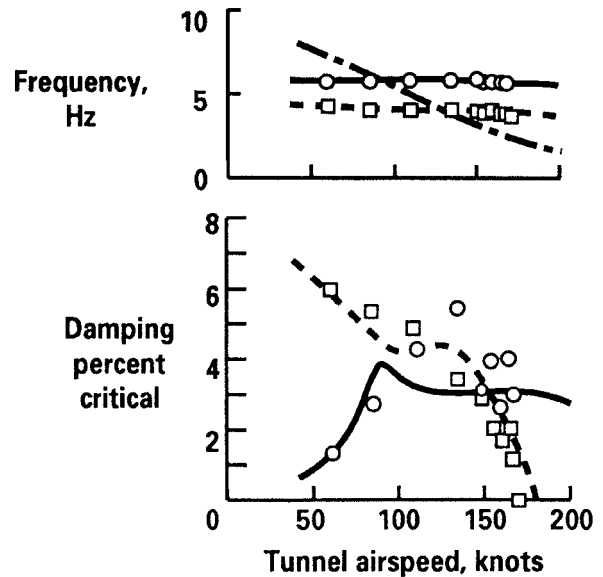


Figure 91.- Stability of wing modes for V-22 model with off-design stiffness wing spar.

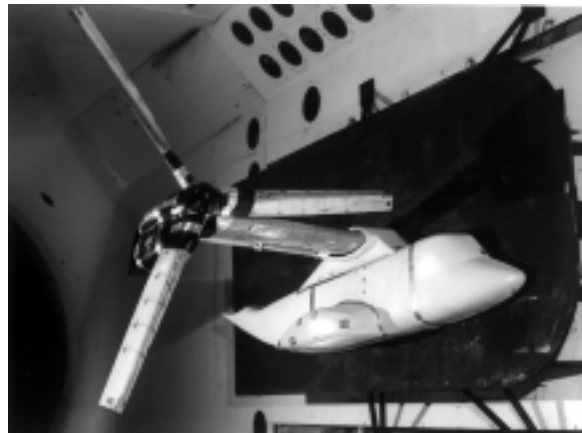


Figure 92.- WRATS testbed installed in TDT.

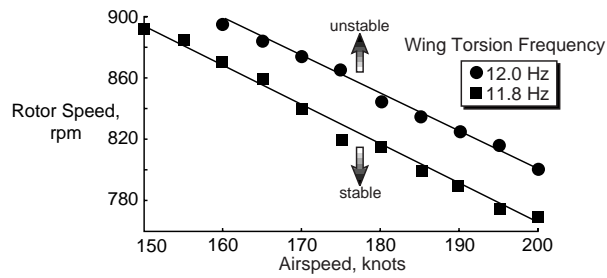


Figure 93.- Effect of wing torsional frequency on stability of WRATS testbed.

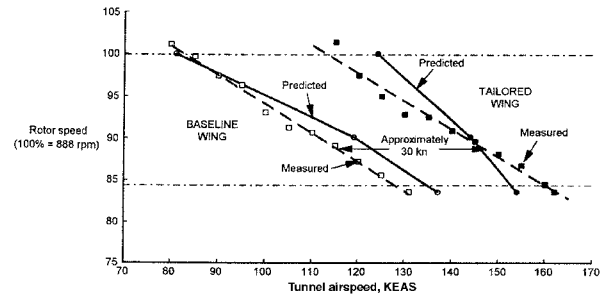


Figure 96.- Stability boundaries for 1/5-scale baseline and tailored wing.

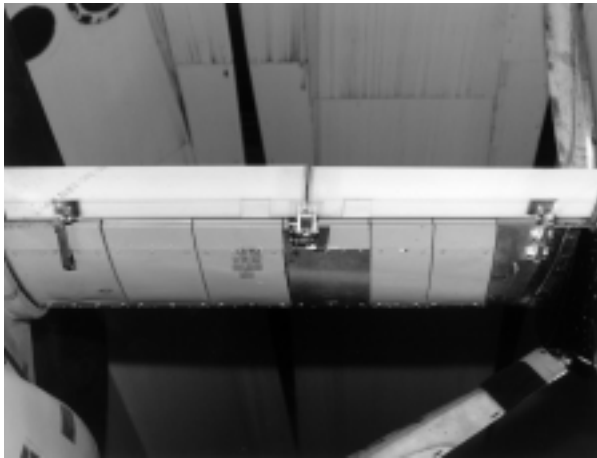


Figure 94.- Active flaperon installed on WRATS testbed.

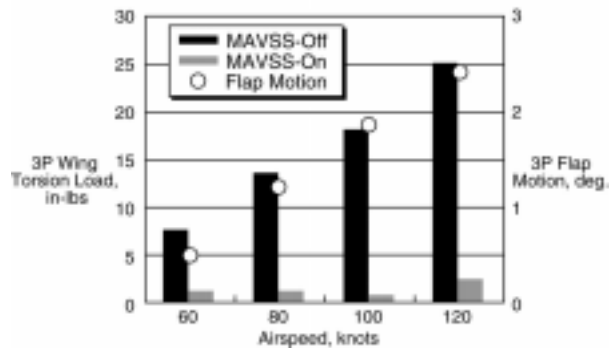


Figure 95.- MAVSS control of 3P torsional vibration using active flaperon.

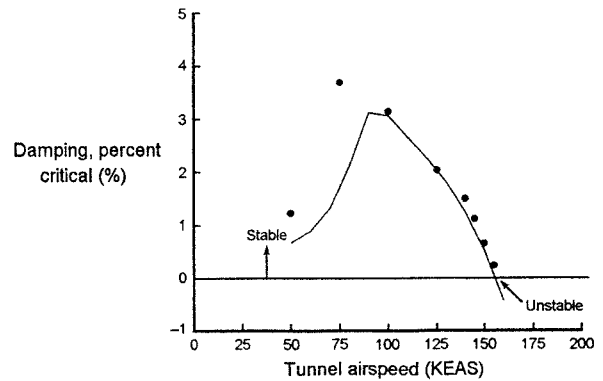
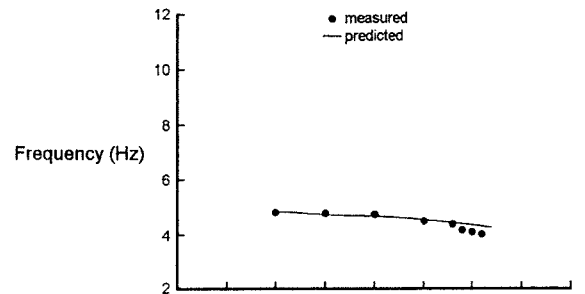


Figure 97.- Stability of wing beam mode for model with tailored wing spar.

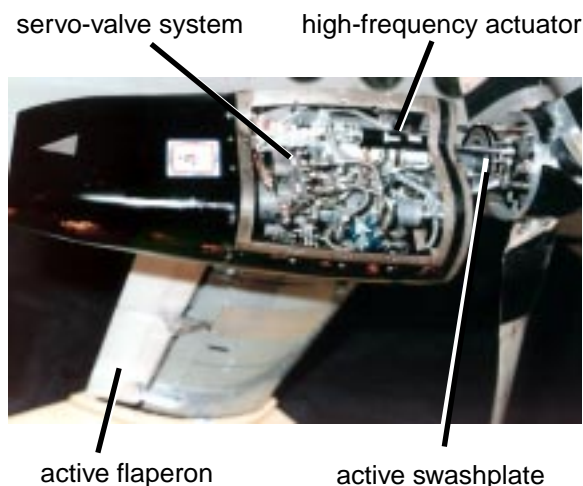


Figure 98.- Hardware components of WRATS active swashplate/flaperon higher harmonic control system.

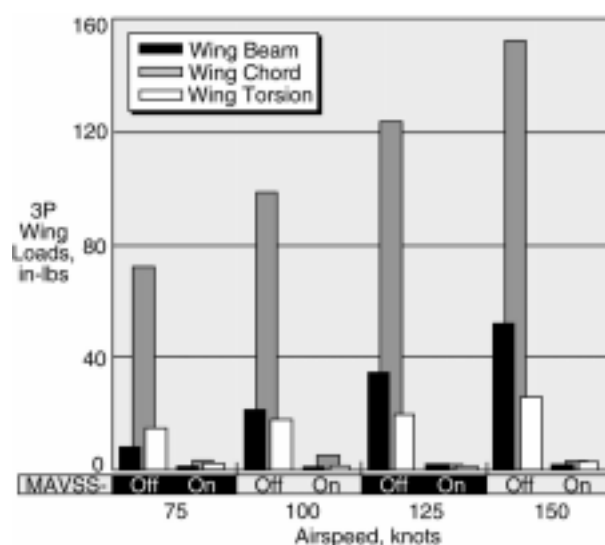


Figure 99.- MAVSS control of 3P wing bending and torsion loads as a function of airspeed.

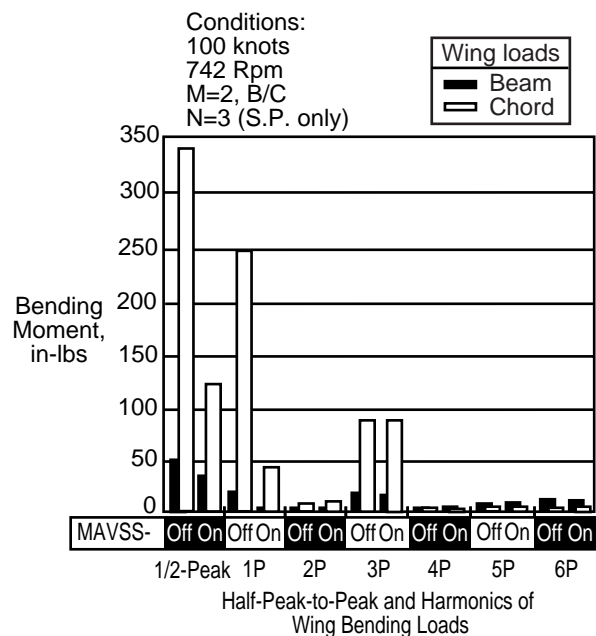


Figure 100.- MAVSS control of 1P wing bending loads.

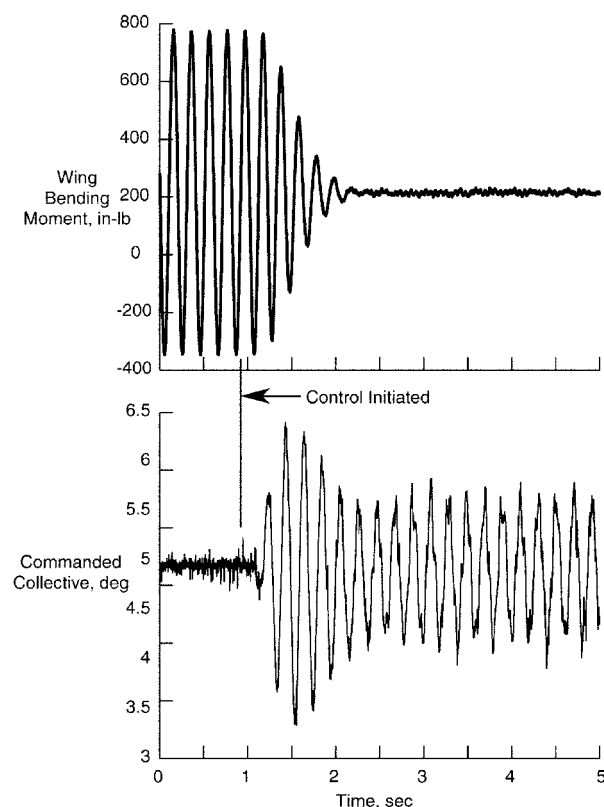


Figure 101.- GPC control of wing vibration on WRATS testbed in hover configuration.

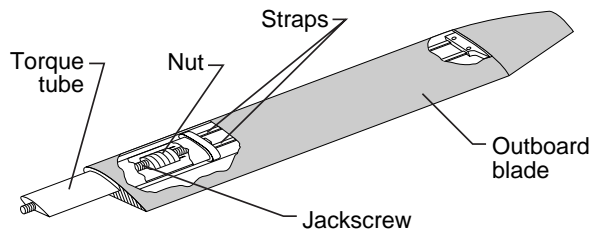
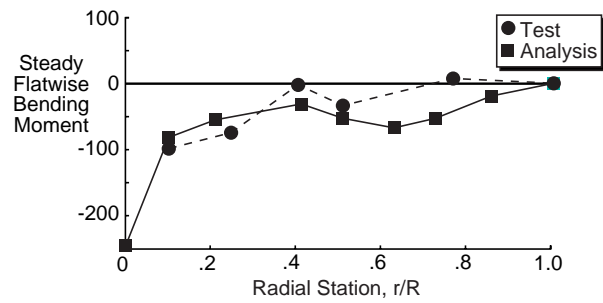


Figure 102.- UMARC/S prediction of torque tube and blade loads on VDTR model.



Figure 104.- Artist's conception of a "Quad Tilt Rotor" under study by Bell.



Figure 103.- Full-scale mock-up of Bell/Agusta BA609 tiltrotor now in development.